

Summer 7-15-2019

Architecture and evolution of the Peace Vallis distributive fluvial system, Gale crater, Mars

Zachary E. Gallegos

University of New Mexico - Main Campus

Follow this and additional works at: https://digitalrepository.unm.edu/eps_etds



Part of the [Geology Commons](#)

Recommended Citation

Gallegos, Zachary E.. "Architecture and evolution of the Peace Vallis distributive fluvial system, Gale crater, Mars." (2019).
https://digitalrepository.unm.edu/eps_etds/258

This Thesis is brought to you for free and open access by the Electronic Theses and Dissertations at UNM Digital Repository. It has been accepted for inclusion in Earth and Planetary Sciences ETDs by an authorized administrator of UNM Digital Repository. For more information, please contact amywinter@unm.edu.

Zachary Ellis Gallegos

Candidate

Earth and Planetary Science

Department

This thesis is approved, and it is acceptable in quality and form for publication:

Approved by the Thesis Committee:

Horton Newsom, Chairperson

Louis Scuderi

Laura Crossey

**ARCHITECTURE AND EVOLUTION OF THE PEACE
VALLIS DISTRIBUTIVE FLUVIAL SYSTEM,
GALE CRATER, MARS**

by

ZACHARY ELLIS GALLEGOS

**B.S. EARTH AND PLANETARY SCIENCE
M.S. EARTH AND PLANETARY SCIENCE**

THESIS

Submitted in Partial Fulfillment of the
Requirements for the Degree of

Master of Science

Earth and Planetary Science

The University of New Mexico
Albuquerque, New Mexico

July, 2019

DEDICATION

This work is dedicated to my great-grandpa, Harold Vaughn Hinchman. Through his mentorship I have become the scientific explorer I am today. He taught me the skills of observation necessary to accomplish this work and directly inspired my career in space exploration. His unrelenting pursuit of knowledge is forever instilled upon me.

ACKNOWLEDGEMENTS

This study is made possible by the teamwork and creativity of the science and engineering teams of the exploration instruments involved: the Mars Science Laboratory rover “Curiosity” team, the ChemCam instrument team, the Mastcam instrument team, the Mars Reconnaissance Orbiter team.

I would also like to acknowledge my long-time advisor Dr. Horton E. Newsom, my advisor Dr. Louis A. Scuderi, and my committee member Dr. Laura J. Crossey for their support in the completion of this study.

ARCHITECTURE AND EVOLUTION OF THE PEACE VALLIS DISTRIBUTIVE FLUVIAL SYSTEM, GALE CRATER, MARS.

by

Zachary Ellis Gallegos

B.S., Earth and Planetary Science, University of New Mexico, 2010

M.S., Earth and Planetary Science, University of New Mexico, 2019

ABSTRACT

The Peace Vallis alluvial fan, located within Gale crater on the planet Mars, is a distributive fluvial system indicating a wet climate in Mars' past. The Mars Science Laboratory rover instrument ChemCam, with the high-resolution Remote Micro-imager, was utilized to remotely explore the Peace Vallis alluvial fan and surrounding areas area. The Peace Vallis imaging campaigns 1 and 2, led by Dr. Horton Newsom and Zachary Gallegos respectively, acquired 20 distinct rover observations with a total of 243 individual images to investigate the fan. Using visual interpretation of the images and GIS techniques, this study interprets the processes and products that lead to the formation and evolution of this complex Peace Vallis distributive fluvial system including: recognition of a new fan structure perched above the Peace Vallis fan, shoreline deposits from Gale lake, nature of the Peace Vallis fan units, and stratigraphic correlation to the Mars Science Laboratory rover traverse.

TABLE OF CONTENTS

LIST OF FIGURES	ix
CHAPTER 1 INTRODUCTION.....	1
Study aim	2
CHAPTER 2 REVIEW OF RELATED LITERATURE.....	3
Alluvial fans.....	3
Alluvial fans on Mars.....	7
Gale crater.....	8
Gale crater alluvial bajada	10
Peace Vallis watershed	12
Peace Vallis distributive fluvial system.....	13
Mars Science Laboratory rover.....	16
ChemCam Remote Micro-imager.....	18
CHAPTER 3 METHODOLOGY	22
Data.....	22
Peace Vallis imaging campaign.....	22
Gale crater HiRISE digital terrain model.....	27

Data processing	28
ChemCam Remote Micro-imager corrections	28
Analysis methods	29
Visual image interpretation.....	29
GIS techniques	30
CHAPTER 4 RESULTS.....	33
Mars Science Laboratory rover results	33
Peace Vallis campaign 1	33
Peace Vallis campaign 2	33
Orbital GIS results	34
Topographic profiles	34
Digital terrain model analysis	35
CHAPTER 5 DISCUSSION.....	37
Gale crater wall layering.....	37
Mass wasting deposits.....	38
Inverted channels	38
Relict alluvial deposits	39

Peace Vallis perched fan	41
Remnant shoreline deposits	43
Nature of the BF fan unit	45
Nature of the AF fan unit	47
Groundwater sapping channels	47
MSL stratigraphic column comparison.....	48
Gale crater wall bajada.....	51
Conclusion	53
APPENDICES	57
Appendix A. Peace Vallis campaign 1 observations	58
Appendix B. Peace Vallis campaign 2 observations	81
REFERENCES	92

LIST OF FIGURES

Figure 1. Top (modified from: Strahler, 1975): schematic illustration of an alluvial fan system. Bottom left: alluvial fan within a hyper-arid environment in Death Valley, CA. Bottom right: alluvial fan in the Zagros Mountains of Iran.	4
Figure 2. Top (from: Davidson, 2013): a schematic interpretation of the DFS depositional classes. Bottom (from: Weissman, 2013): illustration of the class 1 DFS depositional mode. Yellow = active channels. Orange = inactive channels. Blue = wetlands/lacustrine.....	6
Figure 3 (from: Morgan, 2019). The locations of fan structures across the surface of Mars. Red dots represent alluvial fans, green dots represent stepped deltas, and blue dots represent deltas. ..	7
Figure 4. Example of an evolved alluvial fan/delta system within Holden crater, Mars.....	8
Figure 5. CTX mosaic of the of 154 km diameter Gale crater and the surrounding areas.	10
Figure 6. A section of the Gale crater bajada in the north-east quadrant of the crater. The Peace Vallis channel is observed dissecting the crater in the top-left of the figure.	12
Figure 7 (from: Newsom, 2019). The Peace Vallis watershed on the rim of Gale crater, outlined in white dashes (image credit: Fred Calef).	13

Figure 8. Outline of the bajada area containing the Peace Vallis DFS within Gale crater.14

Figure 9 (from: Sumner, 2013). Geologic map of the Peace Vallis fan area with tan representing the AF unit and brown representing the BF fan unit.15

Figure 10 (from: Grotzinger, 2012). A schematic diagram of the Mars Science Laboratory with the scientific instruments annotated.....17

Figure 11 (from: Maurice, 2012). ChemCam mast unit (left) and the MSL mast fully constructed with the ChemCam mast unit integrated (right).18

Figure 12. Top: schematic diagram of the ChemCam telescope (Maurice, 2012). Bottom: orbital image showing the minimum pixel size of the RMI imager at varying distances from the rover (image credit: Fred Calef).20

Figure 13. ChemCam sequence CCAM01237 targeted at distal Peace Vallis DFS deposits.....21

Figure 14. Traverse route of the MSL rover with the two Peace Vallis campaign locations outlined with a blue (1st campaign) and red (2nd campaign) ellipse.....24

Figure 15. HiRISE DTM of the MSL exploration zone area including the Peace Vallis fan system.27

Figure 16. ChemCam long-distance RMI sequence CCAM04981. A: unprocessed, raw ChemCam RMI image. B: RMI image with the standard RMI pipeline processing. C: Peace Vallis RMI image with mean-subtracted RMI processing.	29
Figure 17. Viewshed analysis of the ChemCam long distance RMI sequence CCAM02241.....	31
Figure 18. Correlated view of features in the ChemCam long-distance RMI sequence CCAM02241 (bottom) with orbital data (top). The field of view is ~550 m wide.	32
Figure 19. The Peace Vallis campaign 1: ChemCam long-distance RMI observations on a Mastcam mosaic mcam06038 background.....	33
Figure 20. The Peace Vallis campaign 2: ChemCam long-distance RMI observation on a Mastcam mosaic sequence mcam10228 background.	34

Figure 21. A: Gale crater profile from south to north showing the north-south slope of the crater and surrounding area. Also note the central mound, Aeolis Mons, which covers the Gale crater central uplift. B: North Gale crater profile from above the Peace Vallis fan to the top of the clay unit above the rover. C: Peace Vallis distributive fan down-fan profile. D: Peace Vallis distributive fan medial, cross-fan profile showing a rugged west sector and smooth east sector. E: Large inverted channel profile on Peace Vallis fan with a $\sim 2^\circ$ slope. F: Peace Vallis perched fan down-fan profile with a $\sim 10^\circ$ slope. This profile also shows the Peace Vallis fan trench and a toe bulge.35

Figure 22. DTM analysis of the Peace Vallis fan area revealing the BF unit structure.....36

Figure 23. Crater wall stratigraphy observed in ChemCam long-distance RMI sequence CCAM04262.....37

Figure 24. Inverted channel deposits on the Peace Vallis fan captured by the long-distance ChemCam RMI sequence CCAM04981 and from orbit (bottom right; ~ 2.5 km across). 38

Figure 25. Top: abandoned alluvial deposits captured by the ChemCam long-distance RMI sequence CCAM04300. Bottom: HiRISE orbital view of the abandoned deposits. The yellow box outlines the features in each image and represents ~ 600 m across in the lower figure. 40

Figure 26. Top: A newly recognized fan structure perched above the Peace Vallis fan. The blue arrow indicates a newly activated channel which caused a dam in the Peace Vallis channel. Bottom: Thermal inertia view of the perched fan and Peace Vallis fan area..... 42

Figure 27. Stereo anaglyph of long-distance ChemCam RMI sequence CCAM04300 with dipping layers of the perched fan above the Peace Vallis fan (bottom right). 43

Figure 28. Top (from: Chan, 2011): Paleo-shorelines recorded in Lake Bonneville deposits. Bottom: ChemCam RMI shoreline context image and inset zoom-in within Gale crater.45

Figure 29. Top: outcrops on the of the BF unit observed in ChemCam long-distance RMI sequence CCAM03271. Bottom: threshold adjusted product from CCAM03271 accentuating the lateral continuity of the outcrops. 46

Figure 30. Threshold adjusted image of ChemCam long distance RMI sequence CCAM02011 which shows the undulating, discontinuous surface of the AF fan unit in the middle and the outcropping, semi-continuous BF fan unit at the bottom. 47

Figure 31. Top, bottom-left (inset): groundwater sapping channel observed by the ChemCam RMI sequence CCAM041981. Bottom-right (from: Scuderi, 2019): HiRISE DTM hillshade product....

48

Figure 32. Left: Stratigraphic column for the traverse of the Mars Science Laboratory. Right: Vertically exaggerated profile of the Peace Vallis alluvial system aligned by elevation with the rover stratigraphic column to show correlation to the materials observed along the traverse..... 50

Figure 33. Top: a section of the Gale crater alluvial bajada in the north-east quadrant of the crater. Bottom: a map of the temporal evolution of the bajada in this area. 52

Figure 34 (modified after: Thompson, 2017). Geologic timescale of Mars annotated with important events within Gale crater. 56

Chapter 1

Introduction

The investigation of alluvial fan systems helps to guide interpretation of both regional paleo-climatic and environmental conditions as well as local geologic and depositional processes (Hooke, 1967; Blair & McPherson, 1994; Weissman, 2005; D’Arcy, 2017). The study of terrestrial alluvial fans can be completed in detail due to their accessibility as field sites. Alluvial fan features are also present in abundance on the surface of Mars (Moore, 2005; Kraal, 2008a; Morgan 2019) and record the same environmental information as Earth-based fans (Moore, 2003); however, they are less accessible and can usually only be studied using orbital imagery and data.

NASA’s flagship Mars Science Laboratory rover mission “Curiosity” is currently exploring a region within Gale crater on the planet Mars (Grotzinger, 2012; Grotzinger, 2015). Gale crater is a large complex impact crater situated on the border of the planetary dichotomy boundary, impacted into the crustal highland terrain. This area has a scientifically intriguing deposition and modification history which includes alluvial, fluvial, lacustrine, playa, and aeolian paleoenvironments reflected by the geology observed along the rover traverse. This rich geologic and environmental history led to the selection of Gale crater as the exploration zone for the Mars Science Laboratory rover (Golombek, 2012).

The inner wall of Gale crater rim is host to systems of fan structures (Grant, 2014; Palucis, 2016), known as a bajada, which are exposed in various forms and levels of degradation. This area of the crater is too distant for the MSL rover to ever study *in-situ*, however, it can be evaluated with long-distance imaging (Newsom, 2016; Gallegos 2018) and orbital GIS techniques (Scuderi, 2019).

One fan of particular interest to the MSL mission is the Peace Vallis alluvial fan. This feature lies approximately north of the rover toward the crater rim ~7-18 km from the rover. The rover aspect and the proximity of the fan makes this feature accessible to photo-geologic investigation by the high-resolution ChemCam instrument Remote Micro-imager (RMI) aboard the rover (Newsom, 2016; Gallegos, 2018).

Study aim:

This study will interpret the evolution and architecture of the Peace Vallis fan system and surrounding areas by analysis of long-distance MSL rover ChemCam RMI imagery. This system and the other fans structures in the alluvial bajada of northern Gale crater are also assessed with orbital GIS techniques to compare the architecture and evolution of these fans to each other and to other alluvial forms seen on Earth.

Chapter 2

Review of Related Literature

Alluvial fans:

The investigation of alluvial fans on Earth is important for understanding the past and present regional climate and local depositional environment. In an active hydrologic system, sediments are carried by fluid from areas of higher elevation and deposited in areas of lower elevation. The size and density of the sediment determine how it flows with the fluid. Fine, clay-sized sediment will be transported near the top of the fluid in the wash-load and distributed over a large distance. Larger sediment that is not as buoyant will be carried somewhere within the fluid column as suspended load. Sediment that is too dense to float in the fluid will be transported in the bed load, deposited nearer to the source.

In mountainous regions, sediment from the upstream watershed is transported downhill through fluvial or runoff channels (Fig. 1). When the channel reaches a flat range, sediments are deposited in a cone-shaped fan apron as the flow sweeps side-to-side following the path of least resistance (Blissenbach, 1954; Bull 1972 & 1977; Harvey & Mather, 2005). The point on the fan where it originates near the mouth of the channel is called the apex of the fan. As the fan aggrades and progrades, the sediments at the apex may reach equilibrium with the channel. Retrogradation of the fan back up the channel can occur at this point. The channel may subsequently incise a trench in the fan exposing the previously deposited fan material. The terminus of the fan is referred to the toe of the fan. The segment of the fan apron nearest to the apex is referred to as the proximal fan. The

middle segment of the fan apron is referred to as the medial fan. The segment near the toe of the fan apron is referred to as the distal fan. The sides of the fan are referred to as the lateral sectors of the fan and the central section of the fan is referred to as the central sector of the fan. A general sediment coarsening trend is often observed up-fan as the proximal deposits contain coarse sediments that were deposited due to a change in stream power at the apex (Weissman, 2013). The distal deposits contain finer sediments able to be carried as bed, suspended, or wash load by the less vigorous flow.

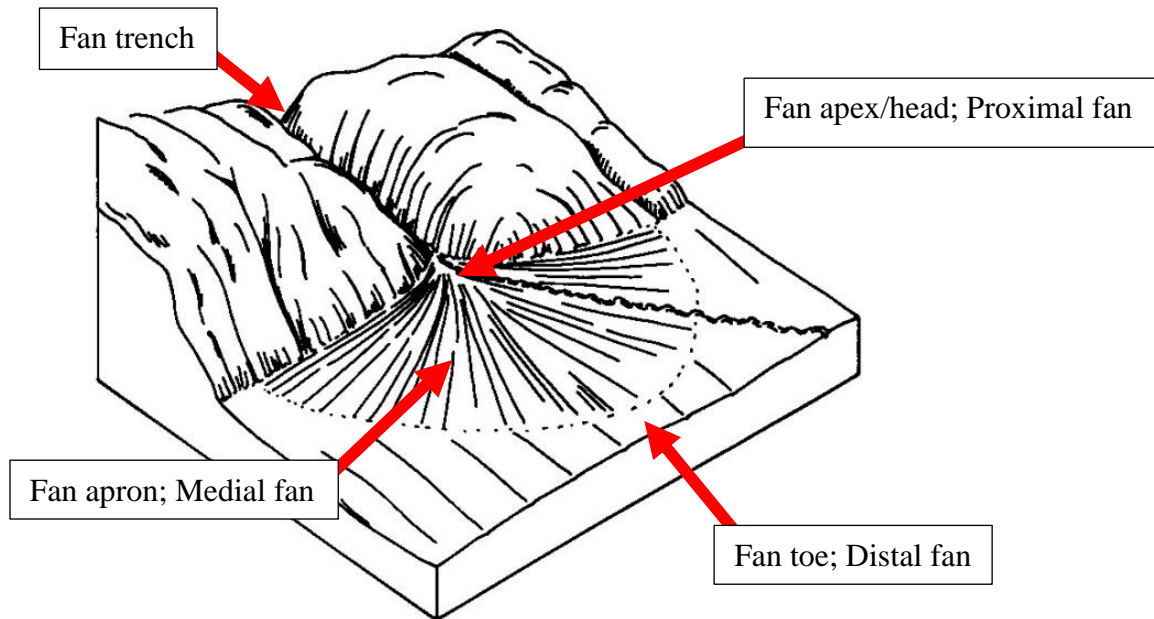


Figure 1. Top (modified from: Strahler, 1975): schematic illustration of an alluvial fan system. Bottom left: alluvial fan within a hyper-arid environment in Death Valley, CA. Bottom right: alluvial fan in the Zagros Mountains of Iran.

There are multiple flow regimes for fan surfaces on a spectrum of sediment size, water availability/regularity, and stream power (Blissenbach, 1954). Debris flow is a viscous mix of sediment, lithics, and water. They are common in areas of high relief and deposit within channels or in lobate features with little internal structure. Sheet flow is a less viscous mix with a higher water to sediment ratio. They are common when discharge is high carrying fines from the upstream watershed during large, infrequent storm events. This leads to thin, regular deposition across a fan surface. Deposition of a fan surface can also be fluvial in nature, with one or more channels delivering the sediment load at a time.

A dominant geomorphic alluvial form of fan structures known as distributive fluvial systems (DFS) (Weissman, 2010) are not dominated by pure lobate debris flow or sheet flow processes but are a result of continual fluvial avulsion, resulting in radial deposition of a fan apron. These features can exhibit varying forms due to variations in surface gradient, sediment supply, and discharge rate of the fluvial source (Fig. 2). Deposition can occur in one or more channels at a time and relates to the normal up-fan coarsening trend (Fig. 2).

Fans can be subaerial or subaqueous in nature and can deposit into a standing body of water. This transition point of the fan into water is difficult to pinpoint. Fans that may have deposited into water are referred to as fan/deltas.

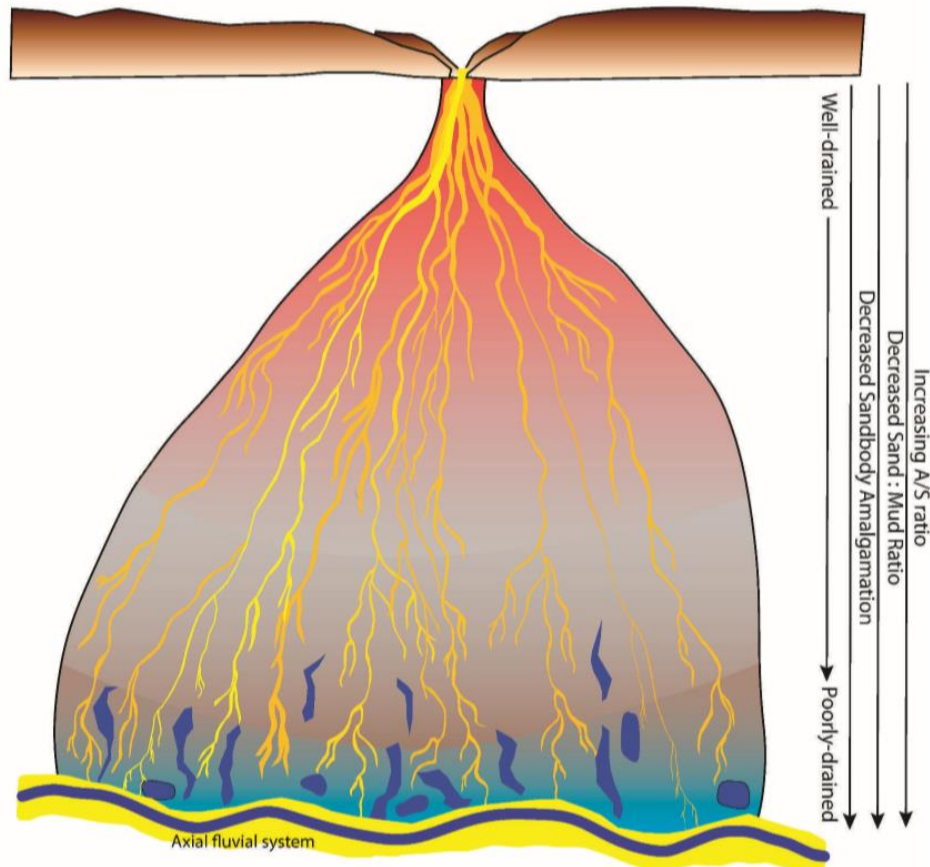
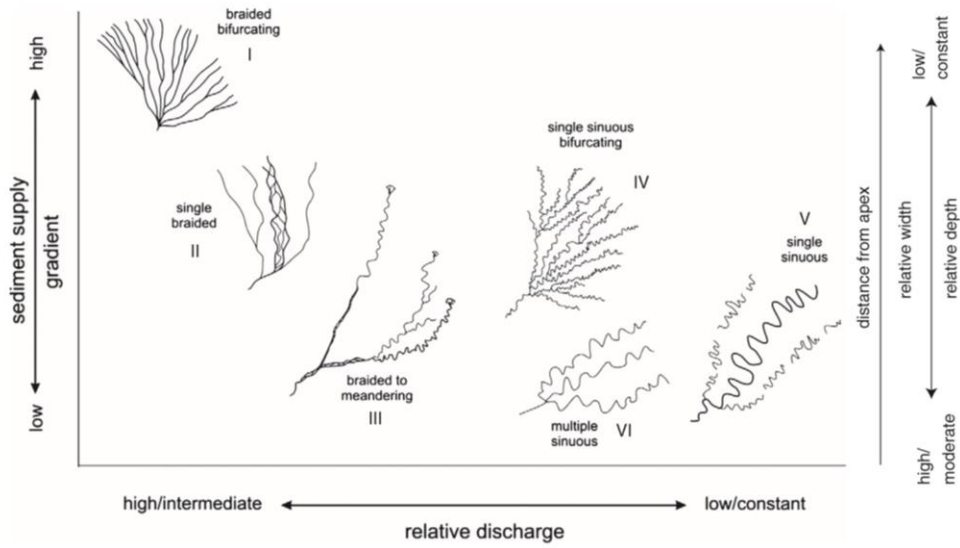


Figure 2. Top (from: Davidson, 2013): a schematic interpretation of the DFS depositional classes. Bottom (from: Weissman, 2013): illustration of the class 1 DFS depositional mode. Yellow = active channels. Orange = inactive channels. Blue = wetlands/lacustrine.

Alluvial fans on Mars:

In the past, Mars has had an active hydrologic cycle which formed many geomorphic features indicative of surface water flow such as: giant outflow channels (Sharp & Malin, 1975; Baker, 1982), inverted channels (Baker, 2001; Newsom, 2010), deltas, and alluvial fans. On Mars, fan structures are observed (Moore, 2005; Kraal, 2008a; Morgan 2019) in many regions (Figure 3) with varying forms including: stepped deltas (Kraal, 2008b), deltas (Malin & Edget, 2003; Fasset & Head, 2005), alluvial fans (Anderson & Bell, 2010) (Fig. 4). With no observed tectonic uplift on Mars, alluvial fans are restricted to other high-relief environments such as within the walls of impact craters, on the slopes of giant outflow channels, and on the flanks of volcanic uplifts. Formation rate of large alluvial fans on Mars have been modeled to $\sim 10^6$ years in a temperate to semi-arid environment and $\sim 10^7$ to $\sim 10^8$ years in long-lived arid environments (Armitage, 2011).

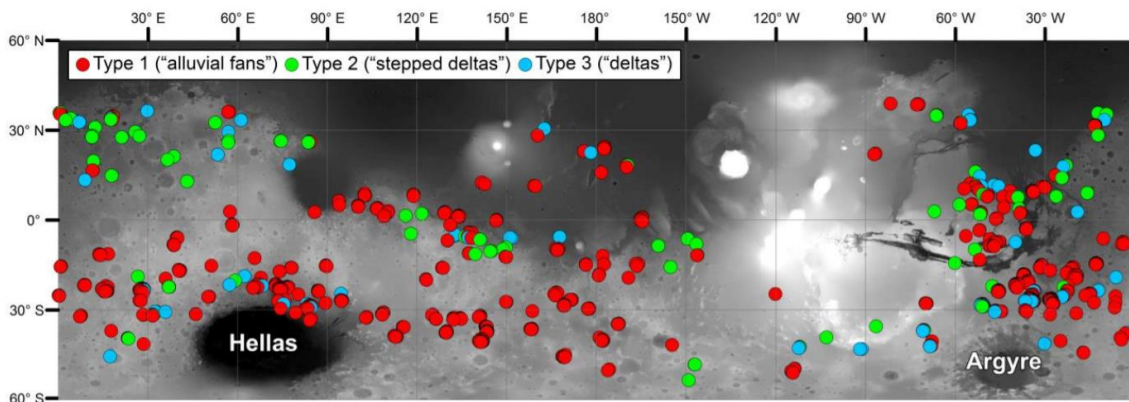


Figure 3 (from: Morgan, 2019). The locations of fan structures across the surface of Mars. Red dots represent alluvial fans, green dots represent stepped deltas, and blue dots represent deltas.

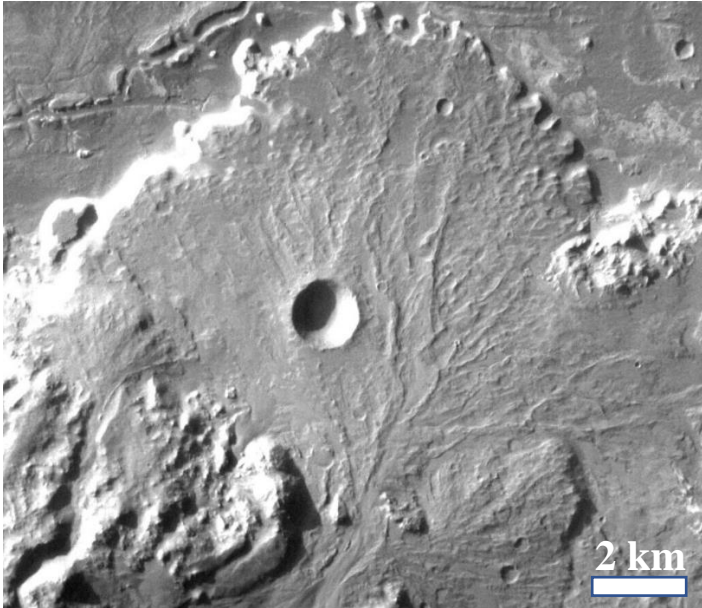


Figure 4. Example of an evolved alluvial fan/delta system within Holden crater, Mars.

Gale crater:

Gale crater (centered at 5.42°S , 137.82°E) is a complex and scientifically intriguing area on the planet Mars. The ~ 154 km diameter crater situated on the highlands side of the planetary dichotomy, ~ 1850 km south of the Elysium volcanic complex, is the result of an impact in the Late Noachian (Thompson, 2011) – Early Hesperian (Le Deit, 2012). The center of the crater is draped by a thick sedimentary mound called Aeolis Mons. The mound rises ~ 5 km above the crater floor and likely covers the central peak of Gale crater.

From orbit (Fig. 5), Gale crater shows evidence for past surface water and groundwater flow. Evidence of one or more paleo-lakes within the crater (Palucis, 2016) comes from orbital spectroscopic analysis of the mineralogies deposited within crater, including the hematite observed on Vera Rubin Ridge and the clays deposited above the

ridge (Anderson & Bell, 2010; Miliken 2010). Geomorphic features around and within the crater also show evidence for past water flow. Fan systems along the crater rim and on the central mound indicate modification by surface water (Anderson & Bell, 2010; Sumner, 2013; Palucis, 2014).

Some models of the Gale crater environment include a lake with deposits partly filling the crater and subsequent aeolian infill of the entire crater (Grotzinger, 2015). This is an unlikely scenario as filling and exhuming a crater of sediment does not need to be called on to explain the past and current environments observed. Conversely, outward dipping slopes of the sediments on the mound reflect the potential for in-place sedimentation and modification of the mound without crater infill (Kite, 2013).

This range of diverse geology/mineralogy, and the inferred environmental conditions that produced it, is the reason Gale crater was selected for the landing site of the MSL rover (Miliken, 2010; Anderson & Bell, 2010; Golombek, 2012)

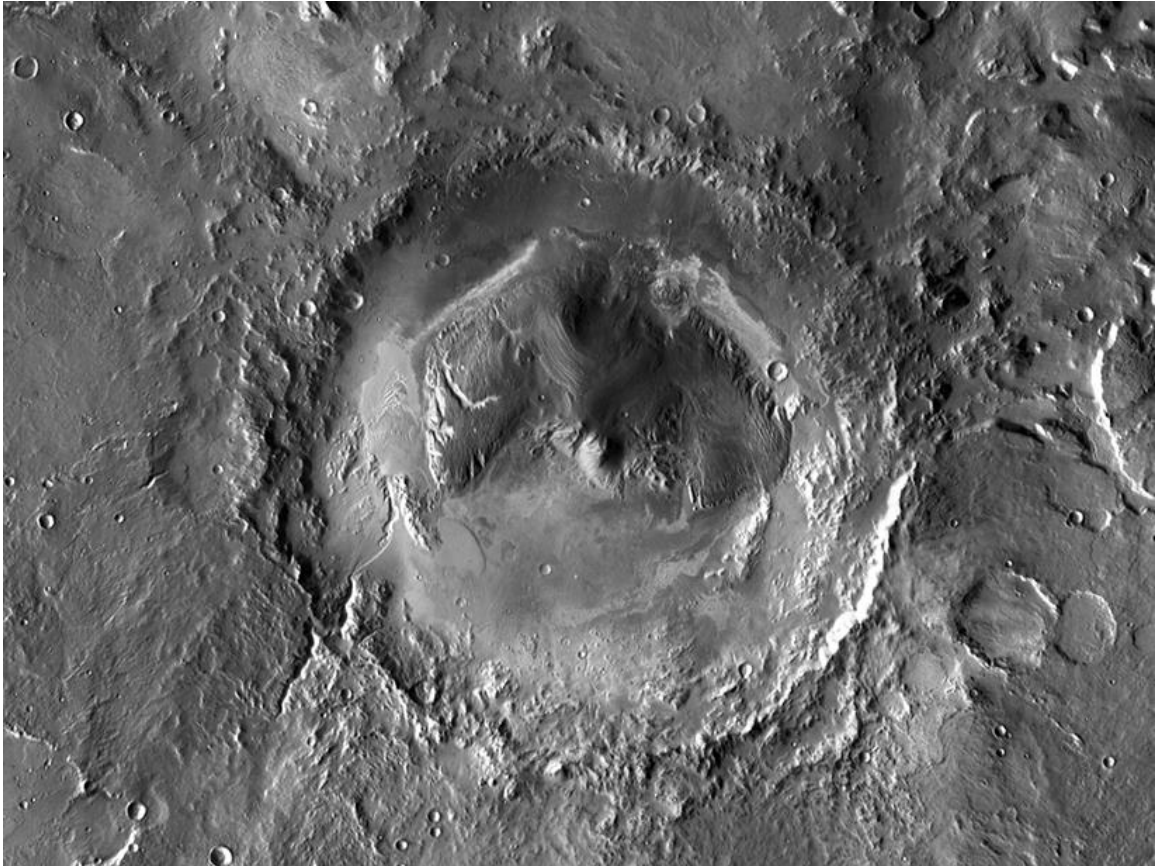


Figure 5. CTX visual mosaic of the of 154 km diameter Gale crater and the surrounding areas.

Gale crater alluvial bajada:

When alluvial deposition occurs along a long-running front, a series of alluvial fan features may form a chain of fans, referred to as a bajada. Segments around the inside rim, or crater “wall”, of Gale crater are partially lined with an alluvial bajada (Figure 6) consisting of fan structures of varying form and stages of degradation. Most of the fans are heavily eroded with prominent, predominantly linear inverted channels forms. These resistant features represent past fluvial channels armored by cemented sediments and/or a unit of fluvial boulders. The sinuosity of the inverted channels is very low suggesting these fan structures represent group 1 (braided bifurcating) of the DFS spectrum. These degraded

alluvial fan structures along the bajada are sourced from crater rim alcove watersheds with relatively small areas but potential for groundwater percolation through the rim.

Most of the watersheds surrounding Gale crater are relatively small due to the precipitous crater rim. These small watersheds carve alcoves within the rim structure that may be due to degradation and mass wasting as part of initial crater modification or with later hydrologic interaction. The rim is dissected in several areas connecting larger watersheds to the Gale crater interior with more developed alluvial structures. These large fans can be mantled by fine grained material from the watershed in periodic climate events (Scuderi, 2019). These deposits are shown by relative crater counts to be significantly younger than the surrounding and underlying deposits (Grant 2018).

Groups of hills are observed intermittently spaced in front of the crater wall. These foothills have little visible internal structure but are often surrounded by small alluvial forms. Areas with larger distributive fluvial systems exhibit a lack of these foothills due to their subsequent erosion in these high-powered fluvial environments. One interpretation is that these hills are mass-wasting deposits that slumped off the crater wall during initial crater modification; the other possibility being they are a result of later crater wall failure due to groundwater percolation through the crater rim or intense alluvial/fluvial activity.

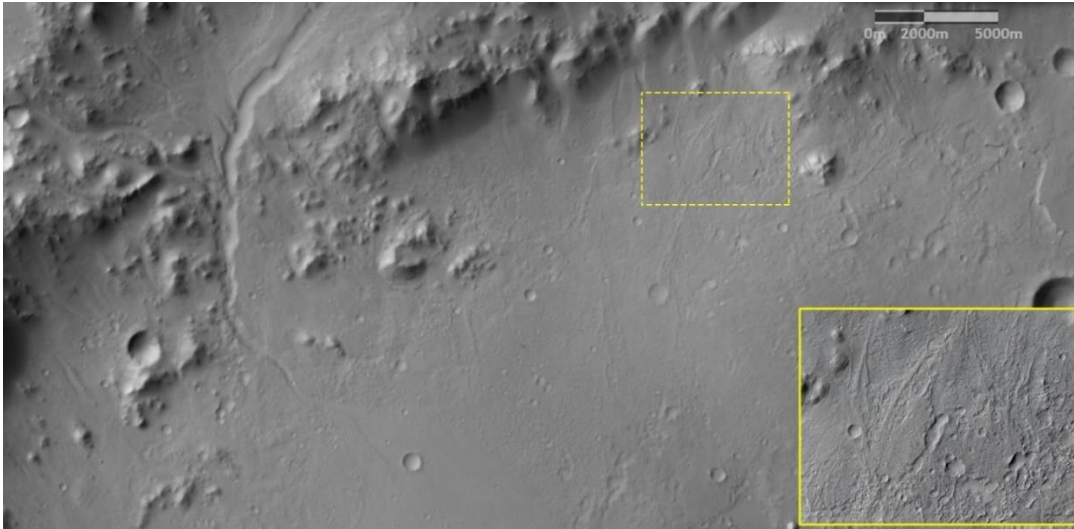


Figure 6. A section of the Gale crater bajada in the north-east quadrant of the crater. The Peace Vallis channel is observed dissecting the crater in the top-left of the figure.

Peace Vallis watershed:

The Peace Vallis watershed is the largest watershed draining into northern Gale crater (Fig. 7). Early studies concluded an area of 1021 km² (Palucis, 2014), however recent evidence shows an area of ~1500 km² with the addition of an extended southern watershed (Newsom, 2019). The watershed records an active fluvial and alluvial history as evident by relatively young fluvial channels, older inverted channels, and small alluvial fans. Most of the terrain is a mottled, light and dark surface suggesting mobilization and transport of sediments into topographic lows. The Peace Vallis watershed drains surface water and groundwater into Gale crater primarily through the Peace Vallis channel. This channel flows from above the crater rim edge (~26 km with 1.4 km elevation change) down through the Peace Vallis alcove to the apex of the sedimentary structure known as the Peace Vallis fan. Other smaller tributaries flow into the main channel, incising new drains into the Peace Vallis alcove. Percolation of Peace Vallis watershed groundwater through the crater rim is also likely.

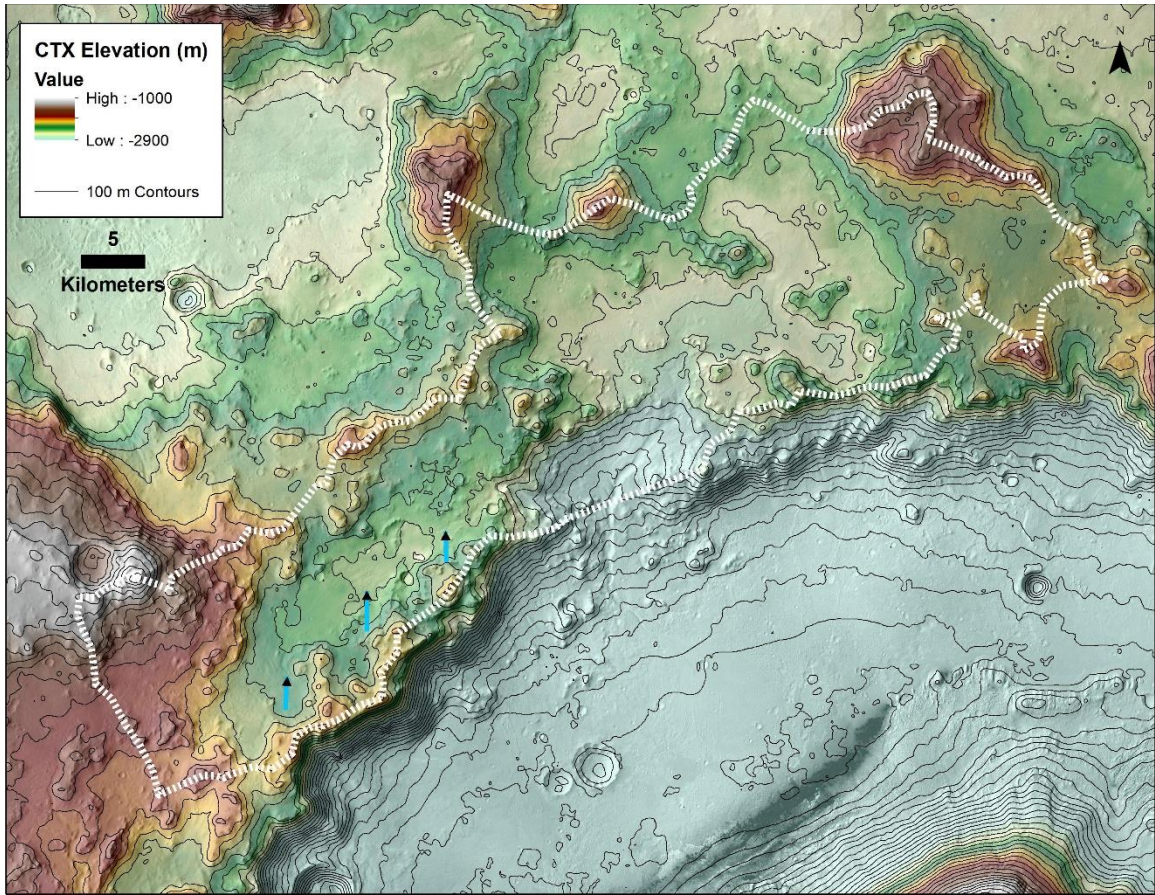


Figure 7 (from: Newsom, 2019). The Peace Vallis watershed on the rim of Gale crater, outlined in white dashes (image credit: Fred Calef).

Peace Vallis distributive fluvial system:

The Peace Vallis alluvial fan (Fig. 8) is located within the north rim of Gale crater. This feature has been the subject of previous study (Anderson & Bell, 2010; Sumner, 2013; Palucis, 2014) due its proximity to the Mars Science Laboratory exploration zone. It shares many similarities with Earth-based fans including: fan-like conical shape, inverted channel topography, and fluvial channels. This feature has been referred to in the literature as an alluvial fan but more closely resembles the definition of a DFS.

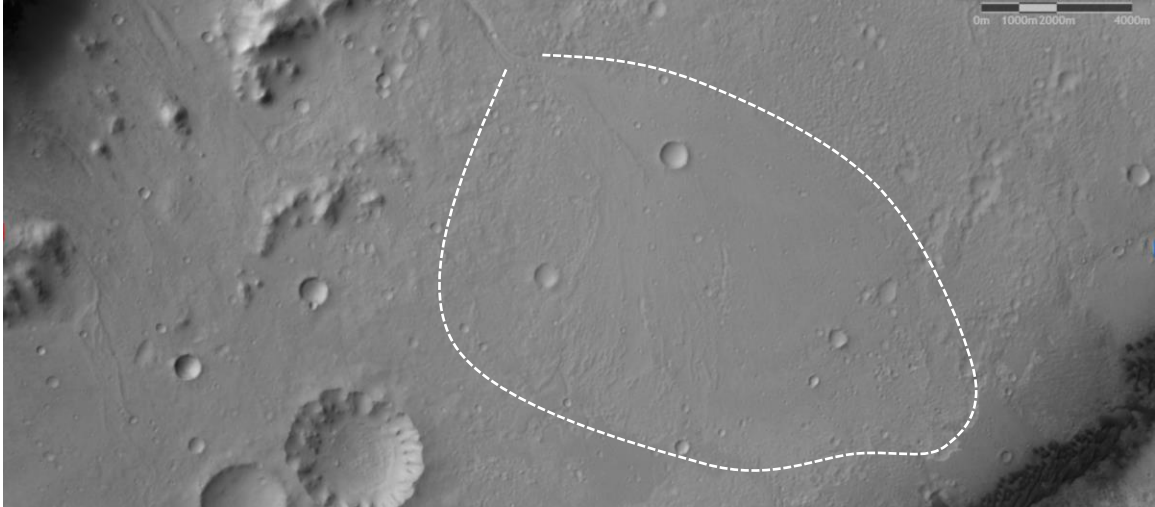


Figure 8. Outline of the bajada area containing the Peace Vallis DFS within Gale crater.

The Peace Vallis fan is supplied with water and sediment by the Peace Vallis watershed. Unlike most other fan watersheds in Gale crater, Peace Vallis watershed represents a relatively large catchment area. This large area provided the water and sediment necessary to account for the individual units of the Peace Vallis fan. Previous research shows the sediments eroded in Peace Vallis alcove to be approximately equal in volume to the Peace Vallis fan (Palucis, 2014). There is likely more input of sediments and lithics from the highlands sourced watershed than this result implies.

The Peace Vallis fan has been mapped (Fig. 9) into two visually distinct units: the BF (bedded and fractured) unit and the AF (alluvial fan) unit (Sumner, 2013). The underlying BF unit is exposed in the left-lateral sector and distal section of the fan. It outcrops in relatively rugged, eroded but continuous beds. The unit also contains polygonal fractures which have been interpreted as paraglacial in origin (Oehler, 2016). The AF unit is present on the proximal and medial sections of the fan. It has a smooth, undulating

surface mantling the underlying topography. This unit has been shown to be a late stage alluvial deposit from <1.6 Ga (Grant, 2018) sourced from sediments and fines accumulated in the Peace Vallis watershed.

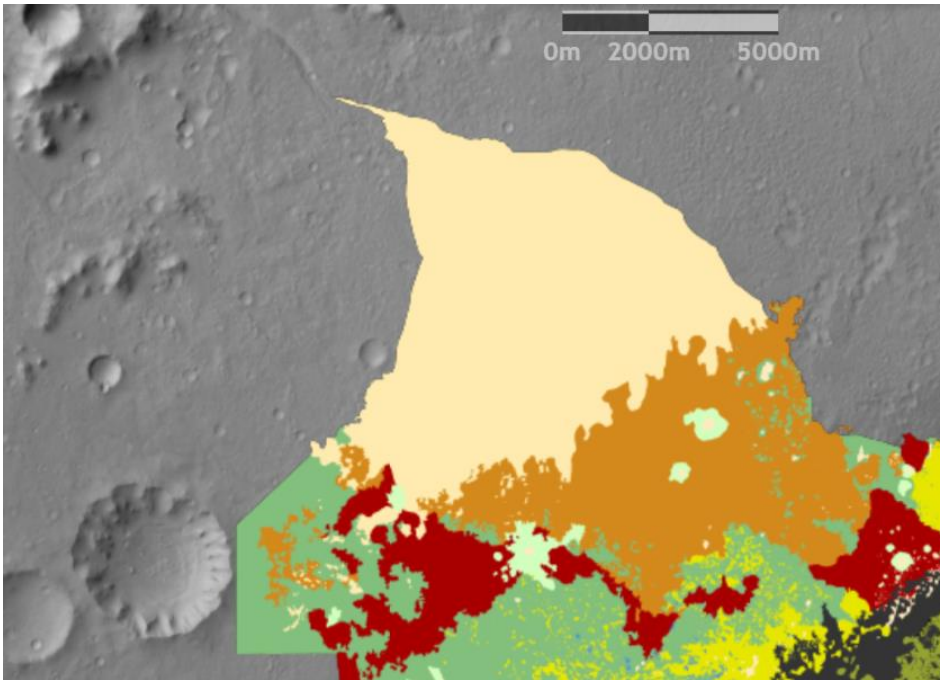


Figure 9 (from: Sumner, 2013). Geologic map of the Peace Vallis fan area with tan representing the AF unit and brown representing the BF fan unit.

Several large inverted channels are observed on the fan originating near the apex and continuing to the medial-distal fan (Anderson & Bell, 2010; Palucis, 2016). These resistive features were likely formed in fluvial environments of the DFS.

Two wide, flat-bottomed channels observed on the fan surface originating at the -4435 elevation contour are result of groundwater sapping at the springline of the fan

(Scuderi, 2019). These features are well preserved with sharp, continuous outcrops and thereby represent the latest major hydrologic activity on the fan surface.

Mars Science Laboratory rover:

The Mars Science Laboratory rover (MSL) (Fig. 10) is a multi-instrument, NASA flagship rover mission which landed within Gale crater, Mars (5.3°S, 137.7°E) on August 6, 2012. It consists of seven analytical instruments for investigating geochemistry, mineralogy, and other geologic/environmental processes in the vicinity of the rover. These analyses are performed via remote science, contact science, and as drill sample (Okon, 2010). The rover also has six photographic instruments for rover navigation, as well as visual and multi-spectral observation of the environment within sight of the rover.

After landing, the rover discovered a sedimentary environment dominated by sandstone and mudstones (Vasavada, 2014). The first leg of the traverse began decreasing in elevation to reach the Yellowknife Bay waypoint. This area is important for understanding the early alluvial, fluvial, and lacustrine environment at Gale crater due to the interbedded conglomerates, sandstones, and mudstones (Vaniman, 2014; Rampe, 2017) representing a prograding alluvial structure. Along the traverse up-section to the sedimentary units on the flanks of Aeolis Mons, the rover encountered more mudstone deposits with a mix with sandstones (Rice, 2017) representing shore or near shore deposits. Diagenetic alteration of the rocks is apparent from veins and nodules observed in certain units (Stack, 2014; Nachon, 2014; Nachon, 2017). Desiccation cracks are also observed in the mudstone (Stein, 2018) indicating past fluid interaction and a drying surface. One of

the main reasons for the selection of Gale crater as the exploration zone for the MSL mission was the identification of Vera Rubin Ridge (previously Hematite ridge) (Fraeman, 2013). Initial orbital spectroscopic mapping indicated a hematite rich signal and the potential for past aqueous alteration. This area was investigated by the rover and shown to be a heterolithic mudstone with elevated hematite (Fraeman, 2018). Clay detections have also been interpreted as past water alteration (Bristow, 2015). The MSL rover is currently traversing across the Clay Unit to investigate the past lacustrine environment while ascending the lower Aeolis Mons sedimentary units.

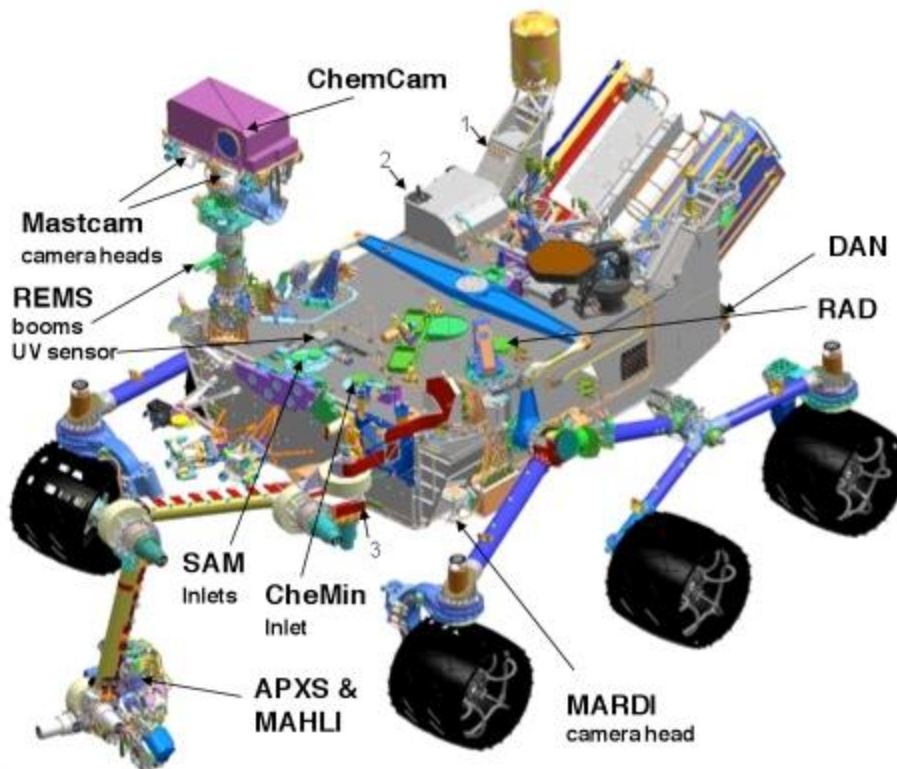


Figure 10 (from: Grotzinger, 2012). A schematic diagram of the Mars Science Laboratory with the scientific instruments annotated.

ChemCam Remote Micro-imager:

The ChemCam instrument (Fig. 11) incorporates two individual remote sensing instruments: a laser-induced breakdown spectroscopy (LIBS) device and the Remote Micro-imager (RMI). There are two individual hardware components to the ChemCam instrument: the body unit (Wiens et al., 2012) and the mast unit (Maurice et al., 2012). The body unit is housed within the chassis of the rover and comprises three spectrometers which each detect a range of plasma light frequencies emitted by the laser target. The mast unit is located atop the 2.1 m tall rover mast and contains the laser and RMI telescope (Fig. 11).

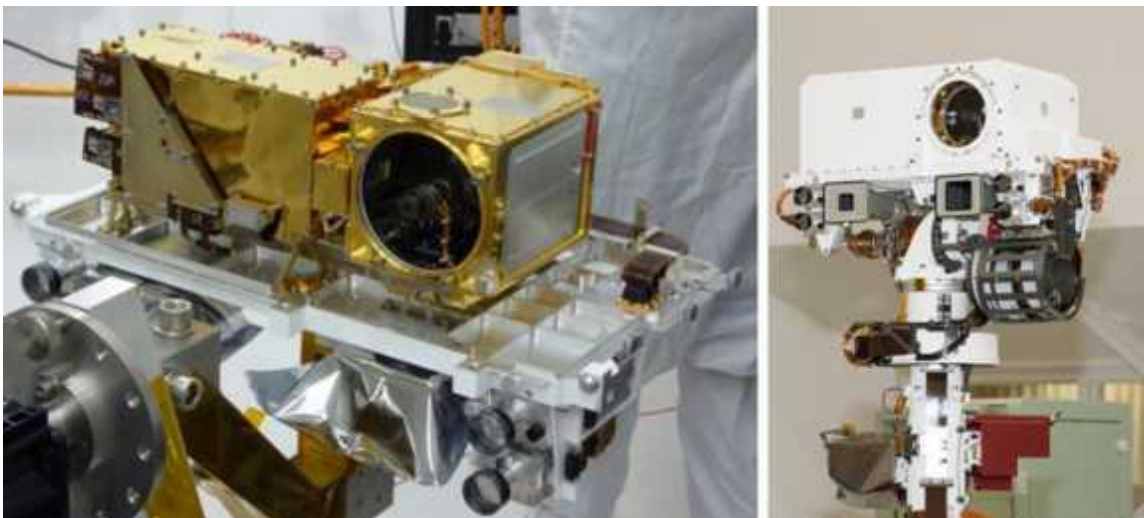


Figure 11 (from: Maurice, 2012). ChemCam mast unit (left) and the MSL mast fully constructed with the ChemCam mast unit integrated (right).

The LIBS instrument is a relatively non-destructive analysis technique, targeting rock and soil samples with a 1067 nm IR laser. Each laser analysis consists of 30-150 individual pulses which vaporizes a small $\sim 300\text{-}500\ \mu\text{m}$ diameter pit on the sample. The super-heated plasma created by the laser emits photons indicative of the target's variable

elemental composition. The light is then collected by the telescope in the mast unit and detected by the spectrometers within the rover body where the data is processed and relayed back to investigators on Earth. The laser has fired over 600,000 individual shots on more than 2,500 individual targets, making it one of the most prolific planetary instruments in terms of geochemical data products. The Remote Micro-imager (RMI) instrument is a Schmidt-Cassegrain reflecting telescope device which uses a system of mirrors to direct to the photons of laser plasma to the ChemCam spectrometers (Fig. 12). The RMI was also designed for locating and documenting the pinpoint laser pits on a target created by the laser with a 1024x1024 pixel CCD at 14x14 $\mu\text{m}/\text{pxl}$. The detector is behind the spectra splitting dichroic filters which causes a “ghost” duplicating anomaly in the imagery when travelling through the front and back of the filter.

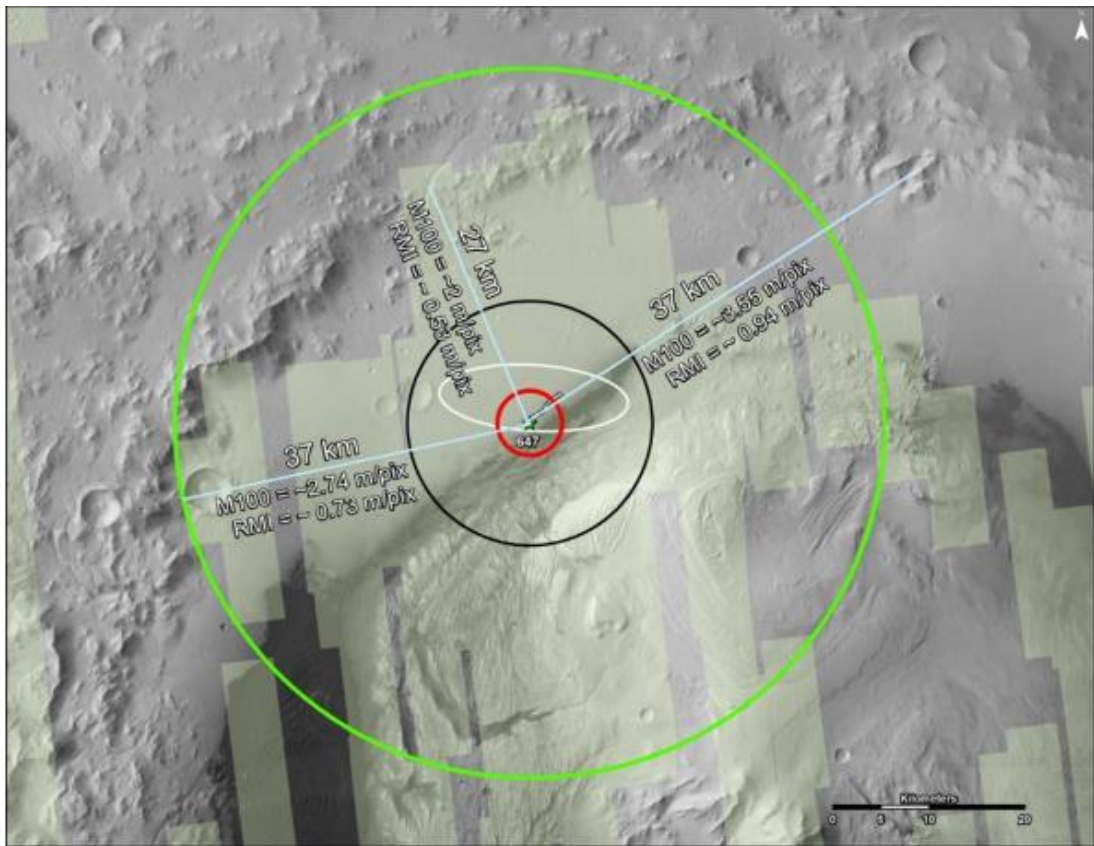
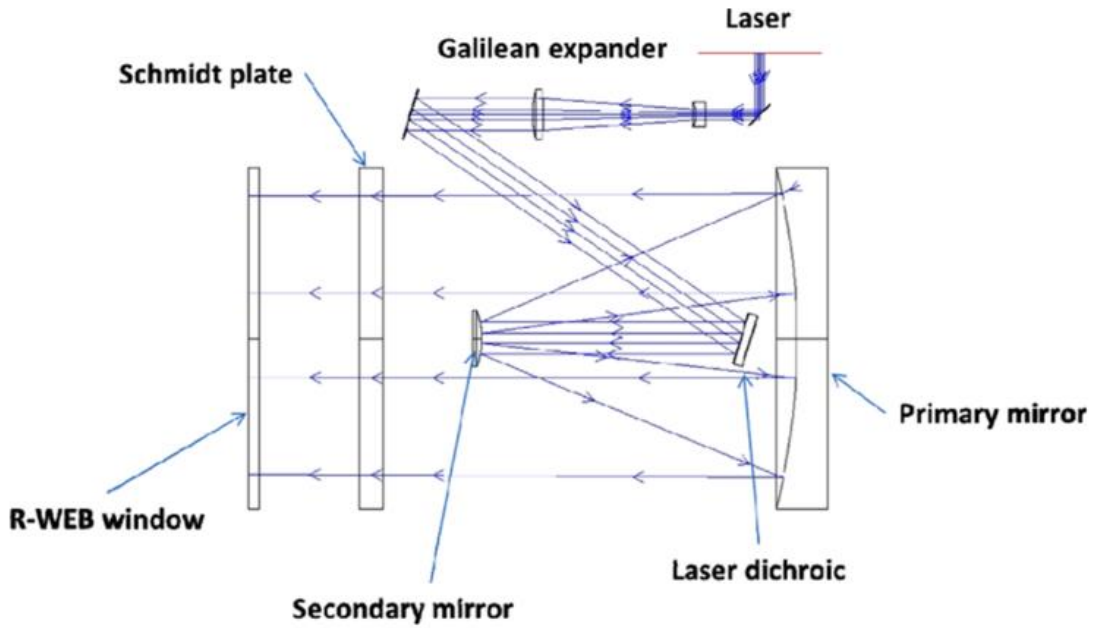


Figure 12. Top: schematic diagram of the ChemCam telescope (Maurice, 2012). Bottom: orbital image showing the minimum pixel size of the RMI imager at varying distances from the rover (image credit: Fred Calef).

The RMI telescopic imaging device was re-purposed on Sol 327 to also make long-distance observations of the areas surrounding the rover (Le Mouélic, 2015). By focusing the optics at or near infinity (equivalent to 52.156 m) the RMI captures a resolution equal to the HiRISE orbiting camera (~25cm/px) at ~12 km distance. The first test on the Peace Vallis system (Fig. 13) targeted an area on the right-lateral, distal edge of the fan. This image shows outcrops of resistant material observed standing above the fan floor. Since this observation, the RMI has been used to image the sedimentary deposits on Aeolis Mons (Dromart, 2018; Le Diet, 2018), dark lineae change detection (Anderson, 2017), and on mid-distance observations along the rover traverse.

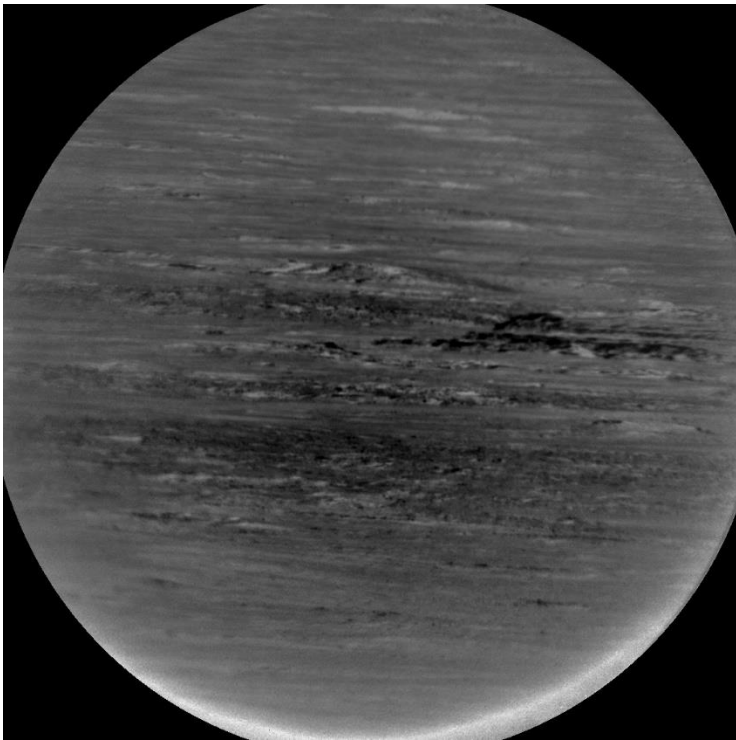


Figure 13. ChemCam sequence CCAM01237 targeted at distal Peace Vallis DFS deposits.

Chapter 3

Methodologies

Data

Peace Vallis imaging campaign:

During the 1st and 2rd extended missions of MSL rover operations, the Peace Vallis campaign acquired ChemCam long-distance RMI imagery of the Peace Vallis distributive fluvial system as well as the surrounding geology (Newsom, 2016; Gallegos, 2018). The Mastcam instrument (Malin, 2010) was utilized as a context imager for the high-resolution RMI imagery in Peace Vallis campaign. This imagery represents the first in-depth photogeologic analysis of a complex fluvial distributive system from the surface of Mars. The Mars Exploration Rover “Opportunity” also observed an alluvial bajada within Endeavour crater along the rover traverse; however, these fans were viewed from the rim of the crater looking down, meaning little geologic information was observed from the system at this high-elevation, down-fan view.

The unique perspective of the Peace Vallis system to the MSL rover makes it a promising target for long-distance photo-geologic analysis. Located approximately north from the rover traverse, the sun illumination angles are advantageous for imaging this up-fan slope. This viewing angle also means that the Peace Vallis system is not within the restrictive “Sun-blob” for the rover: a region surrounding the ecliptic where ChemCam may not point due to the possibility of damaging the optics if focused on the Sun (Maurice, 2012).

The Peace Vallis campaign was completed in two individual campaigns (Fig. 14). The first campaign was carried out by Dr. Horton E. Newsom during 2016 (Sols 1237-1311, Mars year 32; 01/29/2016 – 04/15/2016) from the Namib Dune-Naukluft Plateau section of the MSL traverse. This campaign occurred shortly after the Mars summer solstice during a relatively clear atmospheric period. The second component of the campaign was carried out by M.S. candidate Zachary E. Gallegos during 2018 (Sols 1927-2012, Mars year 33; 01/07/2018 – 04/04/2018) from the Vera Rubin Ridge section of the MSL traverse. This campaign occurred later in the Martian summer just before the onset of a planet-wide dust storm during which the Mars Exploration Rover: Opportunity lost contact with NASA.

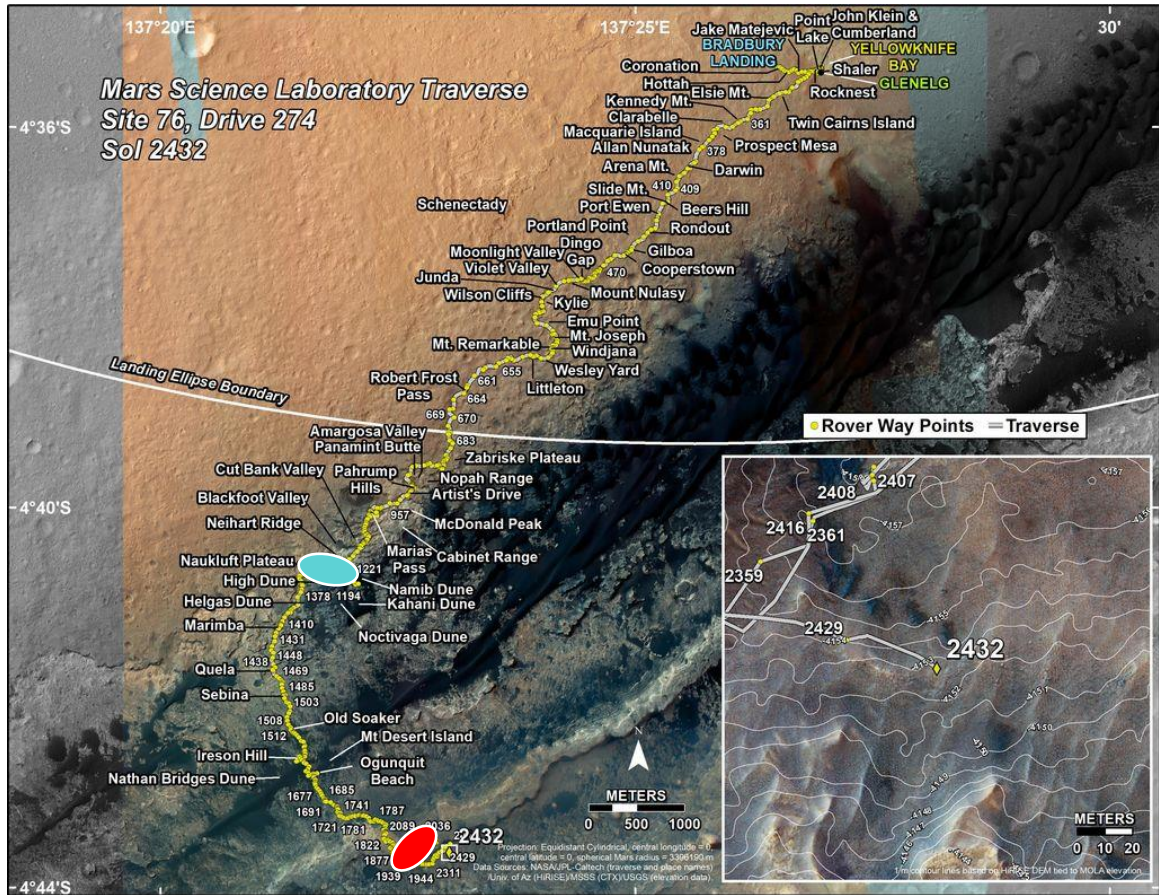


Figure 14. Traverse route of the MSL rover with the two Peace Vallis campaign locations outlined with a blue (1st campaign) and red (2nd campaign) ellipse.

The observations of the Peace Vallis campaign were categorized “opportunistic”, as other recurring rover experiments and engineering processes held precedence. This means that any opportunity to acquire this imagery was utilized. This produced a range of time-of-day for the implementation of the RMI sequences. Having one time for observation would allow for more uniform imagery with regard to light exposure and incidence angle, however, the variable brightness and differing sun angles potentially allow for additional directional aspects and textures to be illuminated

ChemCam RMI observations were acquired in left-to-right mosaics consisting of 4 to 20 individual images. The mosaics were targeted the following raster configurations: 5x1, 10x1, 20x1, and 10x2. Campaign 1 included three 5x1 rasters and ten 10x1 rasters. Campaign 2 included one 10x1 raster, five 20x1 rasters, one 2x2 raster, and one 10x2 raster. The 2x2 observation was intended to be a 10x2 raster but was abbreviated due to a rover anomaly. At times of high rover tilt, diagonal rasters were executed to approximate a horizontal image.

The time and detail required for planning, proposing, and conducting a rover campaign of this scale is not trivial. The purpose of planning a campaign for long-term, high-data observations is to: reduce operator effort, increase rover resource utilization, reduce reliance on ground in-the-loop cycles (Gaines, 2017). This process requires multiple levels of proposal and review presented to the rover science/engineering team hierarchy. This rigorous process is due to a finite amount of daily time and data for all the various rover engineering and science activities. Proposal of campaigns with the scope of the Peace Vallis campaign mean less time for other geologic, astrobiologic, atmospheric, or rover engineering activities during the course of the campaign.

The first step for the Peace Vallis campaign was to propose the plan to the specific instrument required for collecting the data. In this case, the ChemCam instrument team was notified of the initial concept for the Peace Vallis campaign 2 at the Fall 2017 ChemCam science team meeting. This original presentation laid the groundwork for rover resources needed during the entire campaign and the expected results of the study. The initial

proposal was met with hesitation because the amount of time and data required for the campaign was not trivial. This requires reallocation of the resources from other geochemical, photogeologic, and environmental experiments that regularly take place using the ChemCam. After this step, more planning was needed to refine the campaign with the suggestions made by the ChemCam team. The next presentation was made to the Geologic Working Group which includes the teams for all instruments that take part in geologic observations with the rover. The resources used for the campaign would affect the total resources available for these instruments as well so having their approval was important to move forward. The final step was presentation to the entire rover team during a Science Discussion on a rover operations sol. This was a proposal of the campaign as well as an invitation to the team ensuring that anyone on who wished to be involved with the campaign had a chance to collaborate.

After making the rounds with proposals and presentations, the Peace Vallis campaign was given the green-light. Multiple weeks were spent on rover operations waiting for the opportunity to begin the campaign. Anytime there was an opportunity for a Peace Vallis fan observation, another analytical experiment would require the rover time and data. This continued until an extended stay at a potential drill site allowed for saturation of analytical analysis around the rover. Two observations during the campaign were aborted due to rover anomalies. The first was due to the ChemCam instrument being marked “sick” before the observation was executed. The second occurrence was due to the ChemCam pointing crossing the rover “hardstop” resulting in a complete shutdown of rover activities. This produced the abbreviated raster of ChemCam sequence CCAM05991.

Gale crater HiRISE digital terrain model:

As a result of the MSL landing site selection process and continued rover monitoring, a mosaic of HiRISE .25m/px high-resolution orbital imagery was acquired for the characterization of the local north Gale crater area. Stereo imagery processing allowed for construction of a digital terrain model (DTM) representing ~1 m/px surficial data (Fig. 15). This DTM includes most of the Peace Vallis fan system, however, there are major co-location errors and other data anomalies.

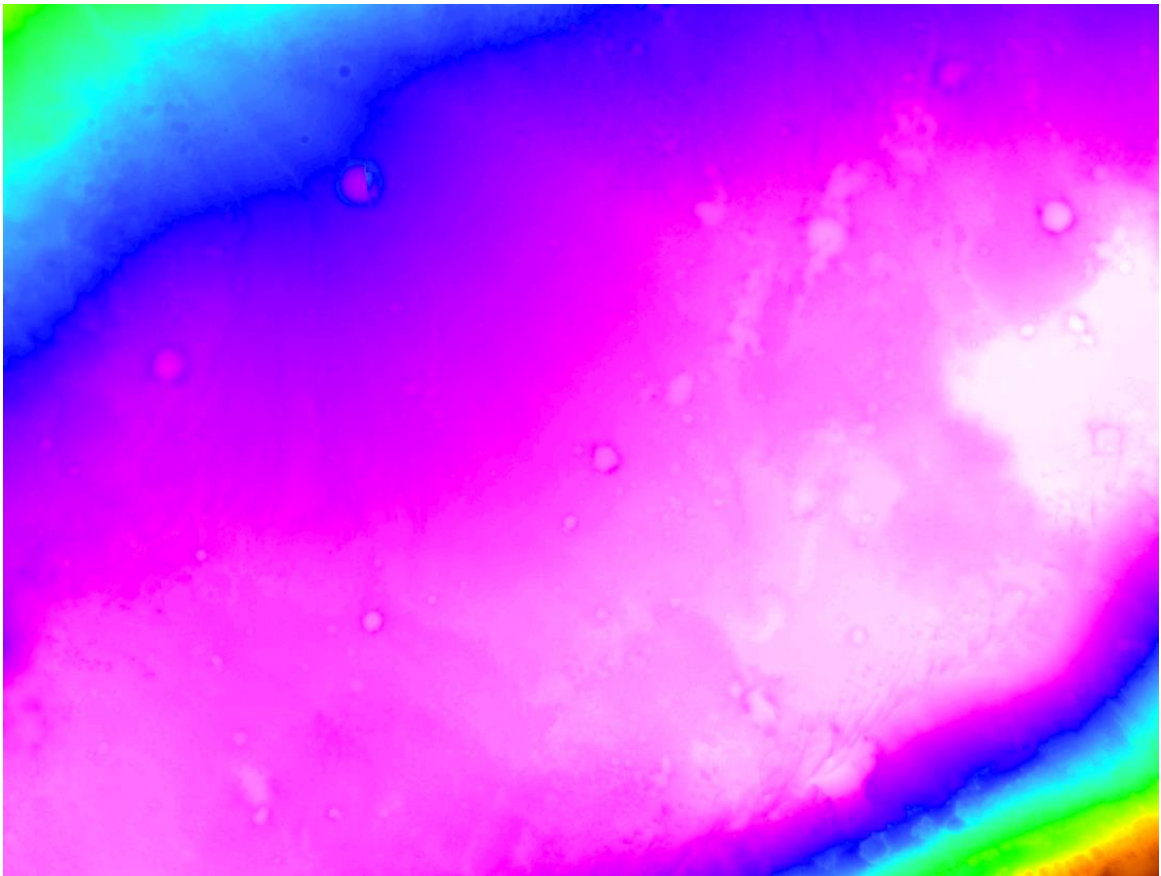


Figure 15. HiRISE DTM of the MSL exploration zone area including the Peace Vallis fan system.

Data processing

ChemCam Remote Micro-imager corrections:

The ChemCam RMI is an effective tool for imaging distant features in the area surrounding the MSL rover (Le Mouélic, 2015). Raw imagery (Fig. 16a) received from the RMI is processed through the RMI pipeline: a set of uniform adjustments performed for every image. Pipeline processed imagery contains anomalies from the camera technology and the optics (Maurice, 2009; Dufour, 2010) which were previously mitigated with manual, non-consistent correction (Figure 16b). One of the anomalies that affects the RMI is a fluctuating flat field value which varies with mirror and lens focus distance. Another anomaly is the result of light intensity varying radially within the image. This means the intensity of light is greater at the center of the image than at the edge. When viewing Peace Vallis fan and areas of Aeolis Mons, a bright halo appears at the edge of the image. This is likely due to stray-light entering the outer 3-4° of the RMI telescope boresight (Le Mouélic, 2019). The uniform corrections made to all RMI images in the processing pipeline do not provide adequate products for complete long-distance geologic/geomorphic interpretation.

The Peace Vallis campaign captured 265 individual images of the Peace Vallis fan area at varying times in the day, times of the year, and at two major atmospheric regimes. This amount and range of imagery has allowed for enhanced, automatic correction of RMI in the Peace Vallis area. Le Mouélic et al. stacked all 265 Peace Vallis images together and applied a median filter to the product. The result is a flat-field filter that when subtracted from the individual images reveals an enhanced product (Figure

16c). This process allows for more accurate visual and enhanced imagery analysis for the Peace Vallis campaign. Currently this processing technique is only effective for correcting images in the direction of the Peace Vallis fan (Le Mouélic, 2019).

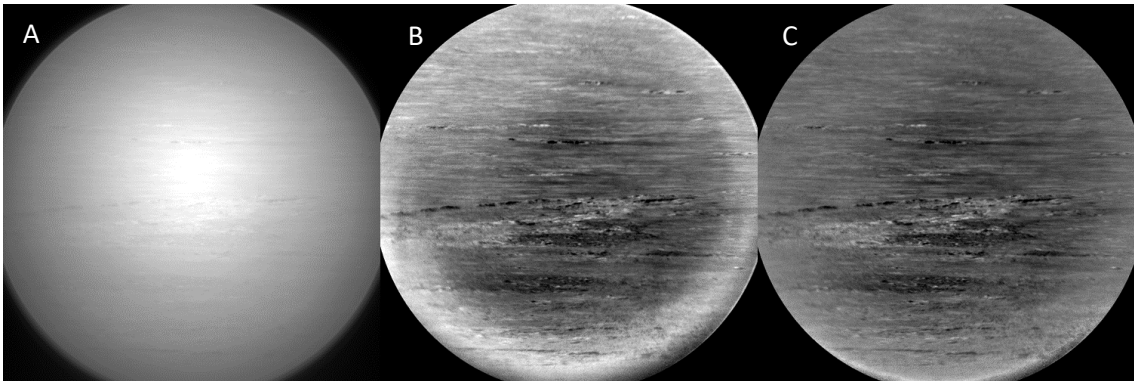


Figure 16. ChemCam long-distance RMI sequence CCAM04981. A: unprocessed, raw ChemCam RMI image. B: RMI image with the standard RMI pipeline processing. C: Peace Vallis RMI image with mean-subtracted RMI processing.

Analysis methods

Visual interpretation:

This study uses visual photo-geologic interpretation as a first order investigation method for understanding the Peace Vallis fan system. Images are analyzed and annotated based on contrast, texture, and structures observed in the frame.

Enhanced image analysis is performed as part of this study by adjusting the threshold of the imagery. For this process, each pixel in the grayscale RMI image is given a value from 0 to 255. Adjusting the maximum, minimum, and mean values will reassign pixel values in the given range. For example, adjusting the maximum from 255 to 200 will

change all the pixels with values above 200 to black and visa versa adjusting the minimum pixel value from 0 to 50 will change all the pixels with values below 50 to white. This technique is used to focus on individual units, layers, or other contrasting features.

Stereo imagery is produced by taking two images from different perspectives of the same target. This was one of the main goals of the Peace Vallis campaign 2: to re-image areas from the Peace Vallis campaign 1, compare the two together, and create stereo anaglyphs. The difference in elevation, viewing angle, and atmospheric conditions between the two campaigns does not yield valuable products; however, useful stereo anaglyphs are constructed using a single RMI image. These products allow for enhanced viewing and analysis of the RMI imagery through increased depth perspective.

GIS techniques:

This study also performs GIS techniques to illuminate the processes and products of the Peace Vallis fan system which are hidden to visual interpretation. The Gale crater HiRISE DTM is utilized as the highest resolution elevation data. Topographic profiles are created to determine differences in elevation and slope between features in the north Gale crater area.

To accurately identify the surfaces on the fan that were within line-of-sight of the RMI field of view, viewshed analysis (Fig. 17) is conducted on the Gale crater DTM from the Peace Vallis campaign imaging locations.



Figure 17. Viewshed analysis of the ChemCam long distance RMI sequence CCAM02241.

Creation of viewshed products allows for accurate recognition of features seen from HiRISE orbital imagery with features seen in the ChemCam RMI imagery (Fig 18). Annotated orbital and RMI correlations are created for context.

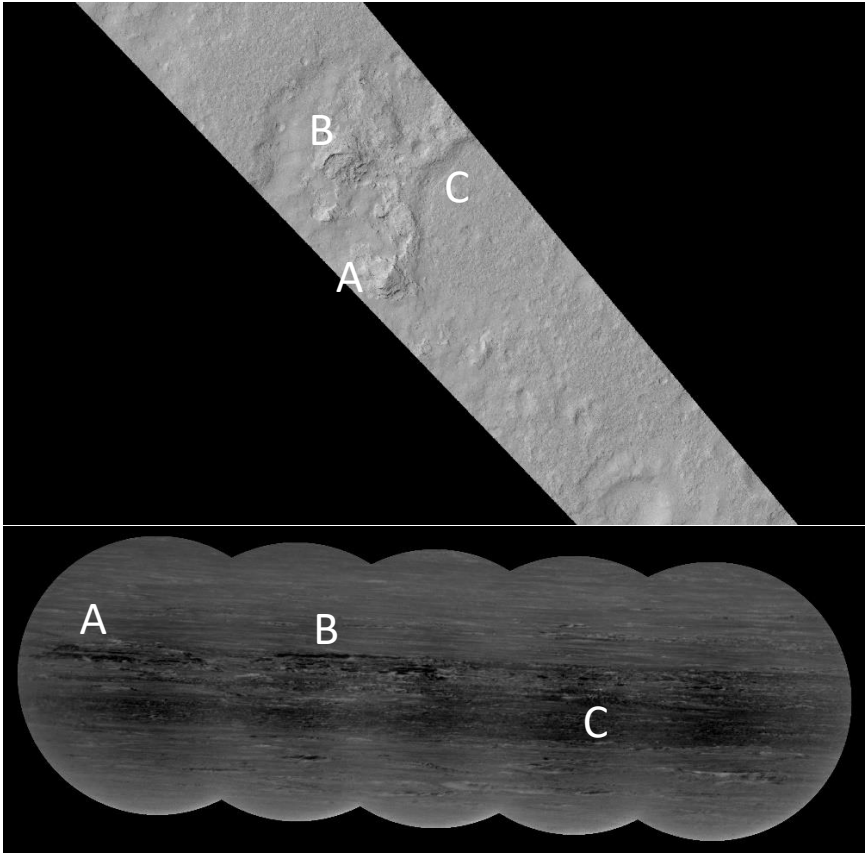


Figure 18. Correlated view of features in the ChemCam long-distance RMI sequence CCAM02241 (bottom) with orbital data (top). The field of view is ~550 m wide.

Chapter 4

Results

MSL rover results

Peace Vallis Campaign 1:

The Peace Vallis campaign 1 (Fig. 19) was conducted from sol 1237 to sol 1311. The objective of this campaign was to acquire imagery of the lateral boundaries of the fan and the fan apex. A total of 13 distinct mosaics were captured for a total of 113 individual images. Each mosaic has an RMI image spacing of 10 mrad for maximum coverage within each mosaic except for the Peace Vallis fan trench mosaic which had a spacing of 8 mrad.

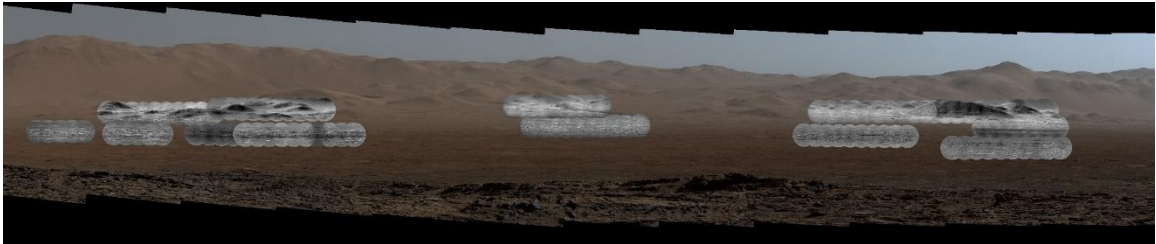


Figure 19. The Peace Vallis campaign 1: ChemCam long-distance RMI observations on a Mastcam mosaic sequence mcam06038 background.

Peace Vallis Campaign 2:

The Peace Vallis campaign 2 (Fig. 20) was conducted from sol 1927 to sol 2012. The objective of this campaign was to acquire imagery of the entire central sector of the fan from the Peace Vallis channel to the toe of the fan. A total of 8 distinct mosaics were captured with 134 individual images. Each mosaic has an RMI image spacing of 8 mrad for maximum overlap near the top and bottom of the mosaics.

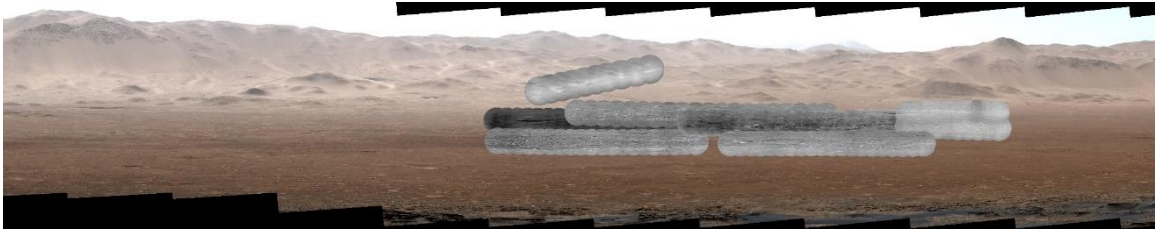


Figure 20. The Peace Vallis campaign 2: ChemCam long-distance RMI observation on a Mastcam mosaic sequence mcam10228 background.

Orbital GIS results

Topographic profiles:

Using DTM data from the HiRISE and CTX orbital instruments, topographic profiles were constructed to illustrate the elevation change between areas key for understanding the Peace Vallis fan system. The south to north topographic profile for Gale crater (Fig. 12a) shows a highly irregular crater interior with the current south crater floor standing more than 1.2 km higher than the north crater floor. The north floor of Gale crater (Fig. 21b) is a gently sloping surface from the north crater rim to the floor, with a steep rise base of Aeolis Mons. The Peace Vallis distributive alluvial fan shows $\sim 2.5^\circ$ slope down the fan (Fig. 21c). This is within the typical range for distributive alluvial surfaces. The cross profile for the Peace Vallis fan (Fig. 21d) shows a concave-down surface, with the left side of the profile more irregular and the right side more smooth. The profile of the large inverted channel running down the center of the Peace Vallis fan (Fig. 21e) shows a slope of $\sim 2^\circ$, similar to that of the Peace Vallis fan profile. A fan shaped structure (Fig. 21f) higher on the crater rim than the Peace Vallis fan has a slope of $\sim 10^\circ$ and shows two

irregularities: a dip more than halfway down representing the Peace Vallis fan trench and a bulge at the toe of the fan.

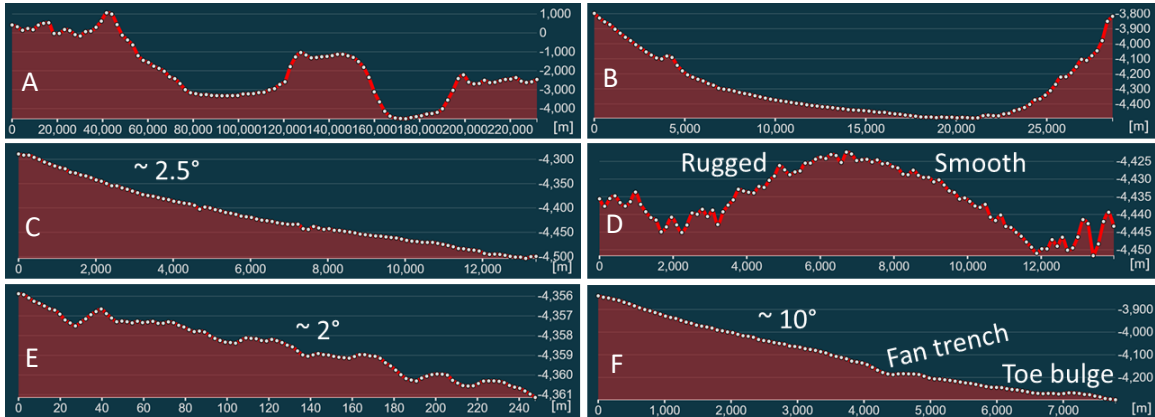


Figure 21. A: Gale crater profile from south to north showing the north-south slope of the crater and surrounding area. Also note the central mound, Aeolis Mons, which covers the Gale crater central uplift. B: North Gale crater profile from above the Peace Vallis fan to the top of the clay unit above the rover. C: Peace Vallis distributive fan down-fan profile. D: Peace Vallis distributive fan medial, cross-fan profile showing a rugged west sector and smooth east sector. E: Large inverted channel profile on Peace Vallis fan with a $\sim 2^\circ$ slope. F: Peace Vallis perched fan down-fan profile with a $\sim 10^\circ$ slope. This profile also shows the Peace Vallis fan trench and a toe bulge.

Digital terrain model analysis:

Analysis is performed on the Peace Vallis DTM to illuminate features not seen in visible imagery. By dividing the DTM values by 121 then subtracting from the original DTM, the underlying structure of the Peace Vallis fan is illuminated (Fig. 22).

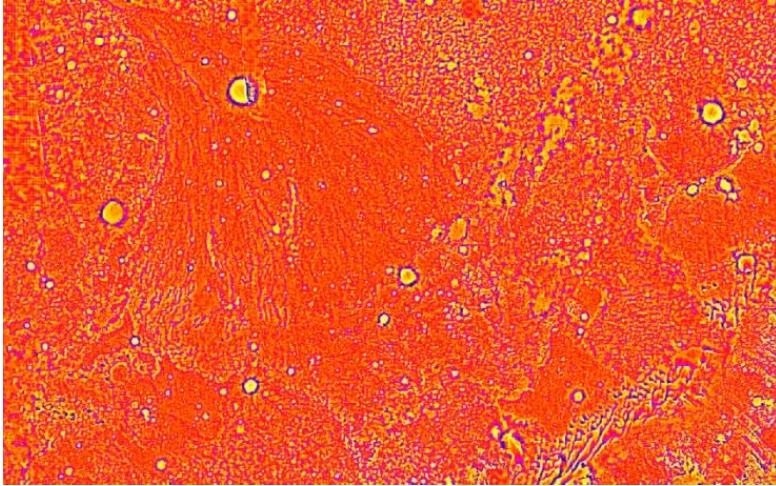


Figure 22. DTM analysis of the Peace Vallis fan area revealing the BF unit structure.

Gale crater wall layering:

Gale crater is impacted into crustal highlands terrain. The nature of the pre-impact stratigraphy is not understood as no bedding relationships have been previously observed in the crater wall. The dominant rock type of the highlands terrain is thought to be mafic volcanic and plutonic lithologies but analysis of float rocks by MSL has revealed a potentially evolved continental-like lithology (Sautter, 2015). A long distance RMI targeted at older bajada surfaces captured the crater wall in the background. After threshold adjustment distinct, horizontal layering can be observed on the crater wall (Fig. 23).

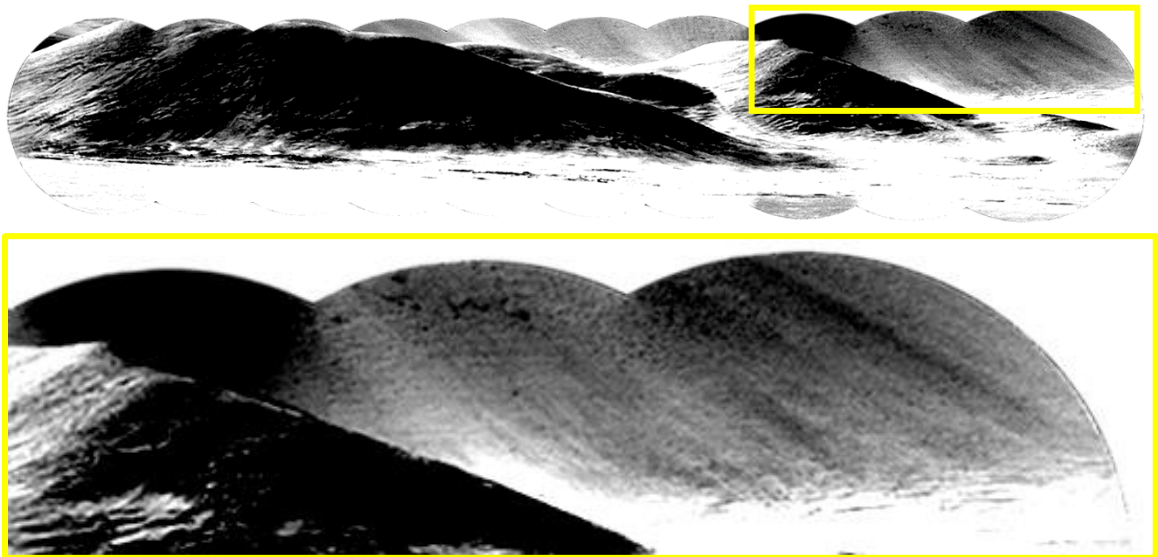


Figure 23. Crater wall stratigraphy observed in ChemCam long-distance RMI sequence CCAM04262.

Mass wasting deposits

A survey of the crater wall foothills, which are observed sporadically from the base of the crater wall extending to the crater floor, reveals no observable internal structure. Therefore, these features are likely mass wasting deposits from the crater rim/wall and not older dissected alluvial deposits. Alluvial bajada deposits skirt the foothills with fan surfaces and inverted channels flowing around them. This implies an emplacement after initial crater modification and before major alluvial bajada activity.

Inverted channels:

There are multiple examples of inverted channels on the Peace Vallis fan, mostly observed in the proximal and medial fan sections and in the left-lateral sector of the fan. These features are discontinuous and have very low sinuosity. They resemble the inverted channel features on the other, older bajada fans and are thereby from the underlying, older BF unit fan. The prominent inverted channel which runs down the central sector of the fan is captured in the long-distance ChemCam RMI sequence CCAM04981 (Figure 24).

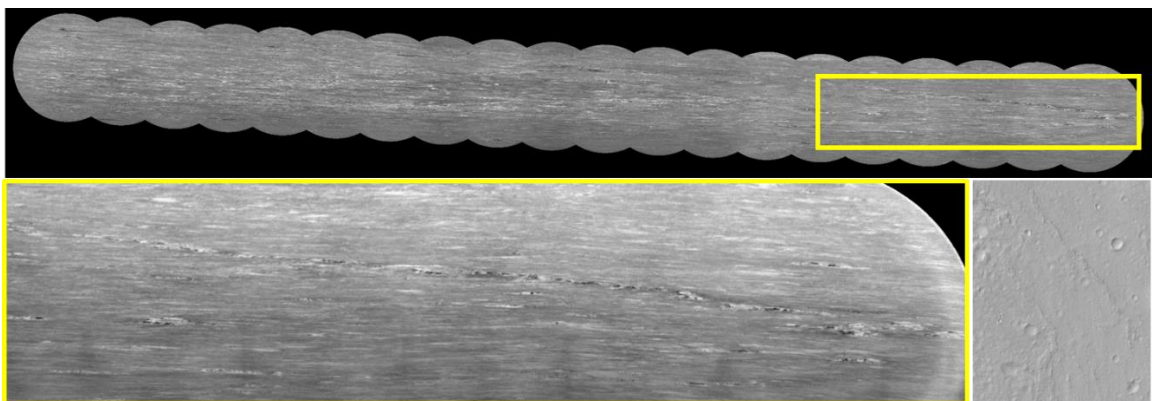


Figure 24. Inverted channel deposits on the Peace Vallis fan captured by the long-distance ChemCam RMI sequence CCAM04981 and from orbit (bottom right; ~2.5 km across).

Another possible explanation for these inverted features is a glacial eskers origin deposited on top of the Peace Vallis fan surface. Several studies (Fairen, 2014; Mège & Bourgeois, 2011) have reported potential glacial activity within Gale crater and in other equatorial regions on Mars. Eskers are discontinuous with gaps between preserved segments and have a non-planar surface. This description matches morphology of the central Peace Vallis fan inverted channel. This is an unlikely origin for the inverted channels as there are no other local glacier indicators e.g. glacial valleys, moraines, or scour marks. Alcoves in the crater rim are seen on the north and northwest facing surfaces. These features are potentially glacial in origin.

Relict alluvial deposits:

There are clear examples of relict fan deposits of the paleo-fan surface now outcropping above the current fan trench surface (Fig. 25). These deposits are older alluvial surfaces that have been incised by the Peace Vallis fan trench and abandoned ~37 m above the current trench floor. Individual layers within these deposits are observed to be laterally continuous for at least 2 km. The origin of these deposits is likely incised proto-Peace Vallis fan deposits or incised retrogradational deposits from the current Peace Vallis fan.

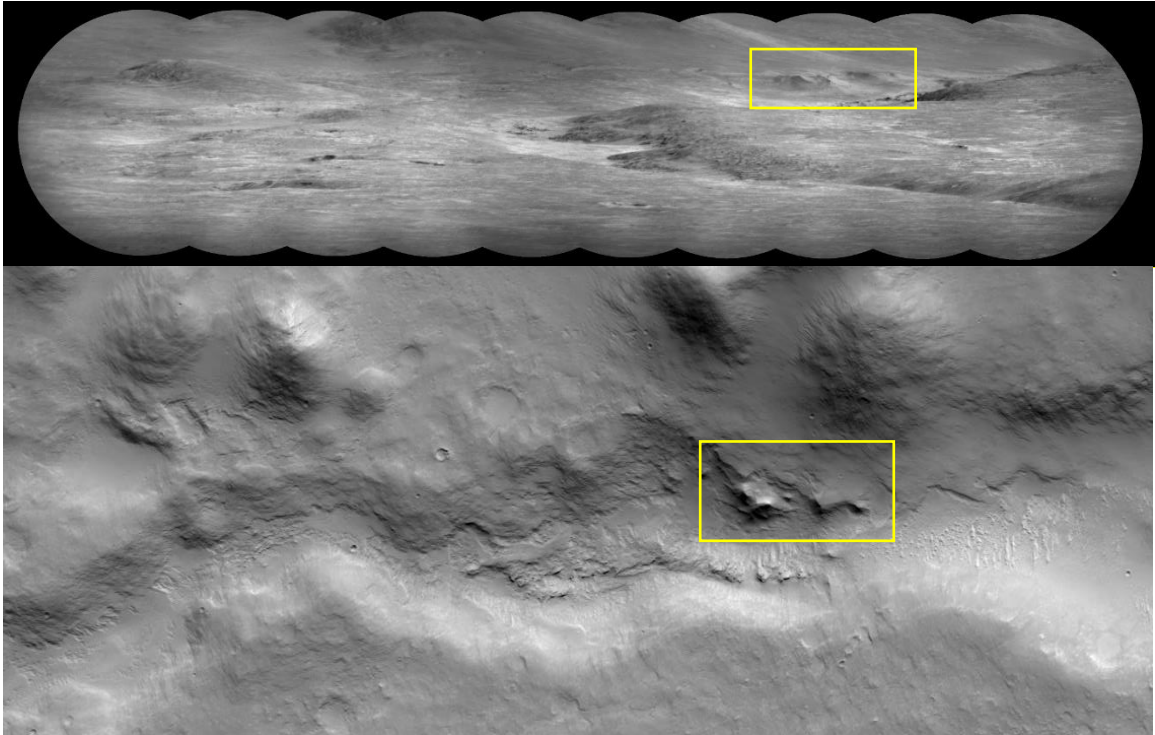


Figure 25. Top: abandoned alluvial deposits captured by the ChemCam long-distance RMI sequence CCAM04300. Bottom: HiRISE orbital view of the abandoned deposits. The yellow box outlines the features in each image and represents ~600 m across in the lower image.

Other relict alluvial deposits exist near the western contact of the AF and BF fan units. These features have two potential origins: 1) resistant inverted channels with the fan surface eroded around them or 2) fan surfaces which have been incised by fluvial flow and abandoned above the surrounding fan surface. The orbital result in Figure 29 showing the underlying DFS nature of the Peace Vallis fan gives evidence for these relicts as inverted channels. Other geomorphic features of DFS can include inactive islands and bars which are incised by current fluvial channels (Davidson, 2013). This geomorphic product would suggest these relicts are not inverted channels.

Peace Vallis perched fan:

Another fan feature has been identified coming from the Peace Vallis alcove system (Fig. 26). This perched fan is located above the known Peace Vallis fan with the fan apex ~6 km away from and ~475 m higher than the Peace Vallis fan and the apex. The toe of the fan extends to the apex of the Peace Vallis fan. This perched fan resembles the AF unit of the Peace Vallis fan in both texture, brightness, and crater density implying a surface younger than the BF unit. Thermal emission measurements from the TES instrument of the Mars Global Surveyor orbiter confirm the shape of the feature as well as the link to sediments similar to the AF unit on the Peace Vallis fan (Figure 26).

This fan also displays a bulge at the toe, potentially indicative of subaqueous slumping due to the overpressure of Gale lake (Postma, 1984). The Peace Vallis river is thought to have deposited sediment into Gale lake through hyperpycnal flow (Stack, 2018) due to lake chemistry and temperature. This flow regime would support the deposition fines in a subaqueous fan. Other subaqueous fans have been observed in a lacustrine environment on Mars (Metz, 2009).

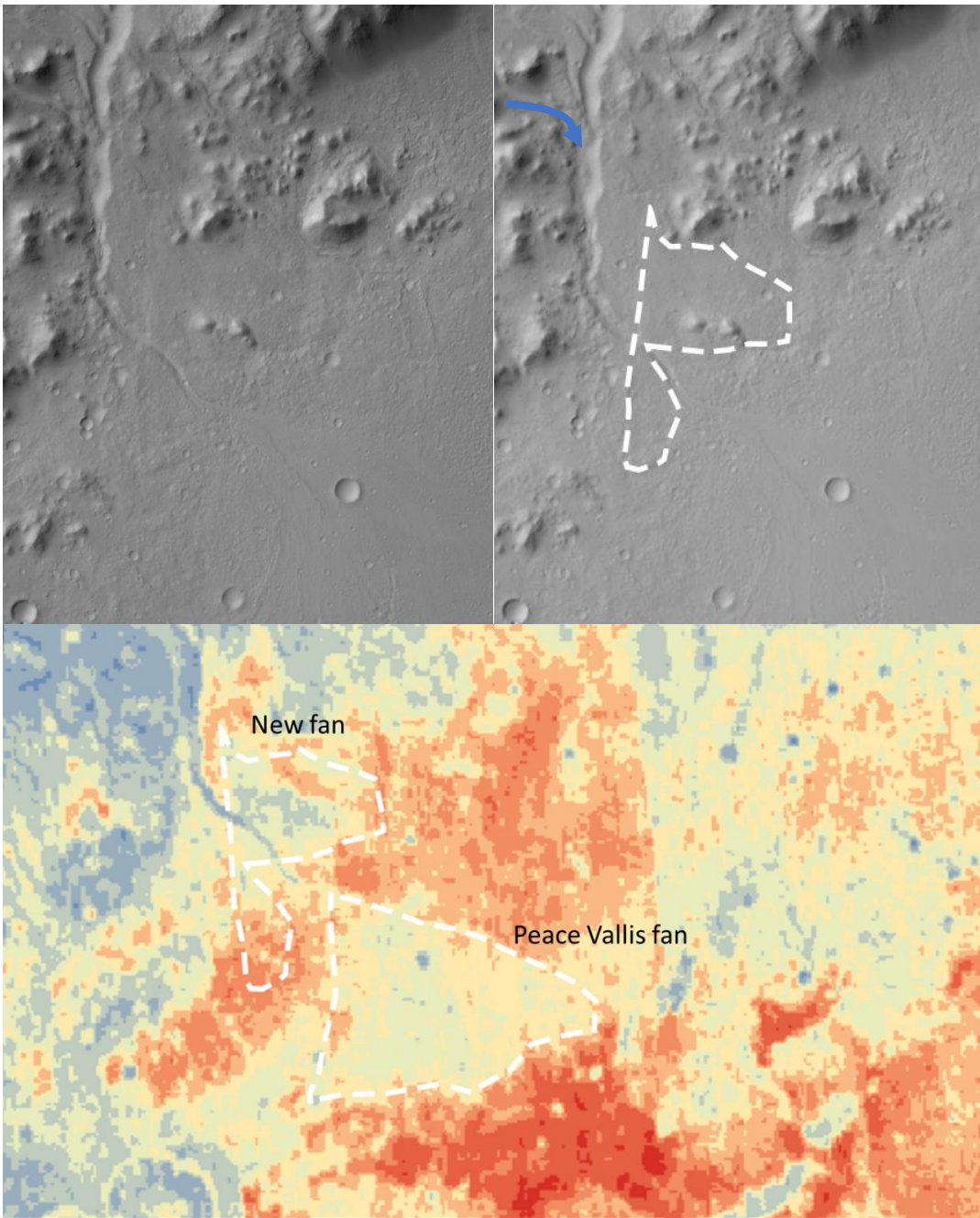


Figure 26. Top: A newly recognized fan structure perched above the Peace Vallis fan. The blue arrow indicates a newly activated channel which caused a dam in the Peace Vallis channel. Bottom: Thermal inertia view of the perched fan and Peace Vallis fan area.

The toe of the perched fan was imaged in a long-distance RMI on Sol 1300 (Figure 27). The bottom right corner shows the sloping layers of the lateral edge of the fan. The fan was then incised by subsequent flow in the Peace Vallis fan trench. This means the perched fan is not the absolute youngest system in the area since it is bisected by the Peace Vallis fan trench. The other alternative is that the systems may be subaerial and active concurrently with the Peace Vallis fan. A landslide dam is observed in the Peace Vallis channel just above the apex of the perched fan. The dam was caused by the activation of a new channel draining into the Peace Vallis alcove from the newly discovered western watershed (Newsom, 2019). This forced water and sediment bound for the Peace Vallis fan to flow outside the channel and deposit at the location of the new fan.

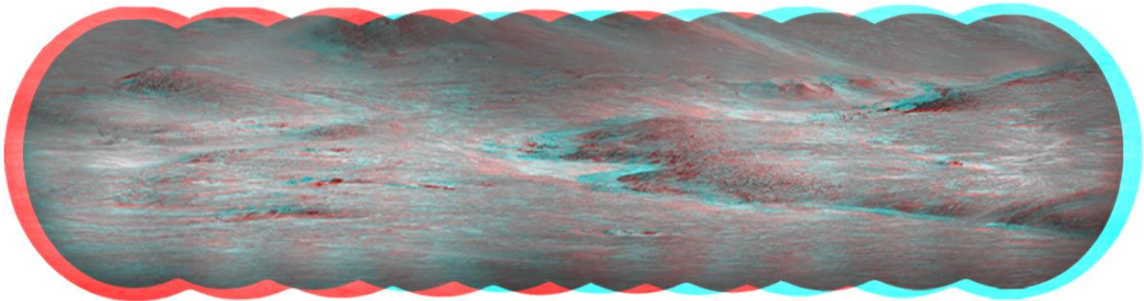


Figure 27. Stereo anaglyph of long-distance ChemCam RMI sequence CCAM04300 with dipping layers of the perched fan above the Peace Vallis fan (bottom right).

Remnant shoreline deposits:

The paleo-lake of Gale crater has been a focus of study since the identification of Gale as a potential landing site for the MSL rover (Anderson & Bell 2010; Golombek, 2010). Assessing the lake level has been accomplished so far by using stratigraphic relationships of lacustrine facies from orbit and with the observations made by the rover.

Terrestrial paleo lake levels are recorded in shore line erosion deposits (Baedke, 2005) due to a process of beach ridge formation and preservation (Johnston, 2007). This study shows lake shoreline deposits on the foothills of the crater floor (Fig. 28). These sets are observed running continuously for >2 km and are ~1-6 m thick. The crater wall layering in Figure 22 may also be recording the paleo-shoreline.

These bedding sets may also be the result of retreating alluvial surfaces which reveal the internal layering of a fan. The uniform periodicity of these potential alluvial layers could record seasonal (Kite, 2013) precipitation and/or melting of ice/snowpack in the watershed producing sheetflood-like flows. This explanation is less probable due to the lateral extent of the individual layers. A single layer can be traced multiple kilometers and the sets have uniform periodicity similar to terrestrial, lacustrine shoreline deposits. The layering is also observed up to 100 m above the current alluvial surface.

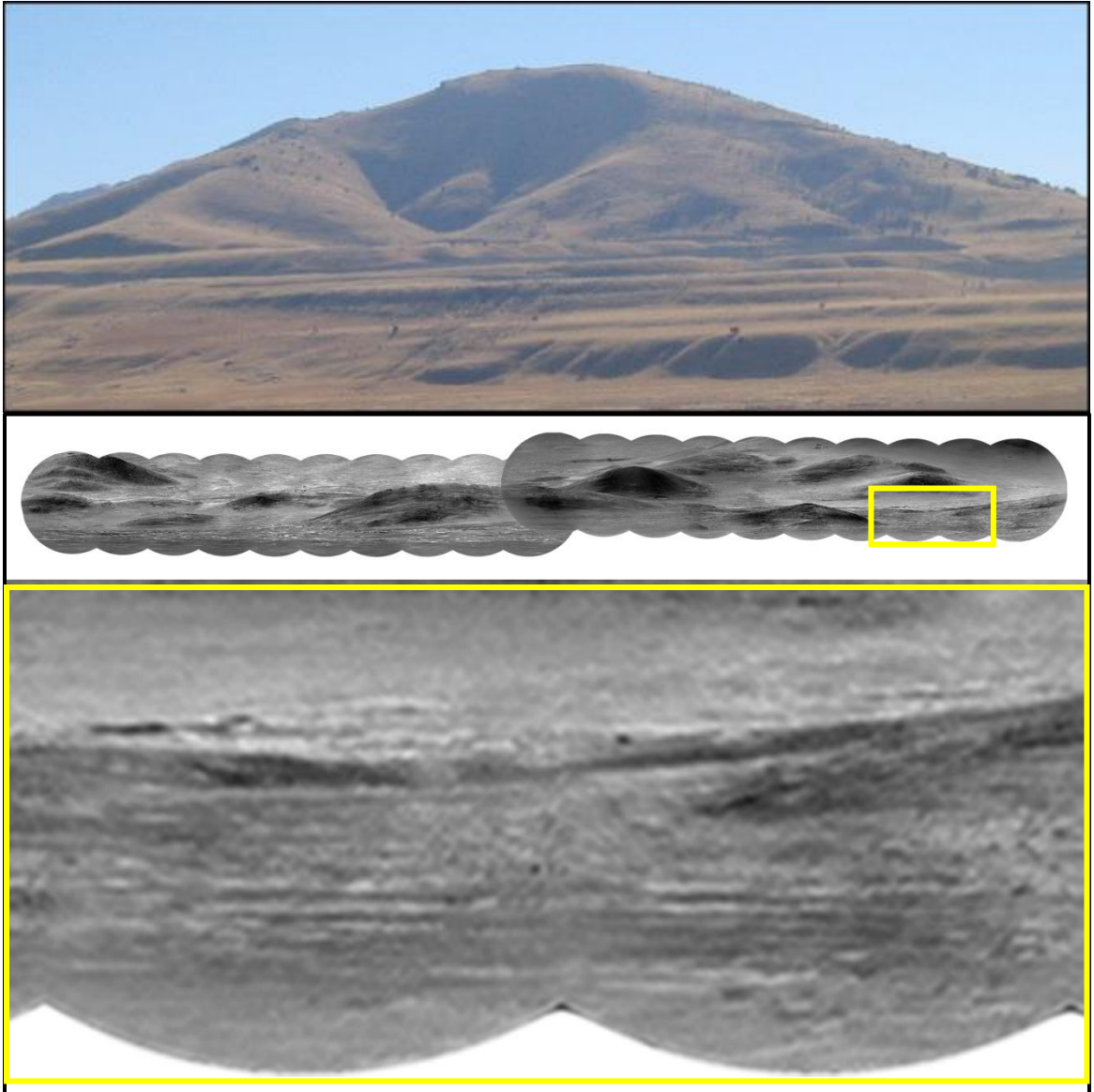


Figure 28. Top (from: Chan, 2011): Paleo-shorelines recorded in Lake Bonneville deposits. Bottom: ChemCam RMI shoreline context image and inset zoom-in within Gale crater.

Nature of the BF fan unit:

In the left-lateral sector of the medial-distal fan deposits, the BF fan displays relict alluvial deposits with laterally continuous, outcropping beds. These beds are observed to continue for 100s of meters and stratigraphically correspond to beds 1000s of meters away. These forms are likely distal inverted channel deposits but may also represent overbank

deposits with the channel deposits eroded out (Davidson, 2013). Where the BF fan is not obscured by the AF fan unit in the central and right-lateral sectors of the fan, it is shown to outcrop in laterally continuous beds perpendicular to fan flow direction (Fig. 29). This suggest a more well-preserved BF fan under the AF fan deposits.

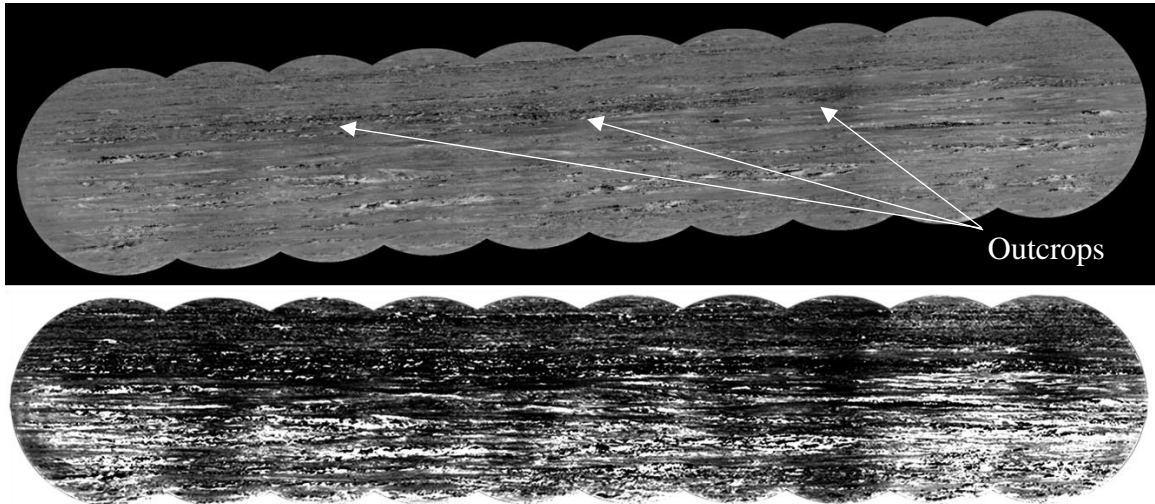


Figure 29. Top: outcrops on the of the BF unit observed in ChemCam long-distance RMI sequence CCAM03271. Bottom: threshold adjusted product from CCAM03271 accentuating the lateral continuity of the outcrops.

The BF fan unit underlies the AF fan unit on the east side of the proximal and medial fan deposits. The AF unit shielded the BF unit from aeolian and fluvial erosion in this area since the ~1.6 Ga (Grant, 2018) AF unit formation. Figure 22 shows the structure of the BF fan to resemble the DFS model with a type 1 braded and bifurcating depositional pattern.

Nature of the AF fan unit:

The AF unit does not represent deposition by a DFS but rather a late-stage (Grant, 2018) sheetflow fan surface. This deposit is a fine grained, undulating surface with little observable structure mantling the underlying BF unit topography (Fig. 30). There is no significant lateral continuation of layers or observable outcrops of this material.

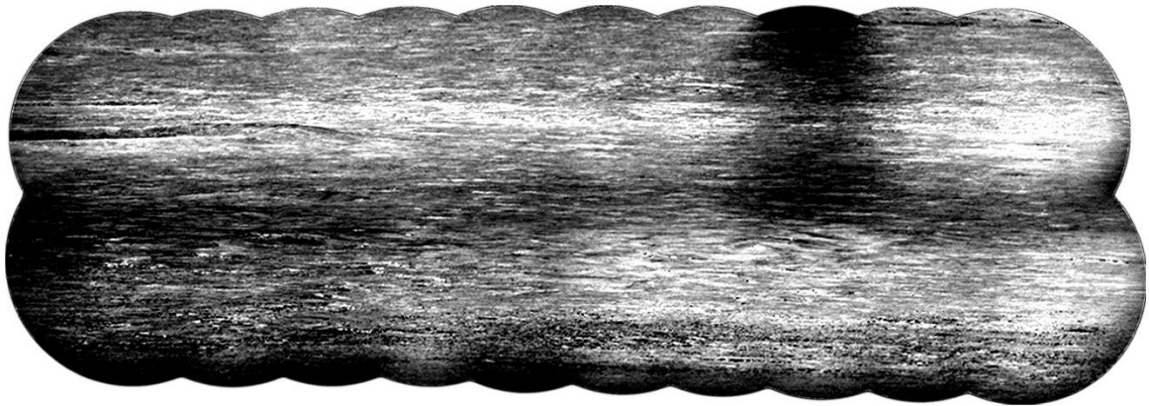


Figure 30. Threshold adjusted image of ChemCam long distance RMI sequence CCAM02011 which shows the undulating, discontinuous surface of the AF fan unit in the middle and the outcropping, semi-continuous BF fan unit at the bottom.

Groundwater sapping channels:

One of the most intriguing findings to come from analysis of the RMI images is the confirmation of proposed groundwater sapping channels on the Peace Vallis fan (Scuderi, 2019). The western scarp of the sapping channel is observed in RMI sequence CCAM04981 (Fig. 31). It is a sharp, continuous feature not heavily eroded or dissected. This preservation state adds to the evidence for a ~1.6 Ga channel formation. The RMI also observes the wide, flat-bottomed nature of these channel features with steep parabolic sides, confirming the groundwater sapping origin. The right side of the channel is obscured

by an inverted channel which bounds the eastern side of the sapping channel. The inverted channel is irregular and eroded confirming an older origin.

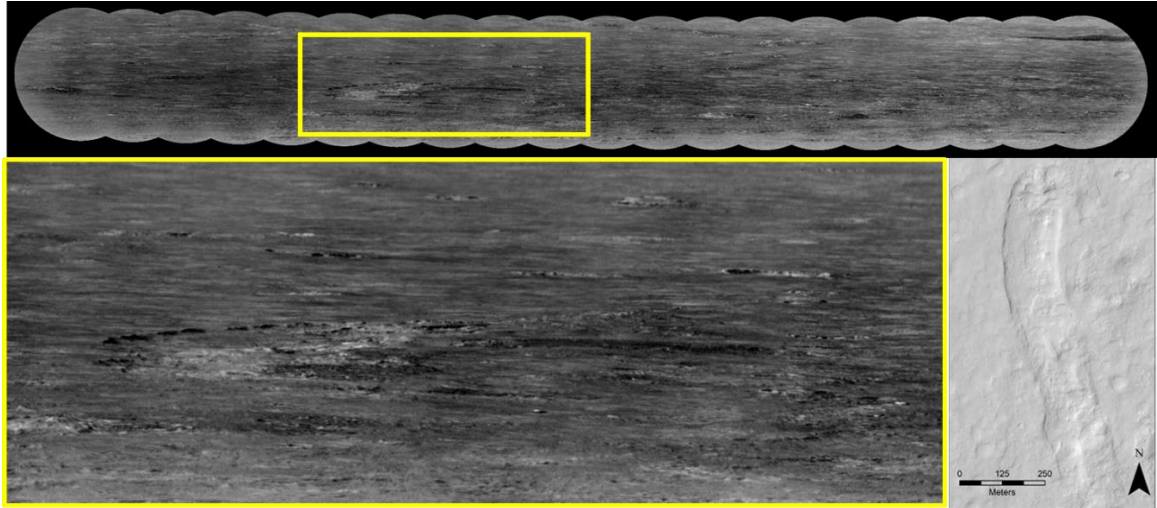


Figure 31. Top, bottom-left (inset): groundwater sapping channel observed by the ChemCam RMI sequence CCAM041981. Bottom-right (from: Scuderi, 2019): HiRISE DTM hillshade product.

MSL stratigraphic column comparison:

The MSL rover acquires detailed, frequent measurements of the areas surrounding the rover along the traverse utilizing its analytical instruments and cameras. This has produced a stratigraphic column for a ~380 m section within Gale crater (Fig. 32). Comparisons of the MSL stratigraphic column and the Peace Vallis fan system provide insight into the deposition of the units along the rover traverse.

The lowest elevation deposits recorded by the rover were at the Yellowknife Bay waypoint. This area contained successions of conglomerates (Williams, 2013), sandstones,

and mudstone and has been labeled a fluvio-lacustrine environment (Grotzinger, 2014). This study finds it probable that these units represent a progradational DFS distal deposits from the crater rim with ephemeral lacustrine mudstones interbedded. The profile from the apex of the Peace Vallis perched fan to the Clay unit (Fig. 21b) illustrates a complete alluvial surface with the Yellowknife Bay units representing the distal alluvial/fluvial deposits from the Peace Vallis alluvial system.

The rover entered the Clay bearing unit after Sol 2300 when it descended the Vera Rubin Ridge at -4143 m elevation. This unit signifies a lacustrine depositional environment. This is ~100 m elevation above the Peace Vallis DFS apex. The elevation of the highest clay/sulfate signatures is -3600 m elevation. The Peace Vallis perched fan has an apex elevation of -3810 m. This stratigraphic relationship gives indication of a subaqueous deposition of the Peace Vallis perched fan. Evidence exists for primarily hyperpycnal flow from the Peace Vallis river including a 13 m section of thinly-laminated mudstone and lake salinity predictions (Stack, 2018). The clay unit represents hypopycnal flow of wash load and suspended load sediments from the crater rim transported to the southern lake shore by dominant wind currents and local atmospheric turbulence within the crater.

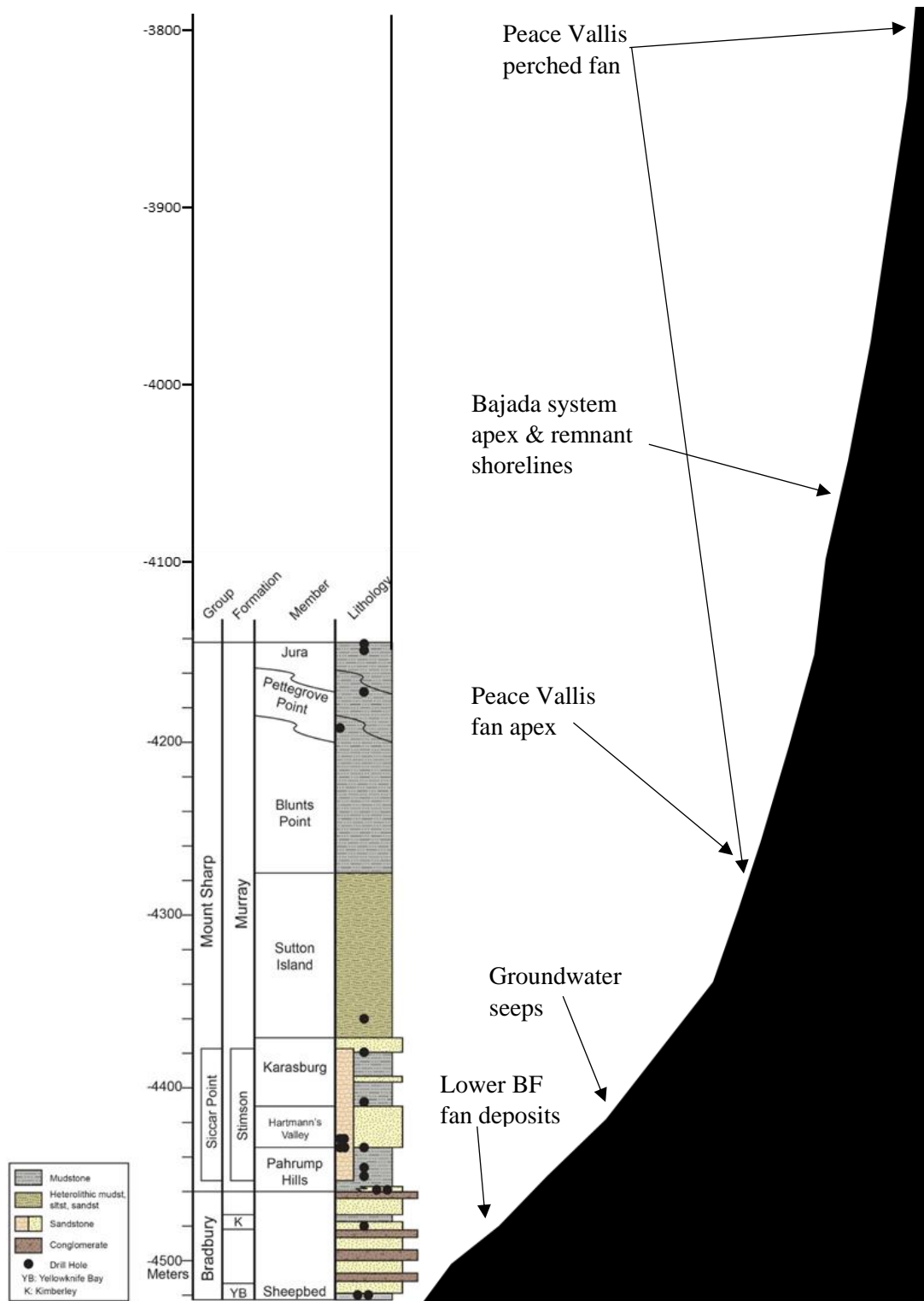


Figure 32. Left: Stratigraphic column for the traverse of the Mars Science Laboratory. Right: Vertically exaggerated profile of the Peace Vallis alluvial system aligned by elevation with the rover stratigraphic column to show correlation to the materials observed along the traverse

Gale crater wall bajada:

The relative timing of the bajada which covers sections of the interior wall of Gale crater can be interpreted by mapping crosscutting relationships and superposition of the fan deposits (Fig. 33). The fan surfaces and inverted channel features are seen overlapping and abutting adjoining fans. A fan surface covered by other fan deposits is older than the overlying fan. In some cases, inverted channel deposits are seen crosscutting other inverted features from another fan. An entire fan sector or a single fluvial channel may become inactive while the remaining fan surface is active. This is the only caveat for these timeline approximations.

The Peace Vallis bajada system displays evidence for no less than three individual fan structures. The first fan formed was the fuchsia colored fan observed through its inverted channel features continuing below the yellow colored fan and overlapping of the beige fan onto the surface. The Beige fan is incised by the Peace Vallis fan trench suggesting that the yellow fan is younger, though they may also be concurrent.

The bajada fan system in northeast Gale consists of at least seven individual overlapping fan systems sourced from individual channels dissecting the crater wall. The youngest possible fans by stratigraphic relationships are the green, orange, and violet fan surfaces which are not overlain by other fan deposits. Nothing can be inferred regarding their relative ages to one another because there are no observed relationships between these youngest fans. The next oldest possible fans are the red and royal blue fan surfaces. These fans are overlapped by the orange and violet fans making them stratigraphically older. The

next possible age is the light blue fan surface which is overlapped by the royal blue fan. The oldest fan observed in this system is the dark purple fan surface which is not observed overlying any other fan deposits. The navy blue and burgundy fans are isolated with no contact to other fan features and therefore can only be mapped.

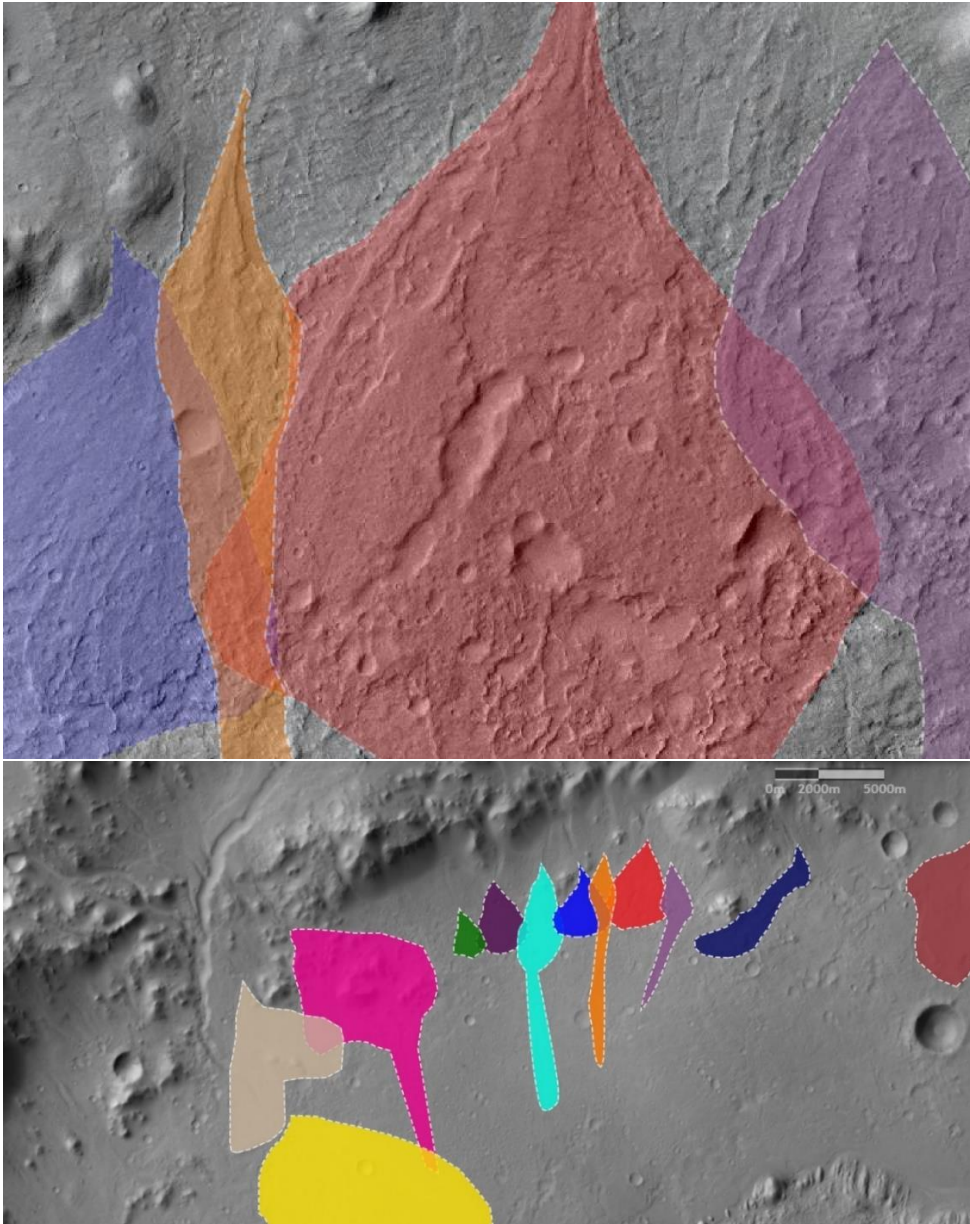


Figure 33. Top: a section of the Gale crater alluvial bajada in the north-east quadrant of the crater. Bottom: a map of the temporal evolution of the bajada in this area.

Conclusions:

Detailed analysis of the Peace Vallis alluvial system reveals a more complex history of deposition and modification than previously determined. This new understanding represents multiple stages of evolution through multiple climatic environments in Mars' history (Fig. 34).

- Initial crater modification after impact produced the bowl-shaped surface of Gale crater with a deep-sourced central peak. This is thought to occur during the Late Noachian to Early Hesperian era. Previous work suggests the lower section of the central mound, Aeolis Mons, was emplaced before the crater was breached by fluvial activity (Irwin, 2013).
- Deposition of early alluvial fans on the Aeolis Palus surface was likely groundwater-sourced through the crater rim. These deposits are likely eroded beyond recognition or covered by subsequent alluvial features.
- The Gale crater bajada lies on the crater modification mass-wasting slopes. The bajada contains fan systems that are relatively small and simple, likely due to small crater rim alcove watersheds. A succession of westward younging within the Peace Vallis alcove bajada system is observed in crosscutting relationships and superposition of the fans. A preliminary timeline is also understood for the DFS activity in the north-east Gale crater wall bajada.

- The Peace Vallis fan system consists of the BF and AF geologic units. The underlying BF fan unit is the oldest visible deposit in the Peace Vallis fan. The unit is rugged and irregular. It comprises an eroded network of inverted channel features deposited by the DFS transporting sediments down-fan. This unit was later modified by lacustrine, fluvial, and aeolian erosion. The BF unit floor continues downslope after the disappearance of the inverted channels. The floor is unconformably topped by Aeolis Palus deposits on the west side of the fan system but can be observed on the right-lateral sector extending to the Yellowknife Bay alluvial formation observed *in-situ* by the MSL rover.
- The Peace Vallis fan system was then modified over the next ~1.5 Ga by mostly dry climate, aeolian erosion and modification in the Late Hesperian and Early Amazonian.
- Around ~1.6 Ga (Grant, 2018) a punctuated climate event reactivated the Peace Vallis system with a deposit of fine-grained, mantling AF unit fan material. From rover view the unit appears undulating with no continuous layering. This unit is sourced from the accumulation of windblown dust and other unconsolidated sediments within the watershed. Well preserved strandlines are observed in several ChemCam RMI mosaics suggesting a late stage lacustrine environment at this time. As the climate event subsided, the flow of sediment rich surface water was reduced to groundwater flow. This led to the formation of the groundwater sapping channels at the fan springline (Scuderi, 2019).

- The newly discovered perched fan above the Peace Vallis fan represents either a high-water level, subaqueous fan depositing fine sediments from the watershed into Gale Lake or an avulsion of the Peace Vallis channel during deposition of the AF fan. Evidence for the former comes from stratigraphic comparison with the lacustrine deposits on the MSL traverse route. Evidence for the latter is the channel plug observed in the Peace Vallis channel above the new fan apex. Crater count statistics are necessary to determine the age of this fan.
- The Peace Vallis fan system was then modified by dry-climate, aeolian erosion and modification producing the present-day form.

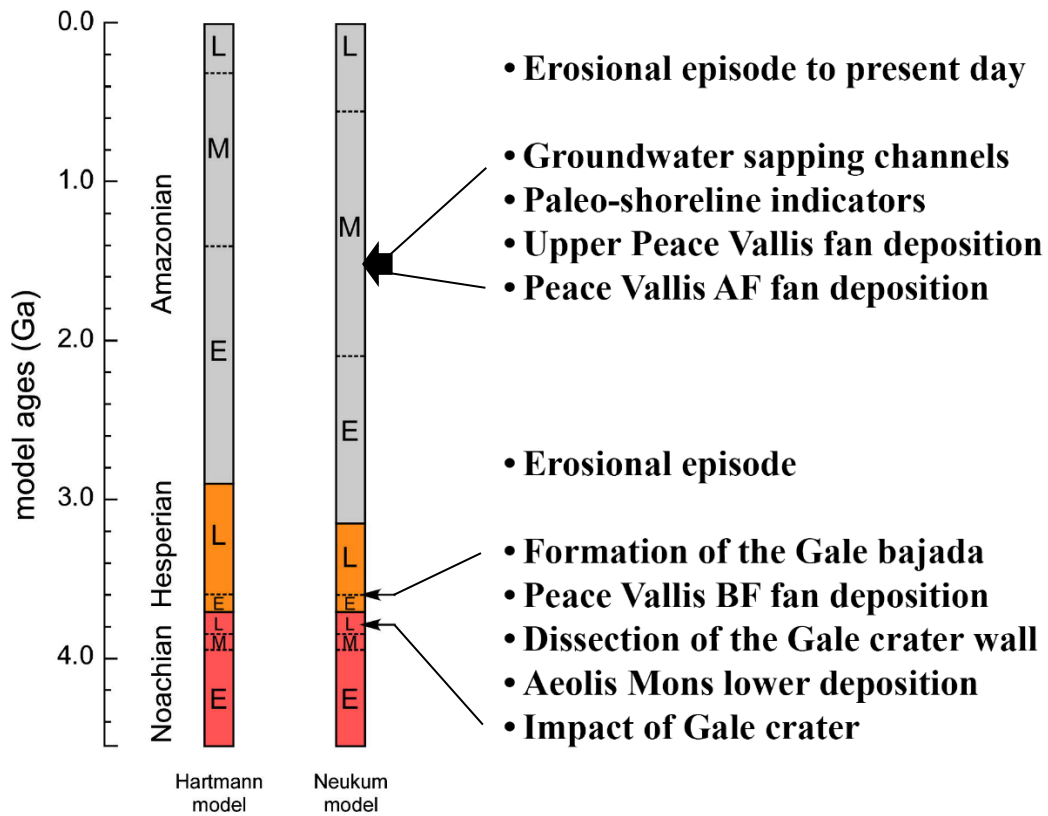


Figure 34 (modified after: Thompson, 2013). Geologic timescale of Mars annotated with important events within Gale crater.

Appendices

Appendix A: Observations and products from the Peace Vallis campaign 1.

Included for each RMI observation in this section are:

- High-level description of the ChemCam RMI image
- Regional RMI context image
- RMI context image
- RMI image
- Threshold adjusted RMI image to accentuate key features
- Stereo anaglyph RMI product

Appendix B: Observations and products from the Peace Vallis campaign 2.

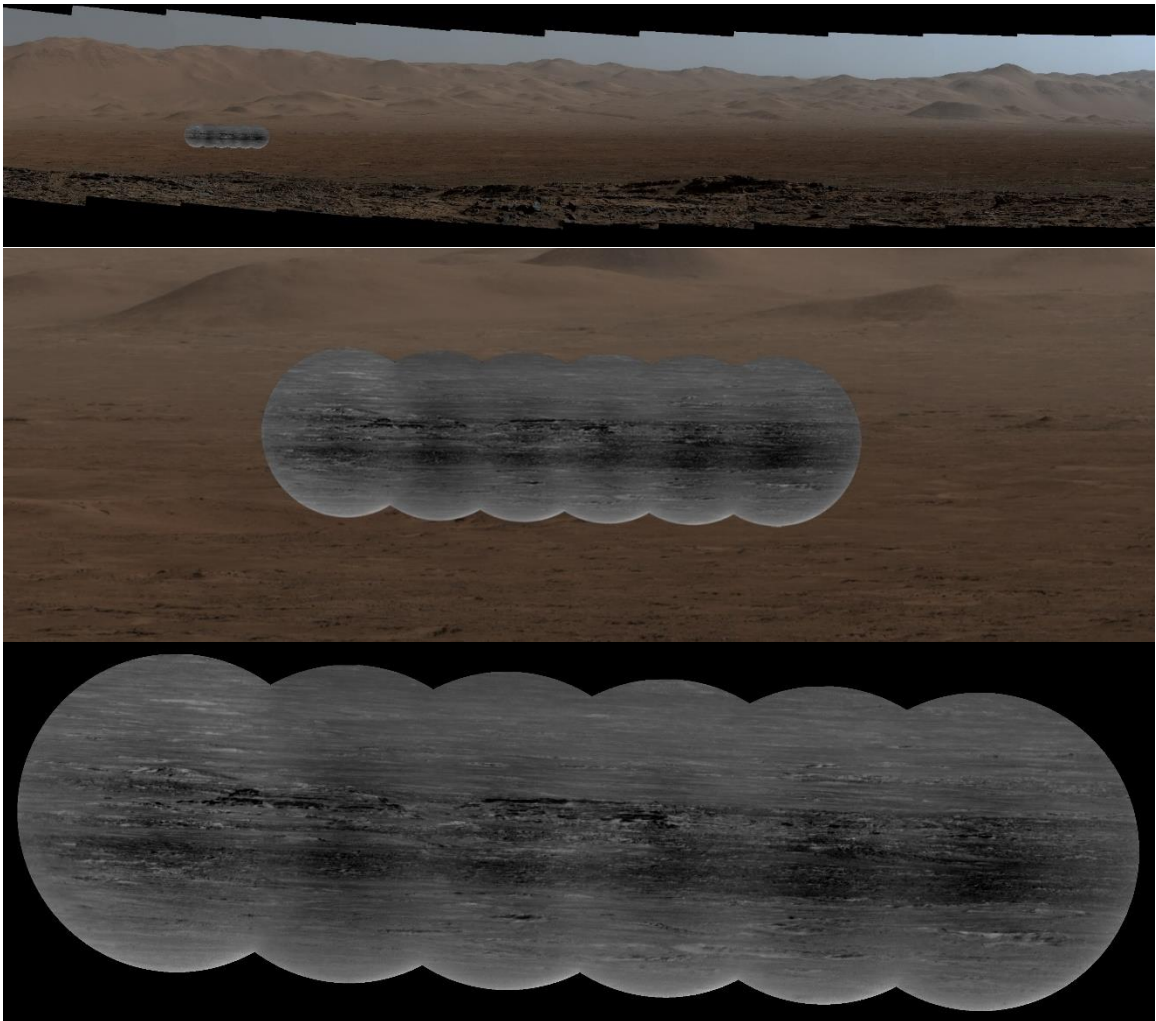
Included for each RMI observation in this section are:

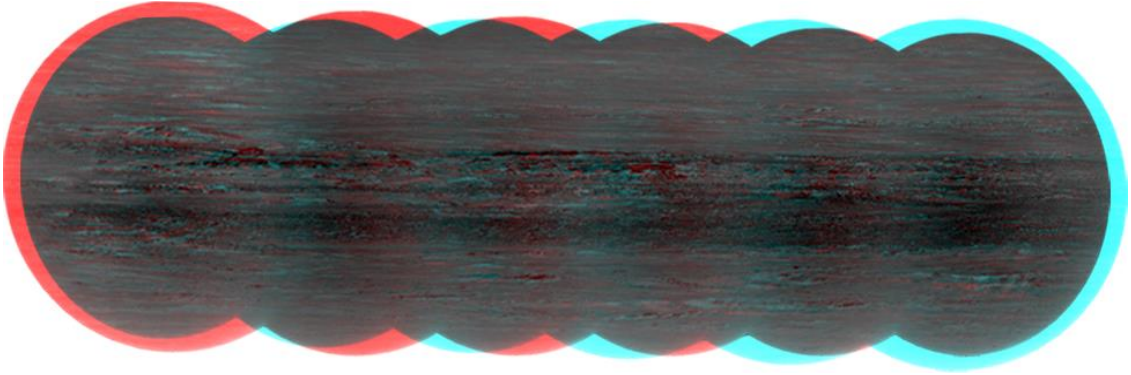
- High-level description of the ChemCam RMI image
- Regional RMI context image
- RMI context image
- RMI image
- Threshold adjusted RMI image to accentuate key features
- Stereo anaglyph RMI product

Appendix A: Observations and products from the Peace Vallis campaign 1.

Sol 1241

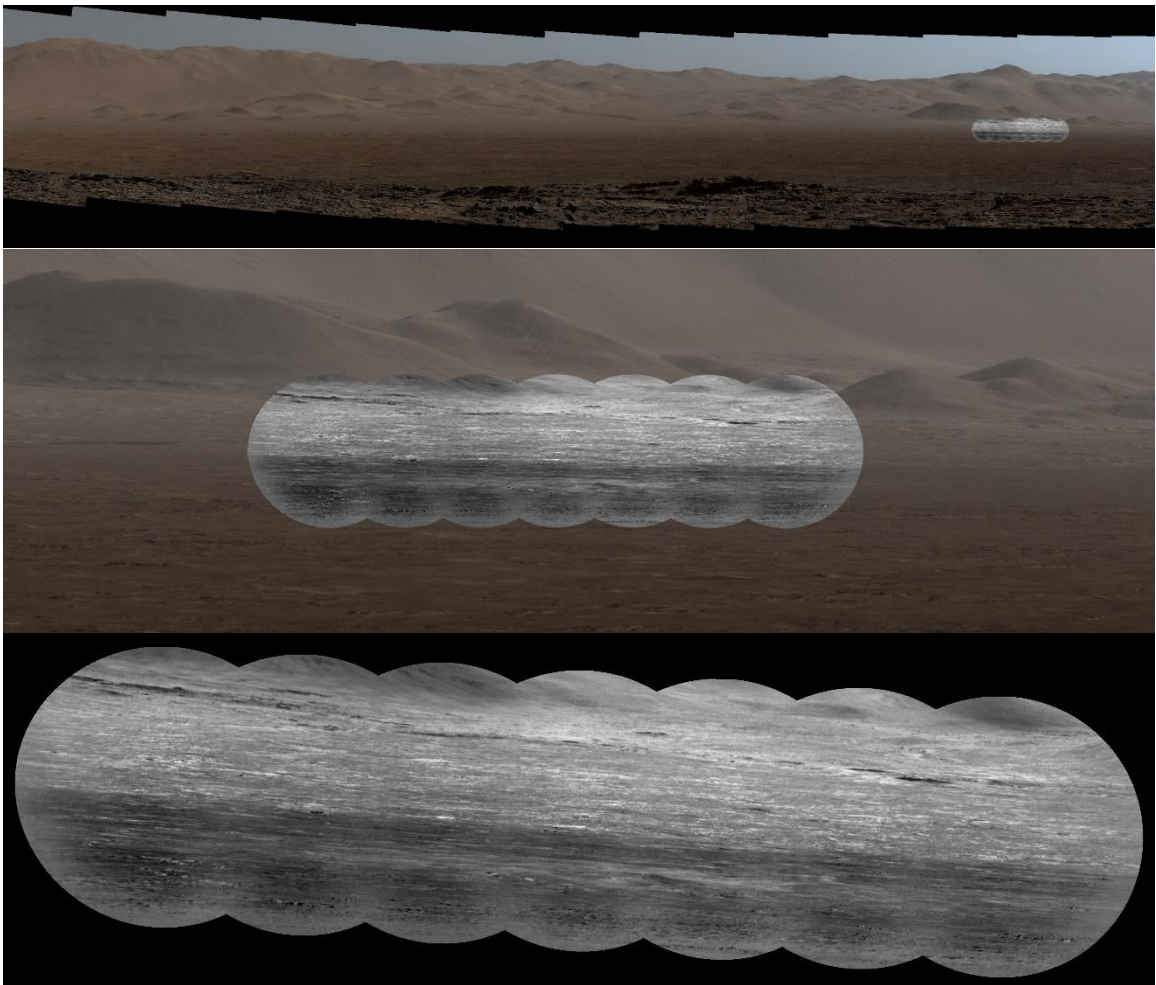
A six-frame mosaic was acquired on Sol 1241 in the ChemCam sequence CCAM02241. The left-most frame is taken from the Sol 1237 test image as this mosaic was a continuation of that observation. This mosaic captures an area in the distal, west-lateral edge of the fan. Several prominent outcrops of the same stratigraphic elevation can be seen protruding above the surrounding surface across the center of the image. These outcrops represent deposits associated with the BF fan unit.

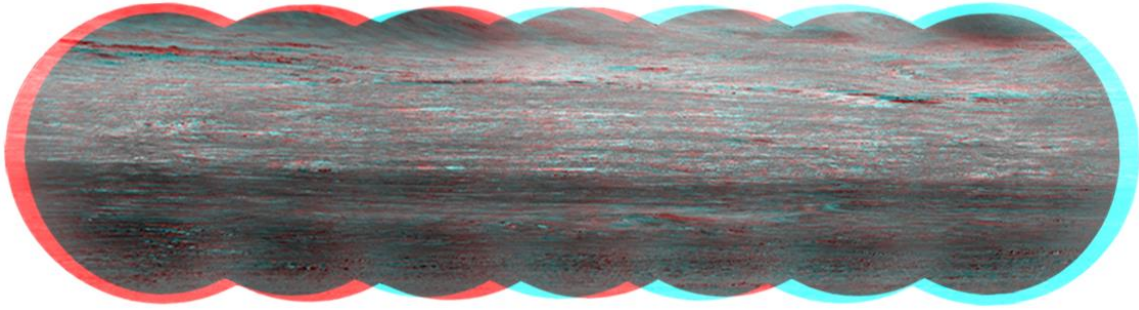
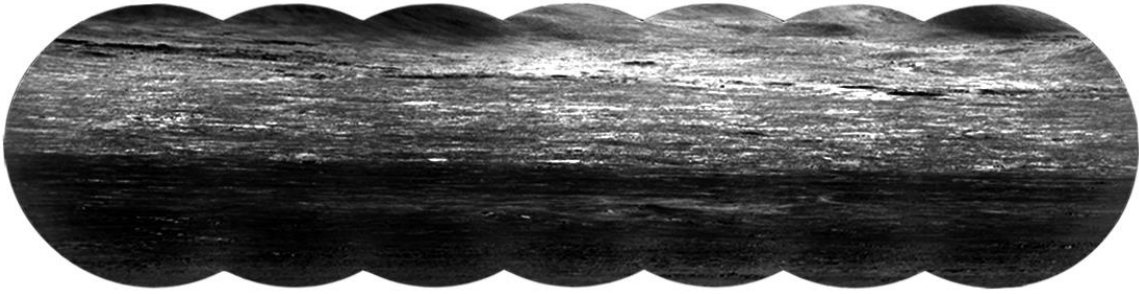




Sol 1251

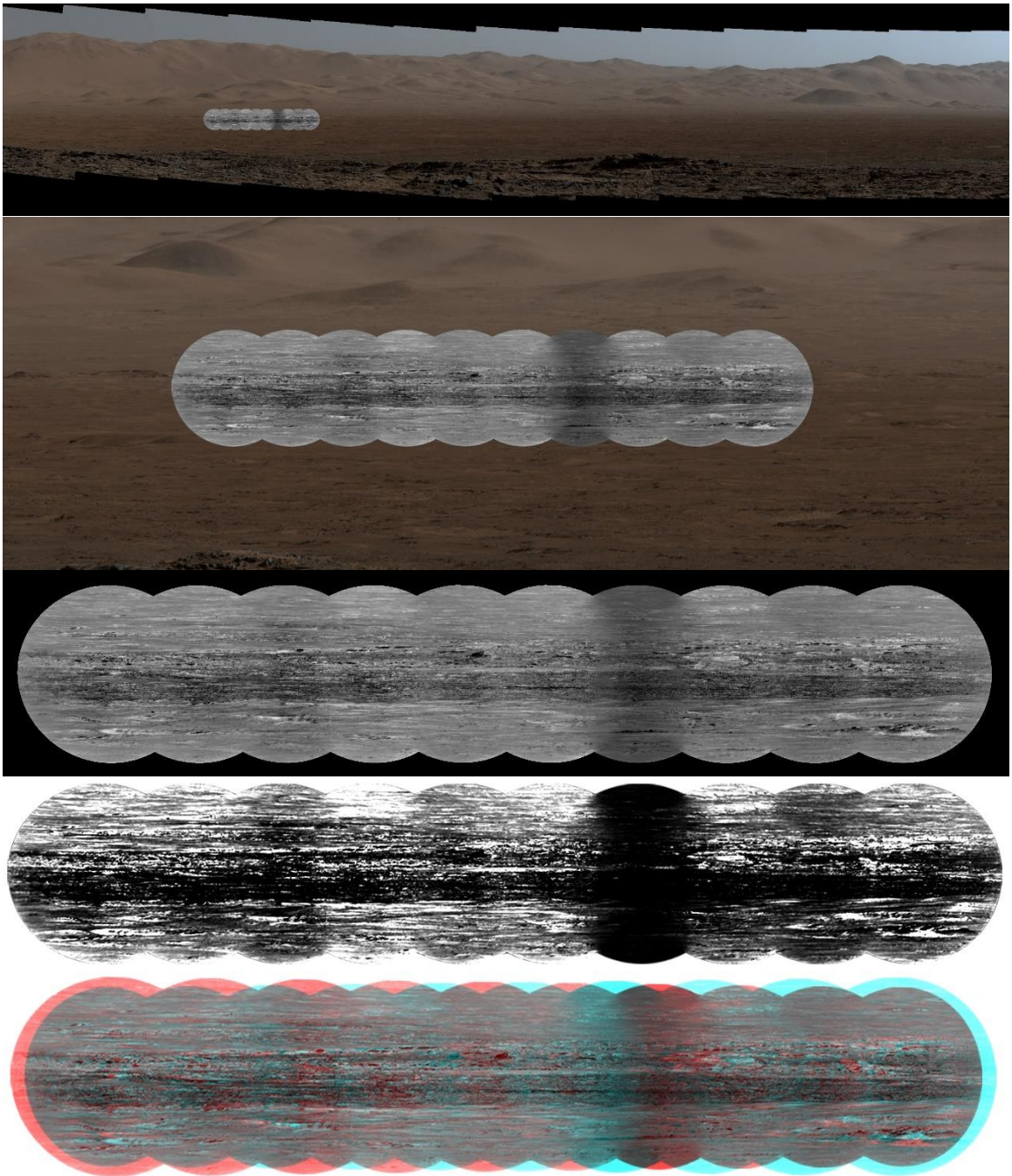
A seven-frame mosaic was acquired on Sol 1251 in the ChemCam long-distance RMI sequence CCAM05251. The mosaic captures an area on the medial, east-lateral edge of the fan. The upper part of the mosaic contains an inverted channel structure skirting the base of a group of mass wasting produced hills. The middle part of the mosaic shows the bright, alluvial surface associated with the inverted channel while the lower part of the mosaic shows the contact of the bajada fan with the Peace Vallis fan proper.



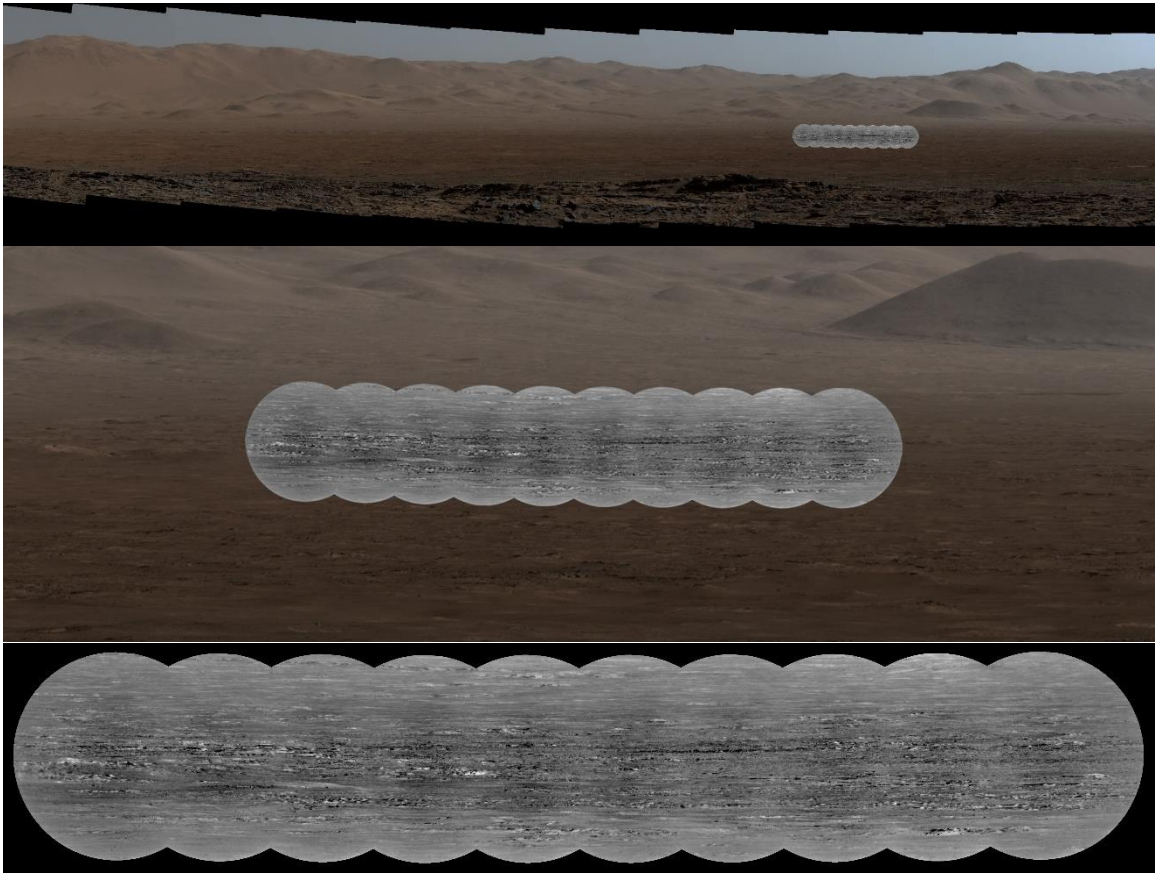


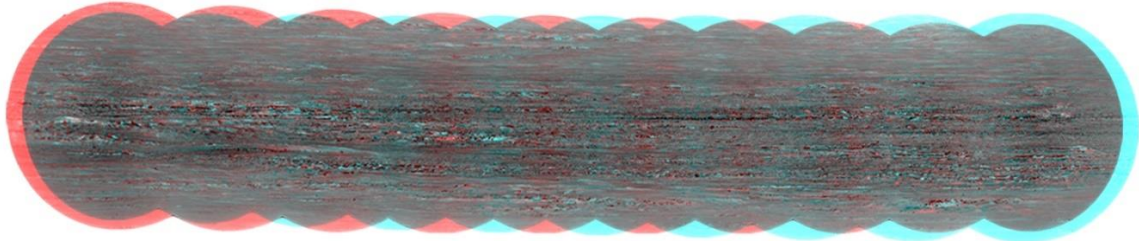
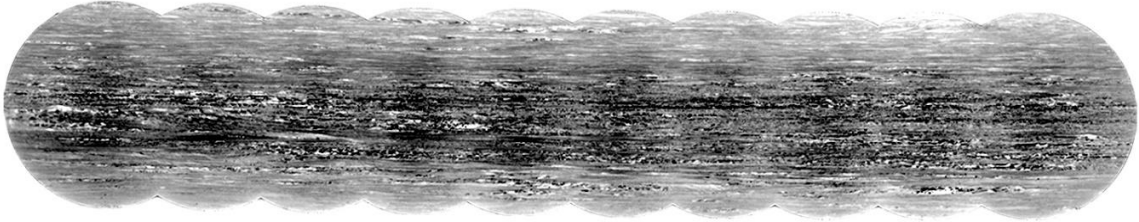
Sol 1257

A ten-frame mosaic was acquired on Sol 1257 in the ChemCam long-distance RMI sequence CCAM01257. Outcropping BF unit fan material can be seen, as well as the distinct contact between the fan and the bounding Aeolis Palus units.



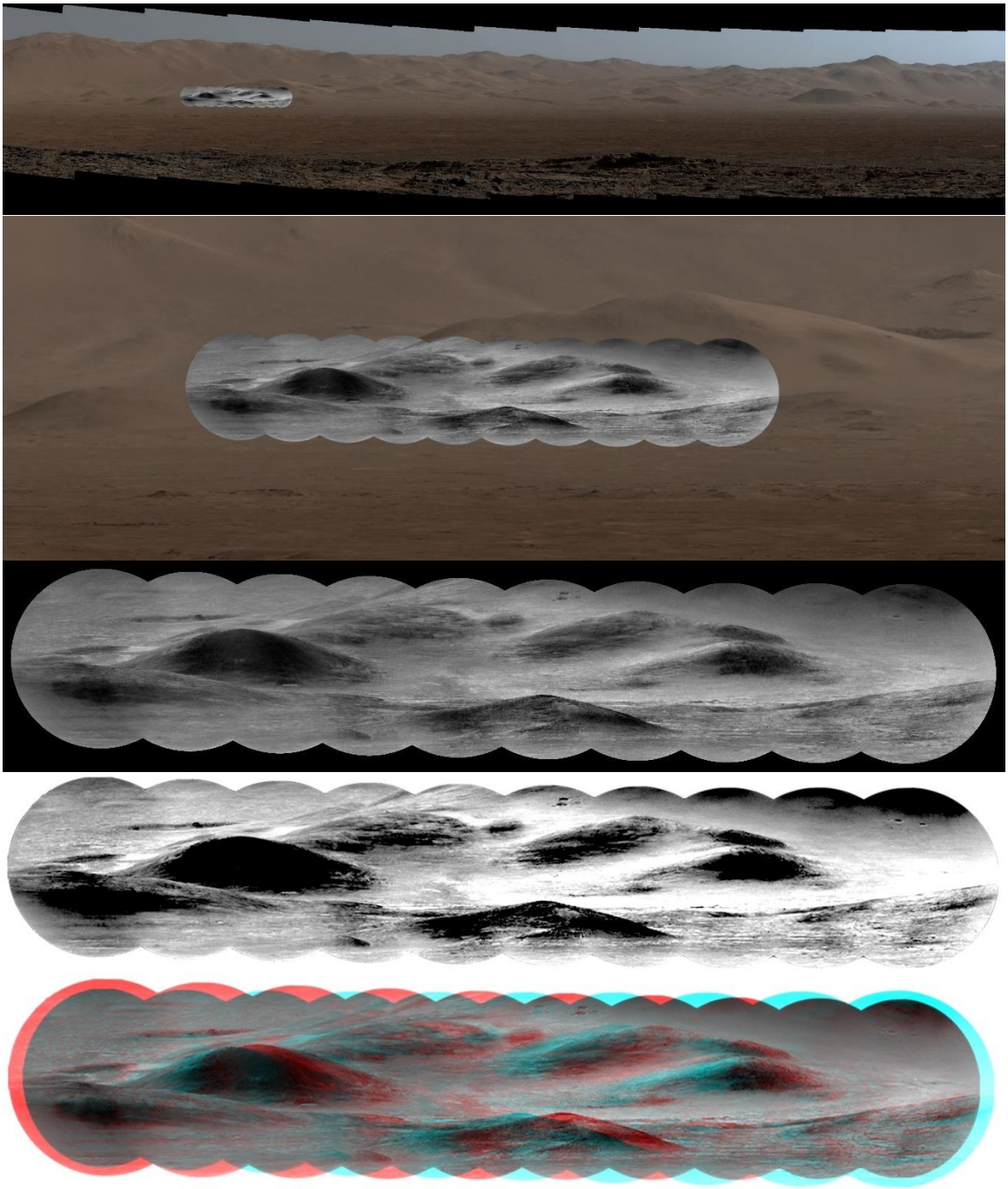
Another ten-frame mosaic was acquired on Sol 1257 in ChemCam long-distance RMI sequence CCAM02257. The top left side of the mosaic contains a prominent inverted channel feature coming across the fan surface toward the southeast and then down the central section of the fan. Outcrops of BF fan material are exposed in the middle of the image.



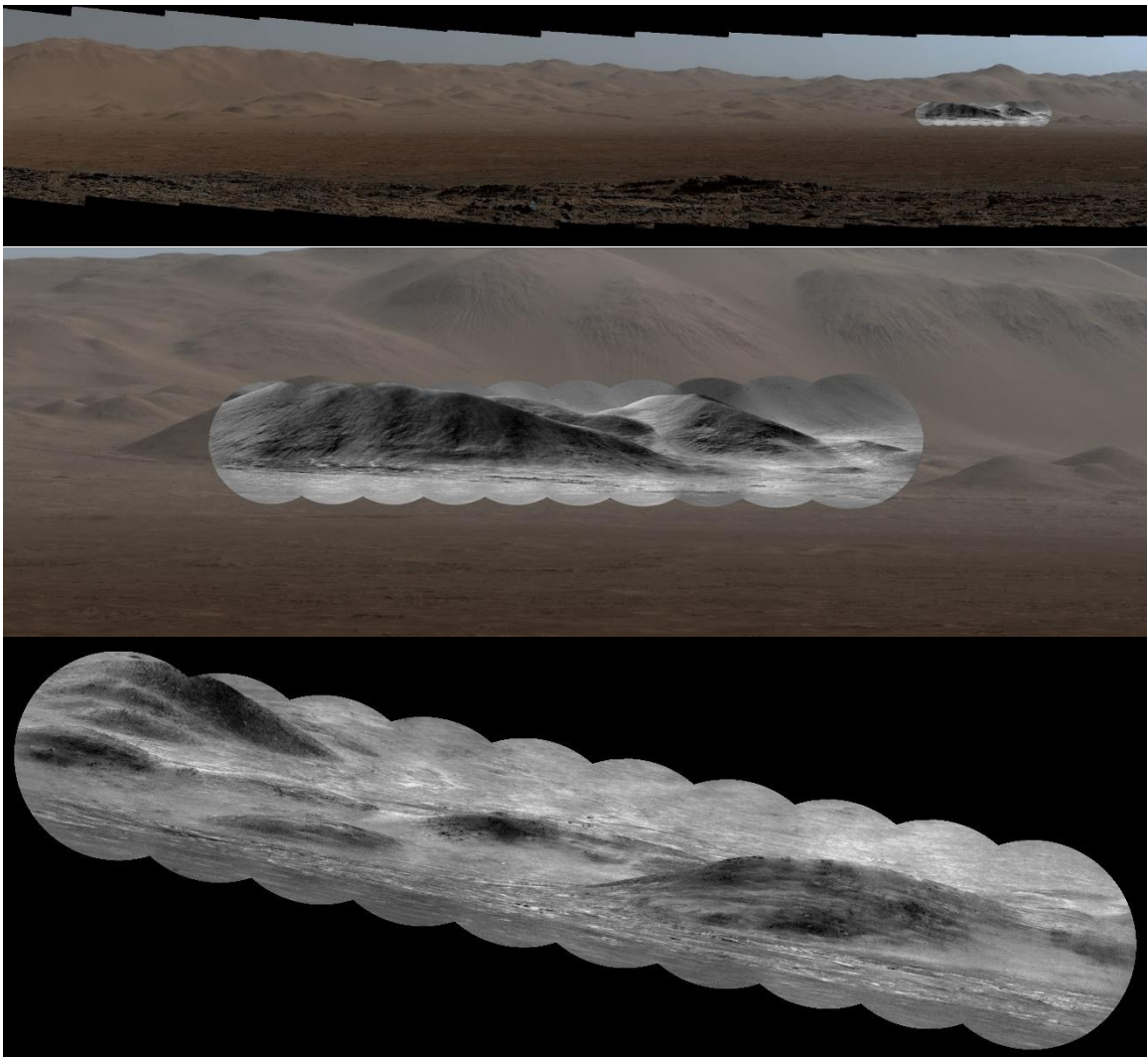


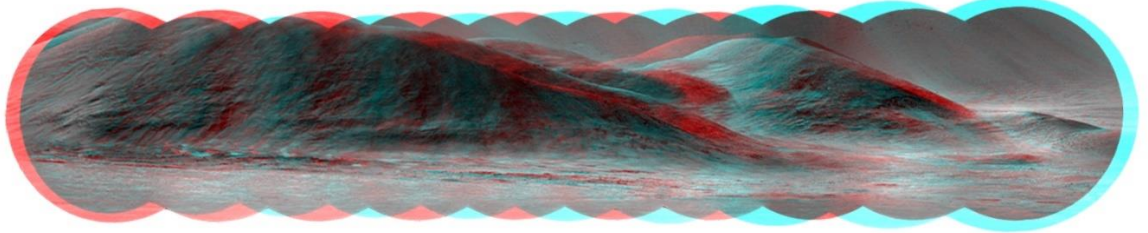
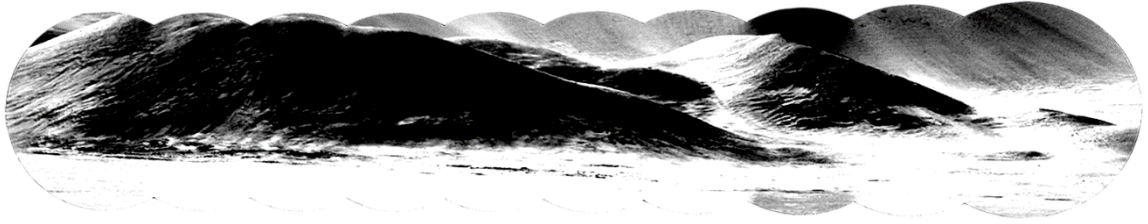
Sol 1262

A ten-frame mosaic was acquired on Sol 1262 in the ChemCam long-distance RMI sequence CCAM03262. This image captures a series of foothills of the slope of the crater wall. Laterally continuous beds are observed abutting the hills in the mosaic.



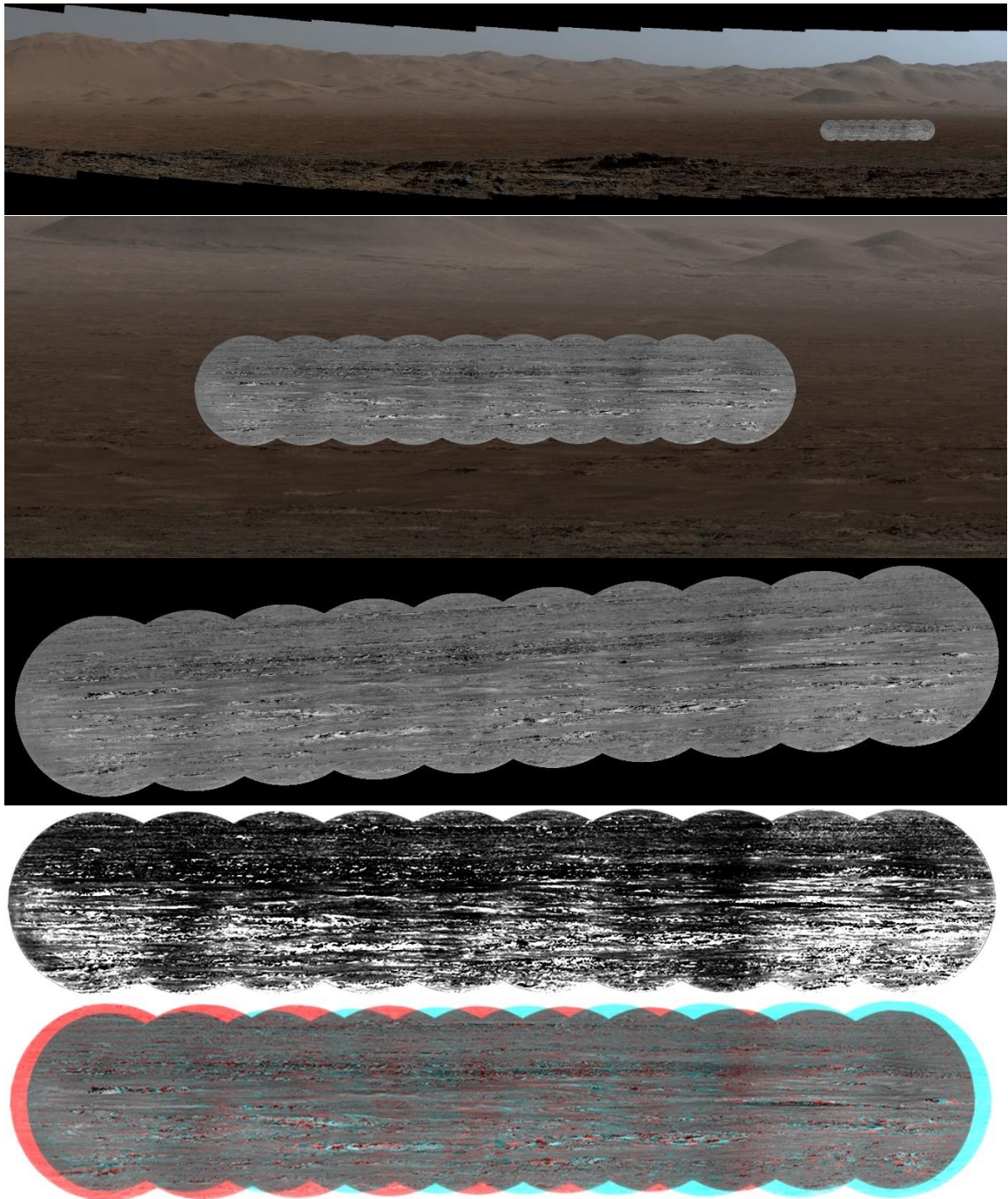
Another ten-frame mosaic was acquired on Sol 1262 in the ChemCam long-distance RMI sequence CCAM04262. This observation targeted a chain of prominent foothills to the east of the Peace Vallis fan apex on the crater wall slope. These hills are mantled with alluvium and show little to no internal structure with the exception of possible horizontal layering near the bottom middle of the left-most hill. The base of this hill is also lined with a resistant, inverted channel feature that follows the slope of the underlying surface. Below the inverted channel is another alluvial surface in the Peace Vallis DFS area.



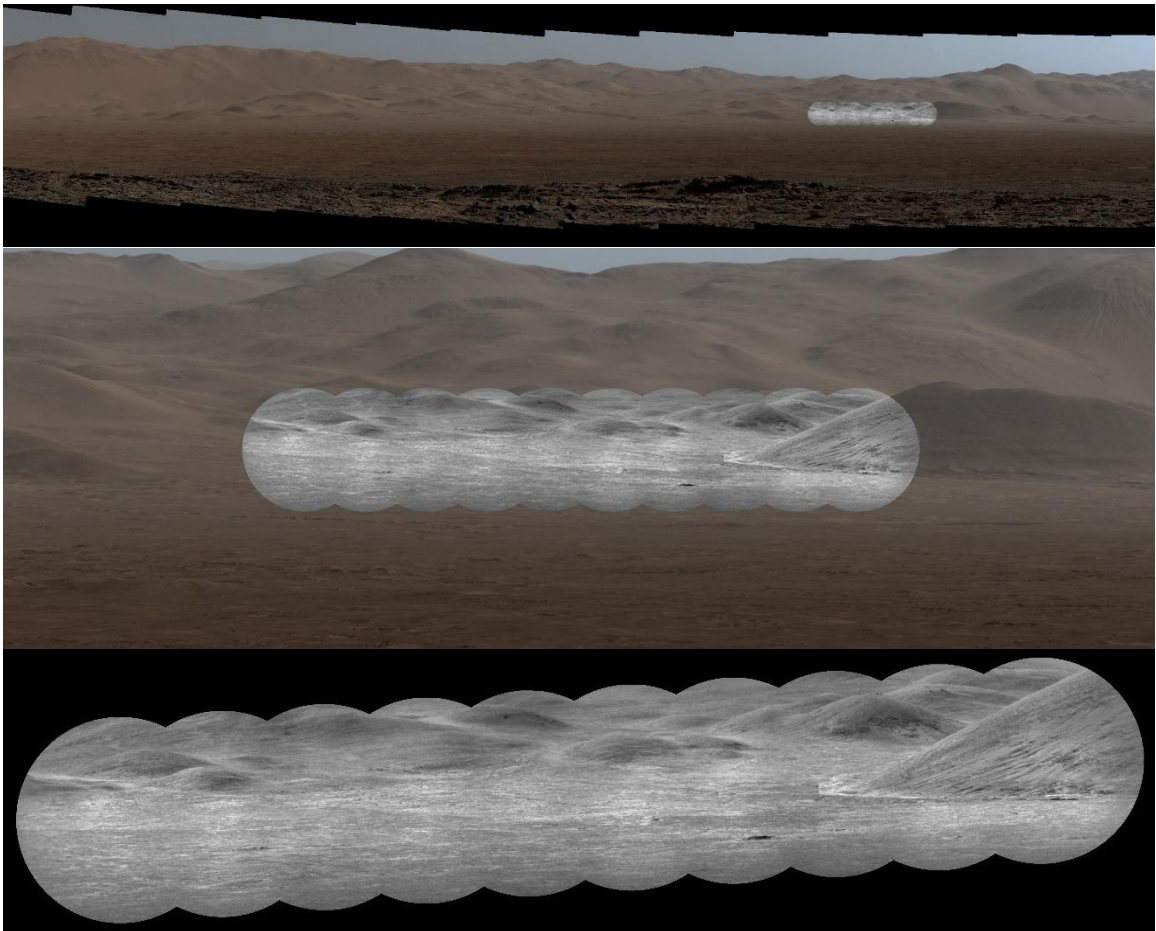


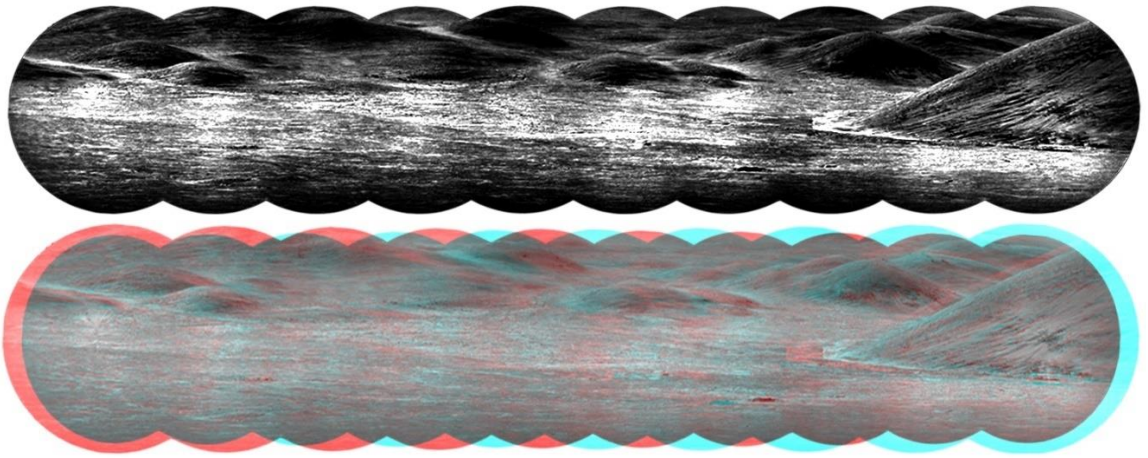
Sol 1271

A ten-frame mosaic was acquired on Sol 1271 in the ChemCam long-distance RMI sequence CCAM03271. This observation targeted the distal deposits on the right-lateral sector of the fan. Outcrops of BF unit are seen above the fan surface.



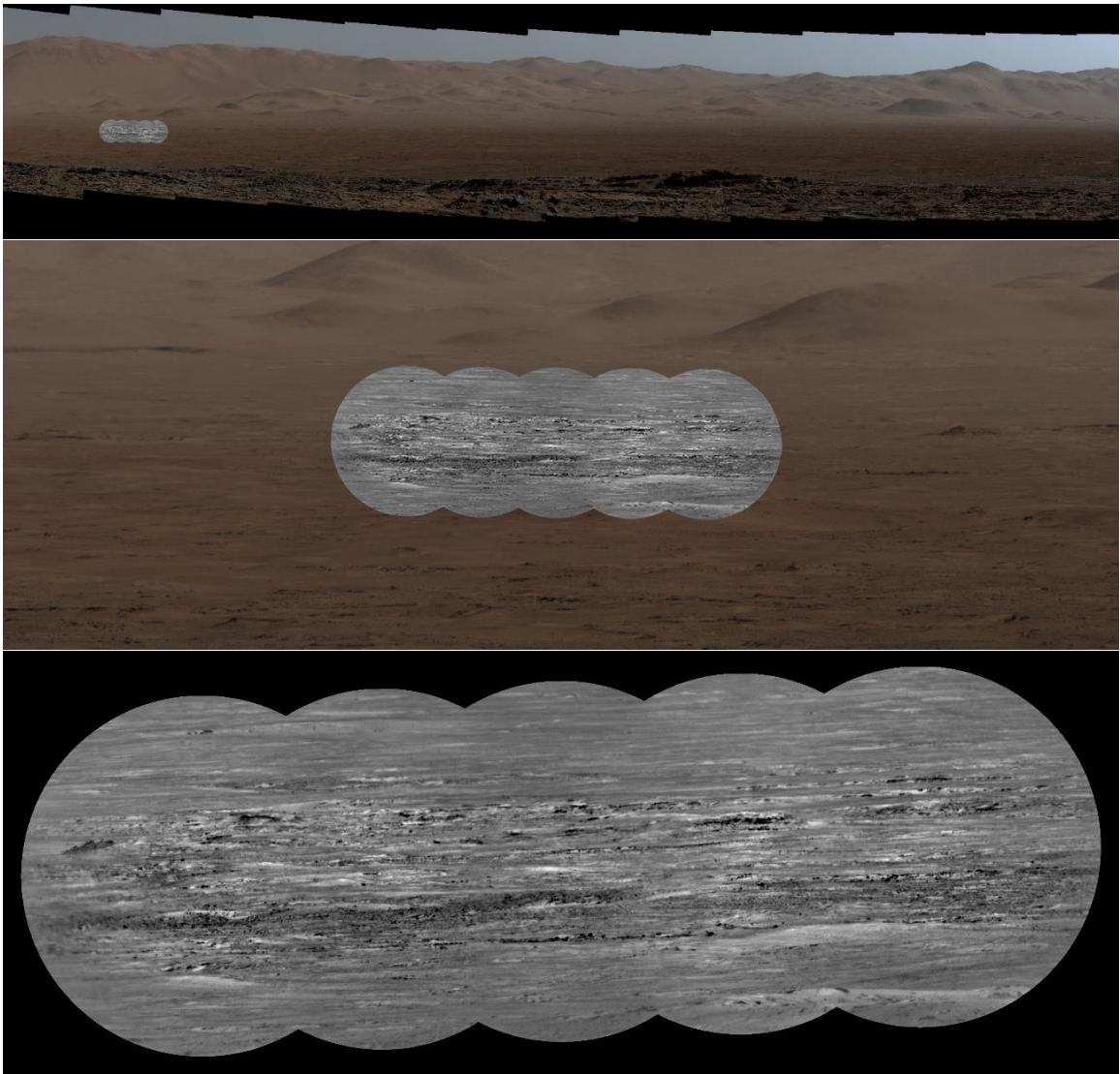
Another ten-frame mosaic was acquired on Sol 1271 in the ChemCam long distance RMI sequence CCAM04271. This observation captures a prominent foothill on the right with inverted channel deposit skirting the side. Other fan surfaces are seen sloping up to the foothills against the crater wall.

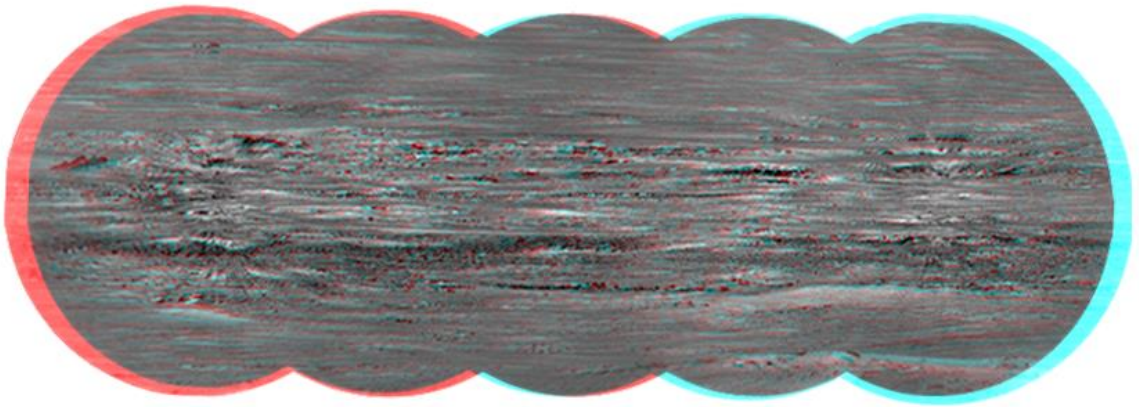




Sol 1293

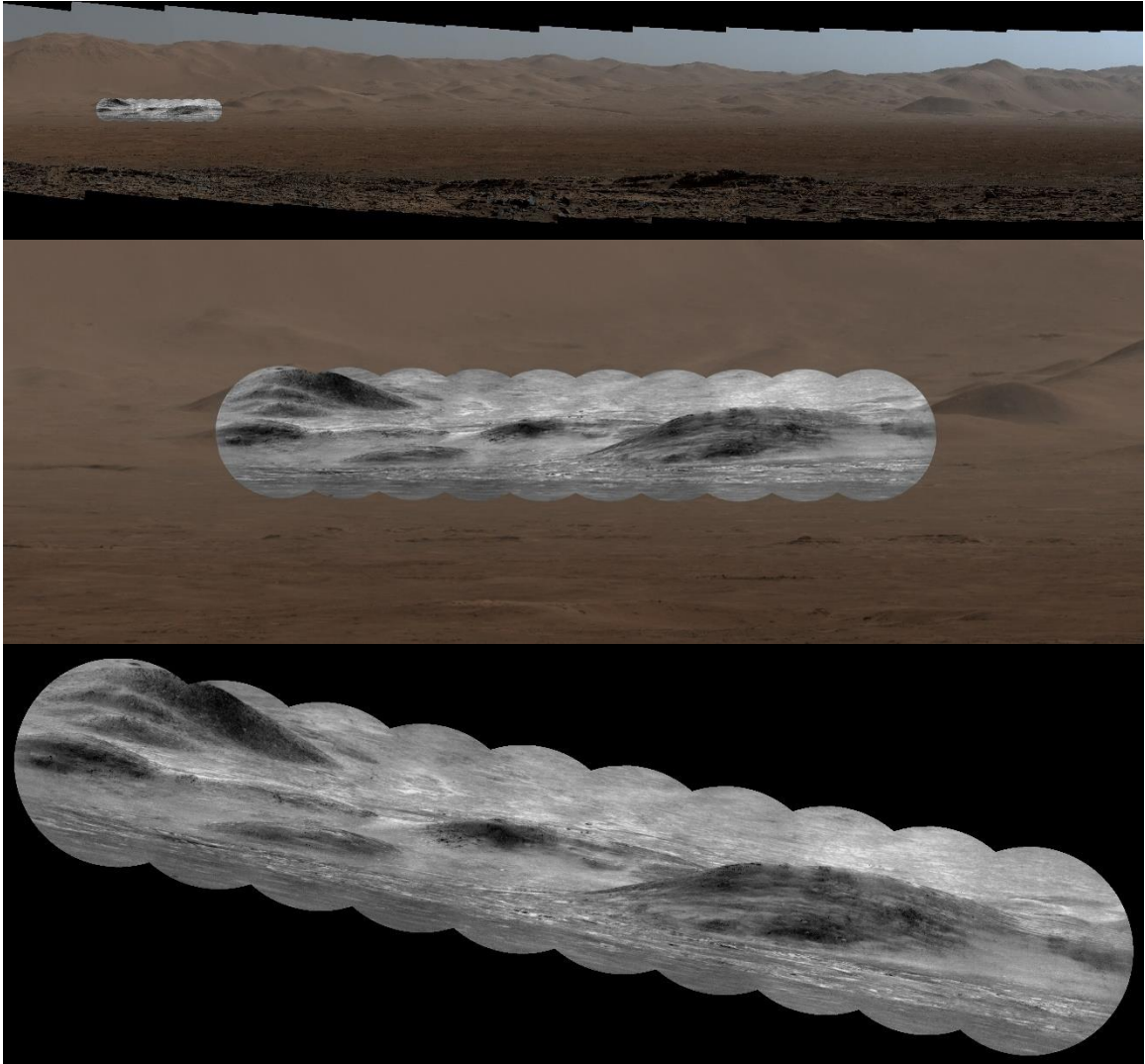
A five-frame mosaic was acquired on Sol 1293 in the ChemCam long-distance RMI sequence CCAM03293. This observation targets the distal deposits on the left-lateral sector of the fan. It shows highly eroded BF unit outcrops.

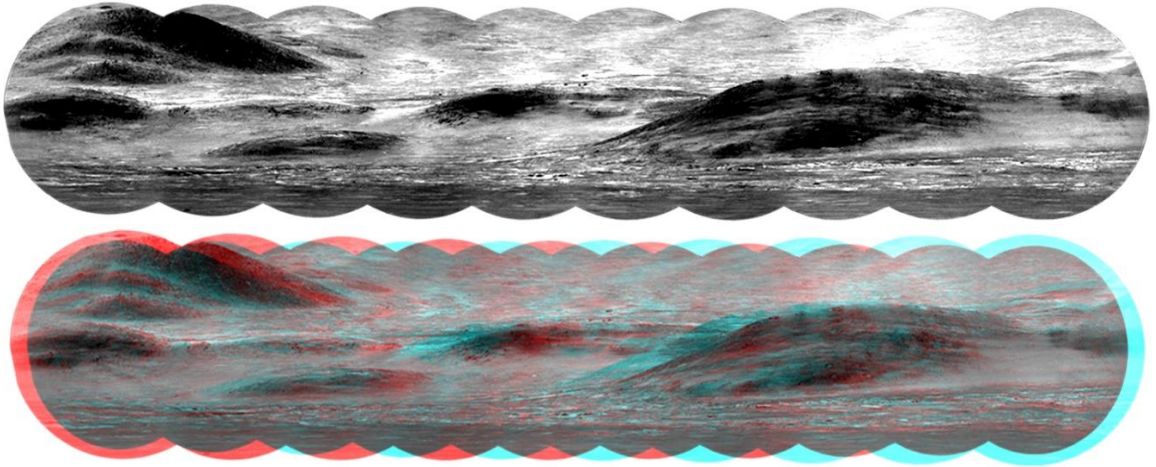




Sol 1296

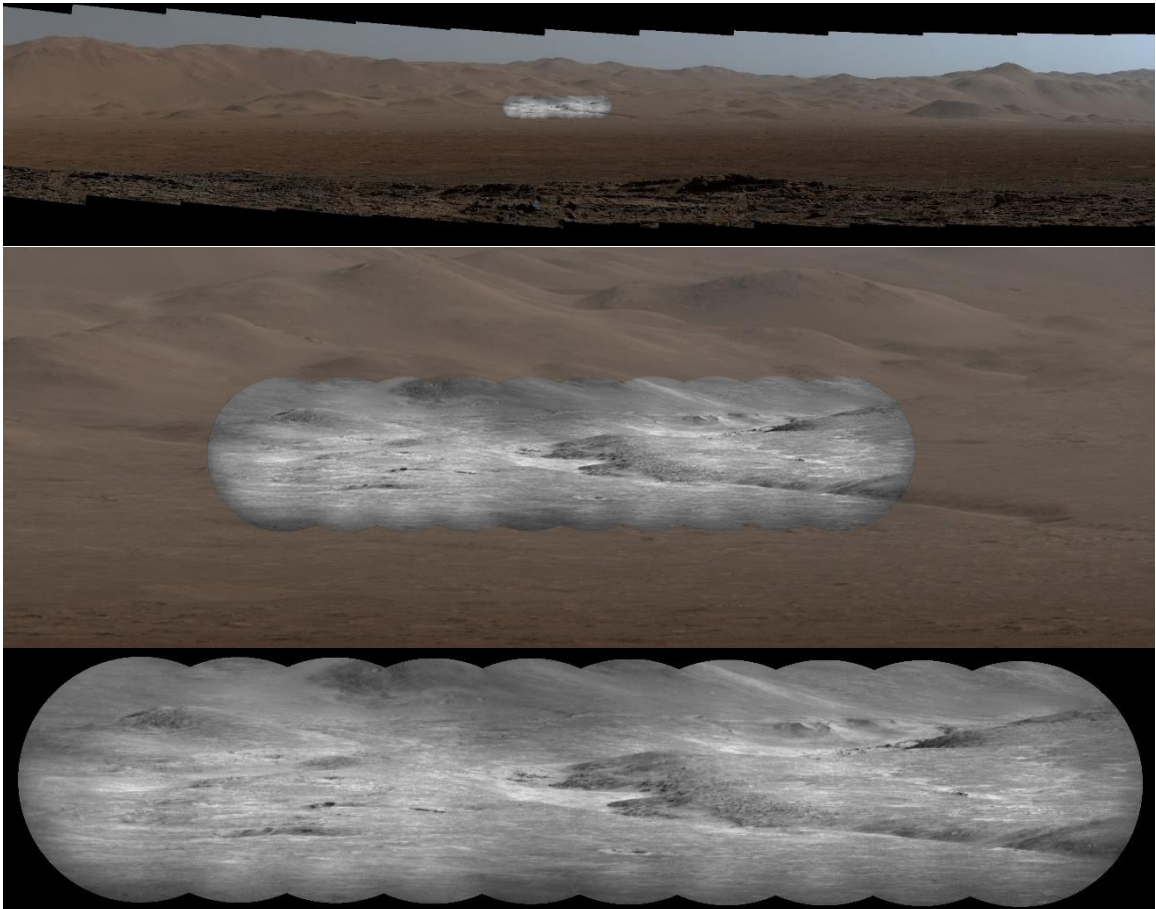
A ten-frame mosaic was acquired on Sol 1296 during the ChemCam long-distance RMI sequence CCAM04296. This observation shows a series of foothills on the lower crater wall. Alluvial flows can be seen flowing through the hills. The same horizontal beds can be observed over 2 km suggesting laterally continuous layers.

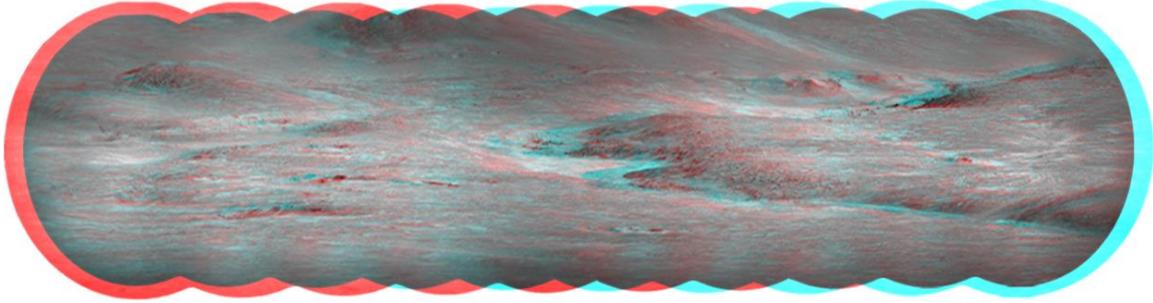
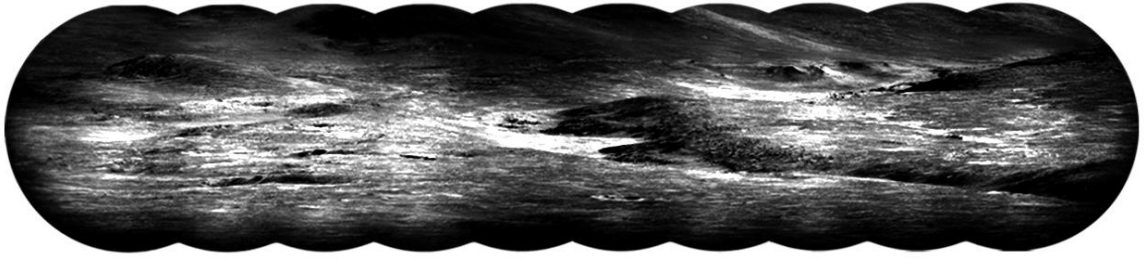




Sol 1300

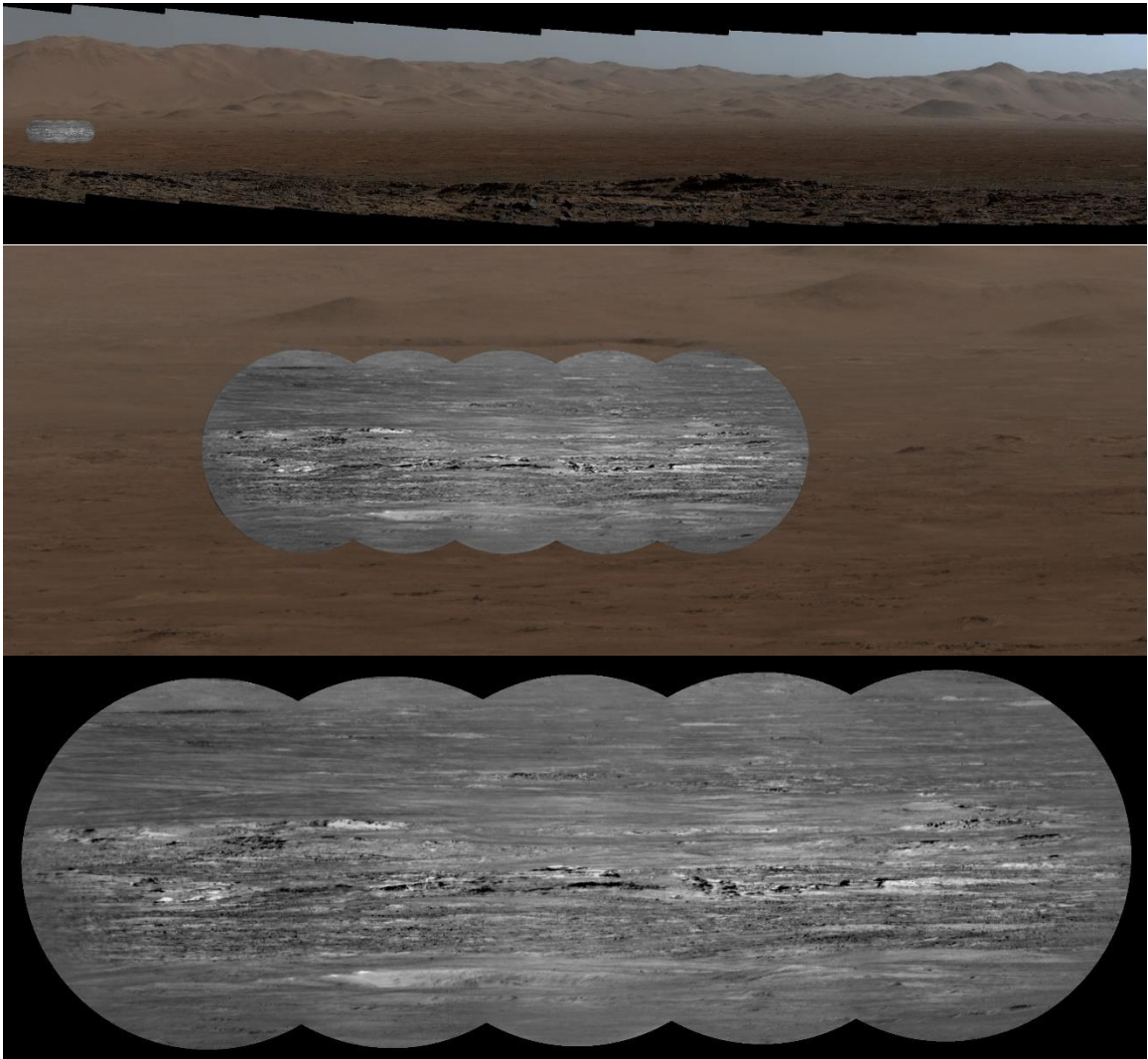
A ten-frame mosaic was acquired on Sol 1300 in the ChemCam long-distance RMI sequence CCAM04300. This observation was targeting the Peace Vallis fan trench and surrounding areas. Other tributaries to the Peace Vallis system can be seen in the bright deposits coming down from the crater rim in the top right section of the image. Another bright tributary on an alluvial surface above the Peace Vallis trench is observer

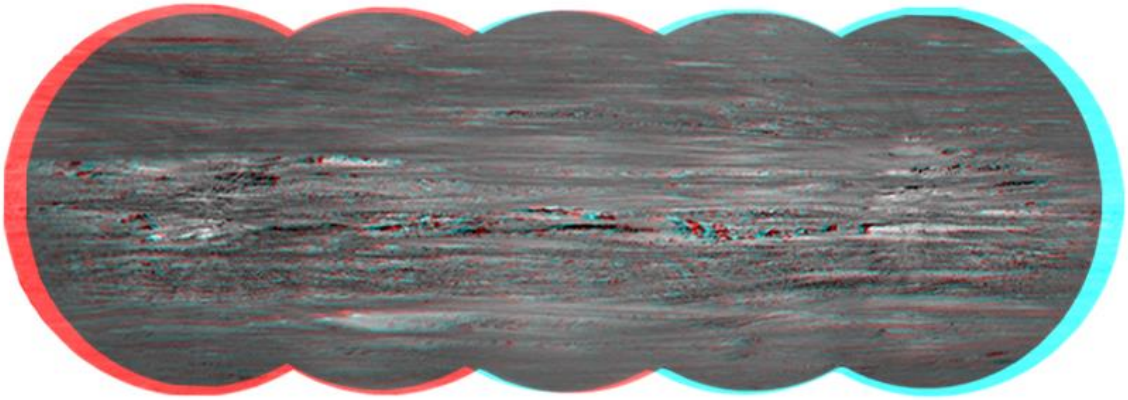
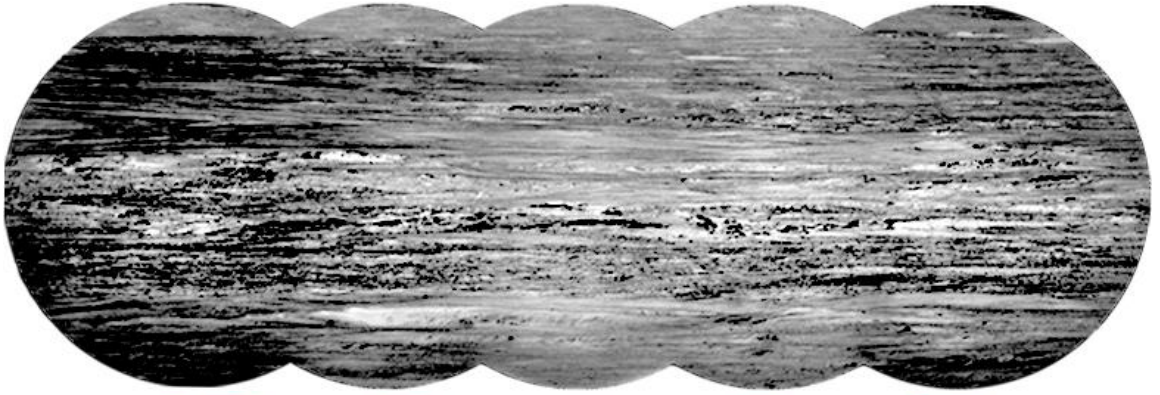




Sol 1309

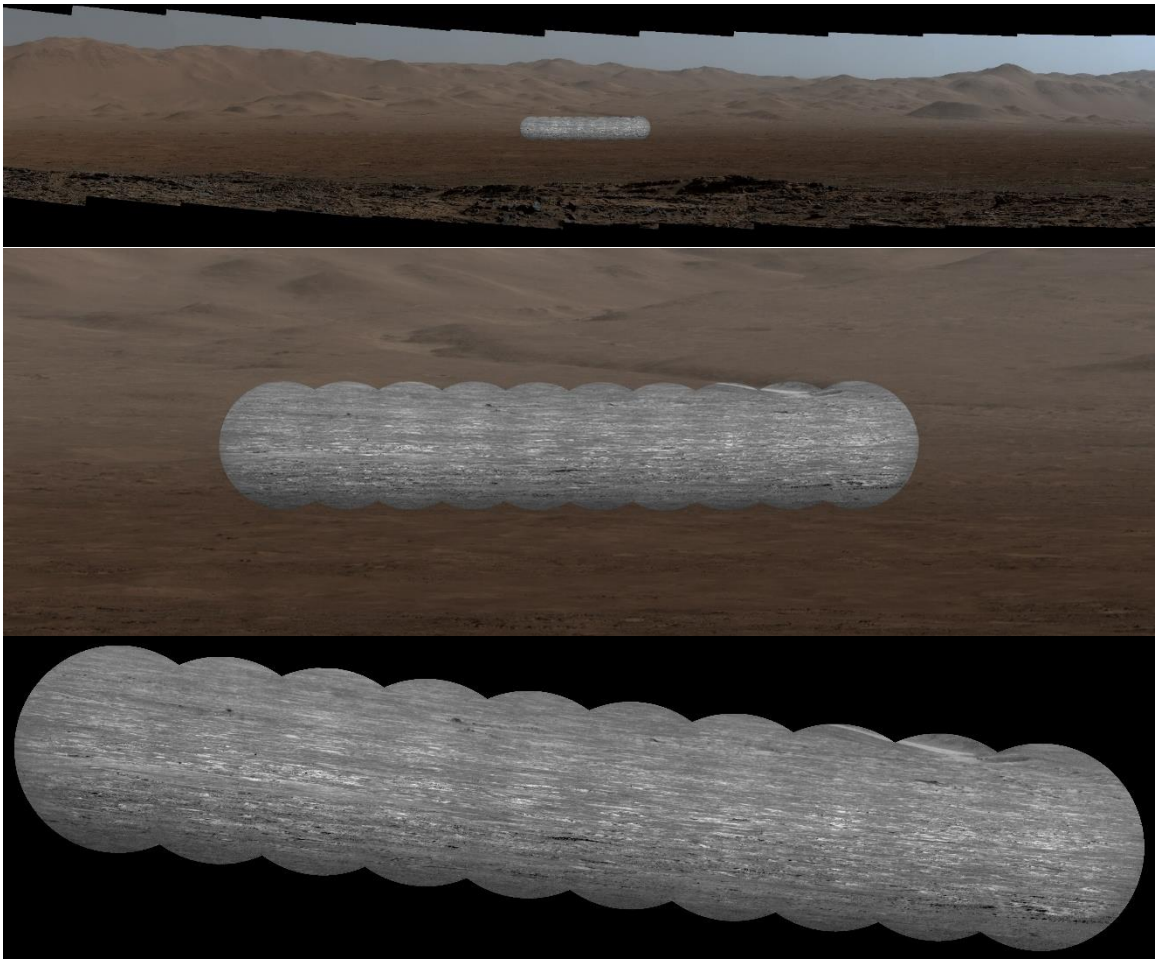
A five-frame mosaic was acquired on Sol 1309 in the ChemCam long-distance RMI sequence CCAM01309. This observation targeted the very distal deposits on the left-lateral sector of the fan. Outcrops of BF fan unit are seen standing above other fan deposits. The ~3.5 km impact crater dubbed “ellipse edge crater” is seen in the top right section of the image.

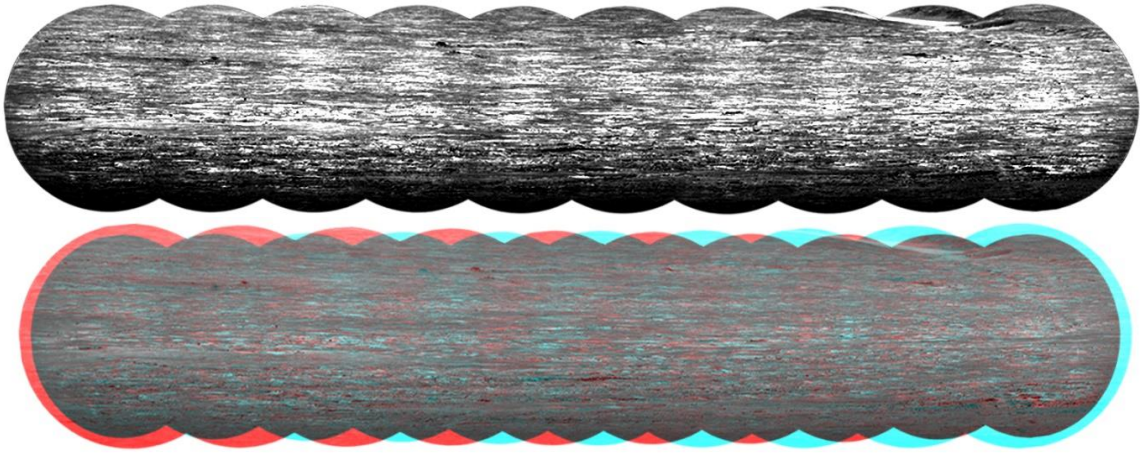




Sol 1311

A ten-frame mosaic was acquired on Sol 1311 in the ChemCam long-distance RMI sequence CCAM05311. This observation targeted proximal fan deposits in the left-lateral sector of the fan apron. Older fan surfaces are also seen in the top left portion of the image.

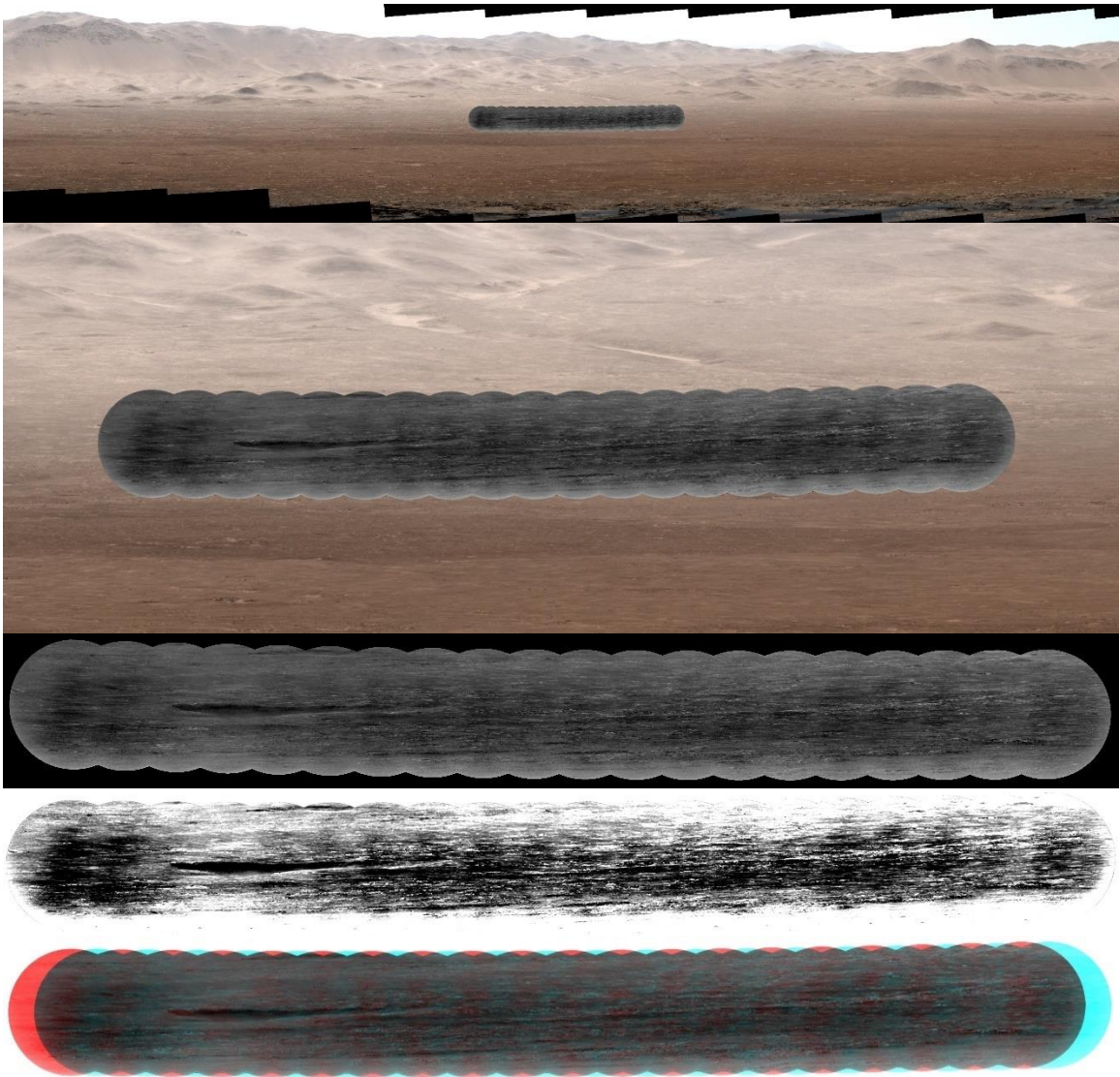




Appendix B: Observations and products from the Peace Vallis campaign 2.

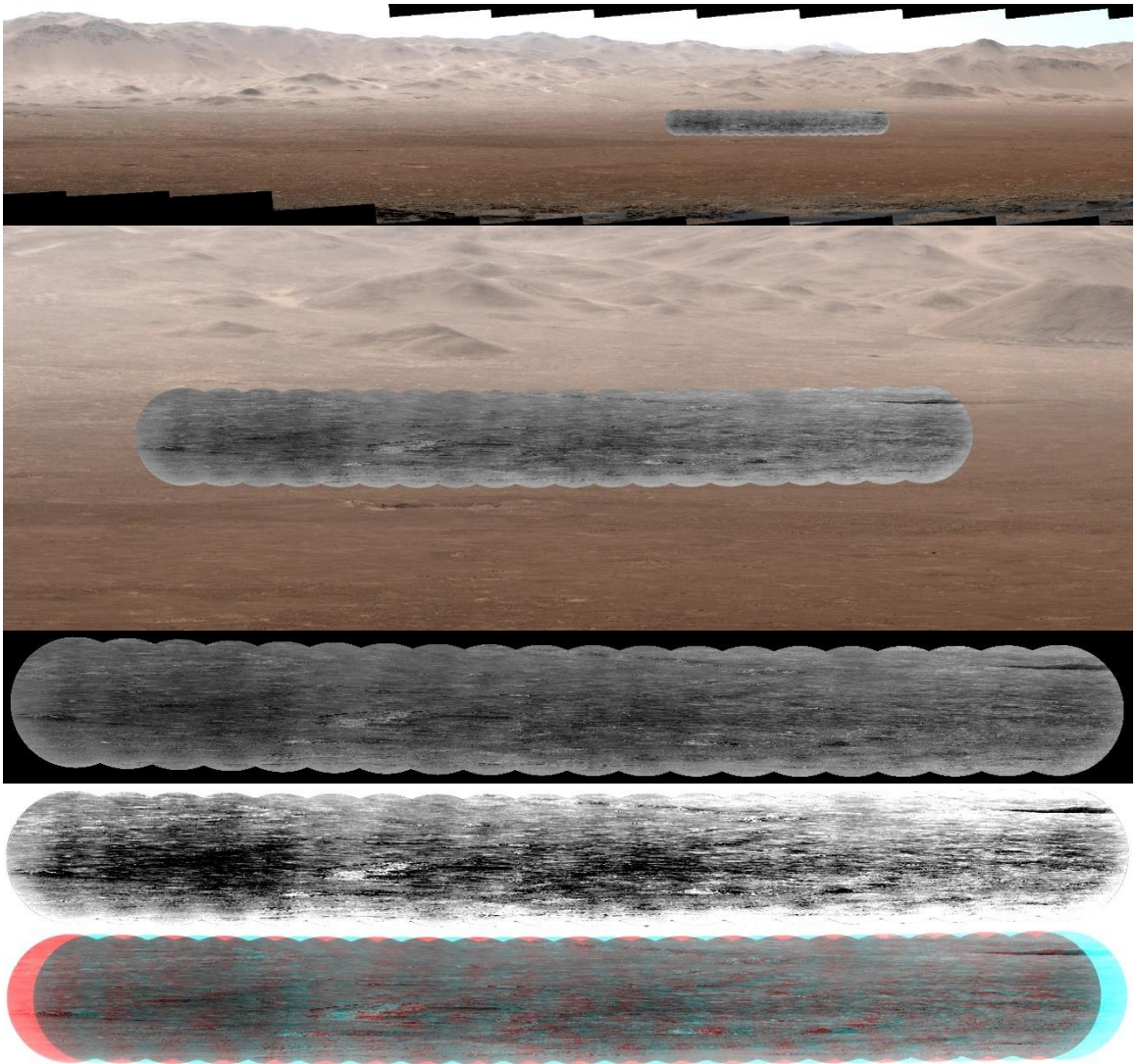
Sol 1980

A twenty-frame mosaic was acquired on Sol 1980 in the ChemCam long-distance RMI sequence CCAM04980. This observation was targeted at the left-lateral sector of the medial fan surface. An impact crater is seen in the middle right section of the image. An inverted channel feature runs just below the crater.



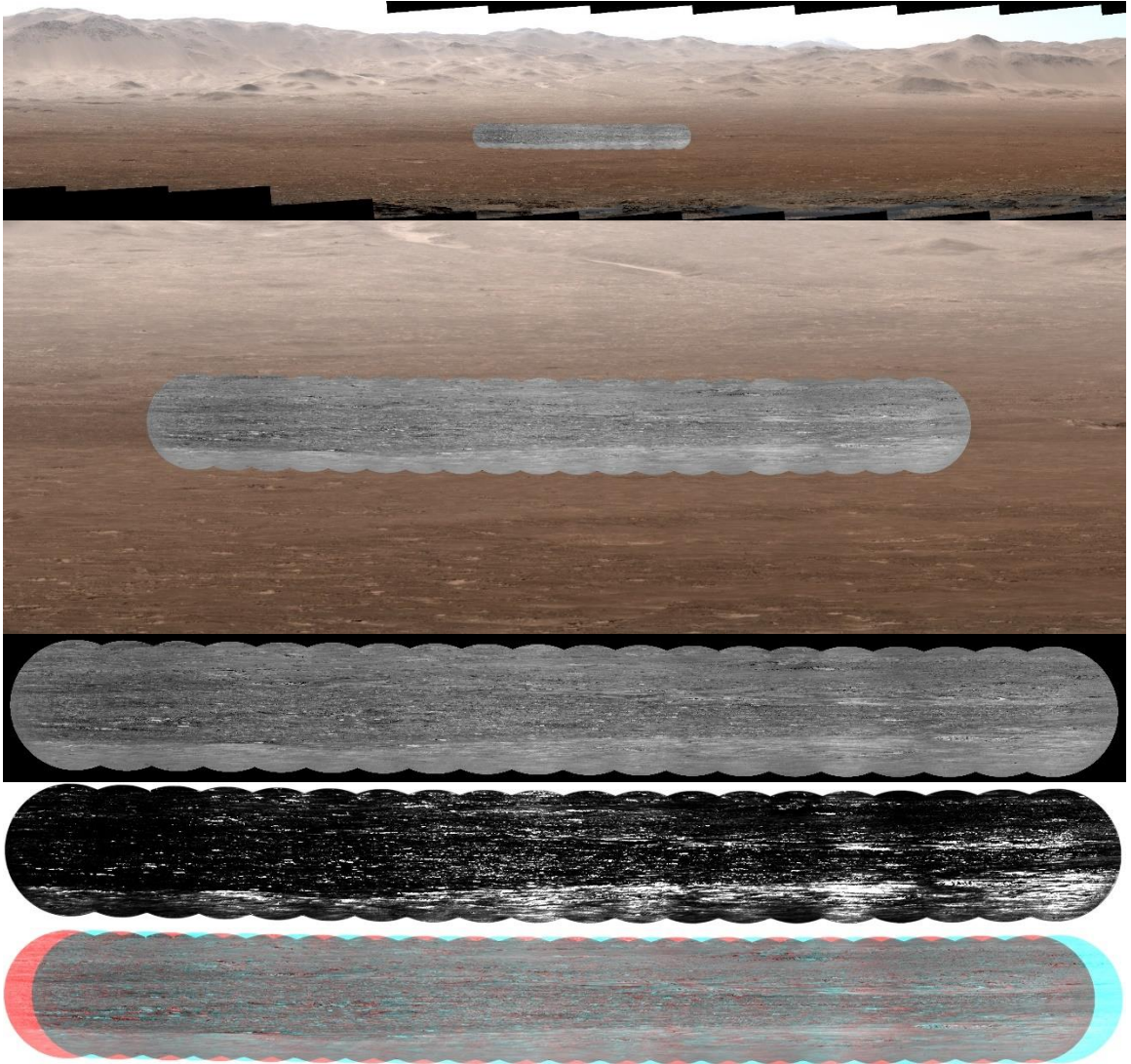
Sol 1981

A twenty-frame mosaic was capture on Sol 1981 in the ChemCam long-distance RMI sequence CCAM04981. This observation targeted medial fan deposits on the central sector of the fan. The .75 km impact crater on the fan is seen in the top right corner of the image.



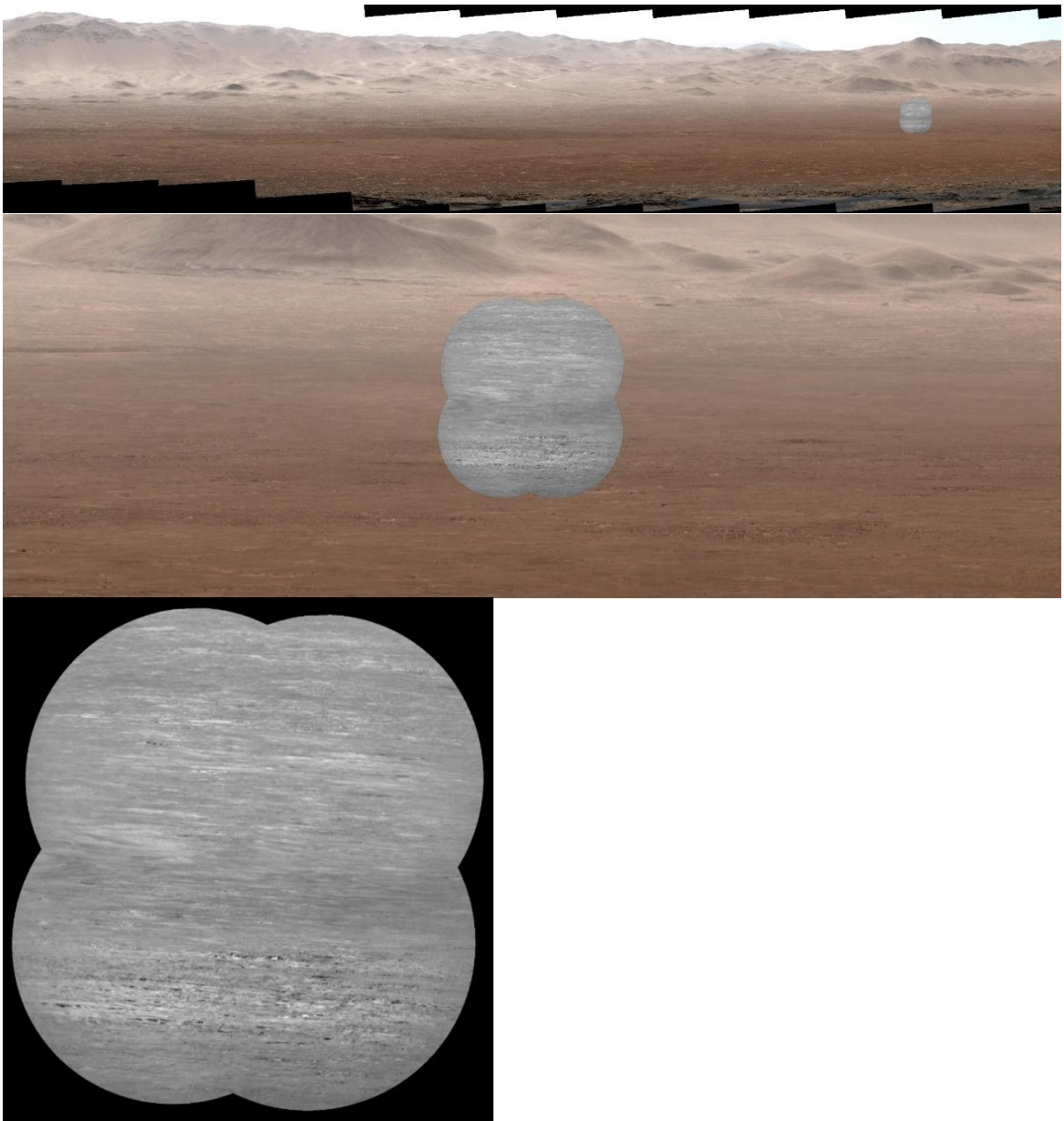
Sol 1984

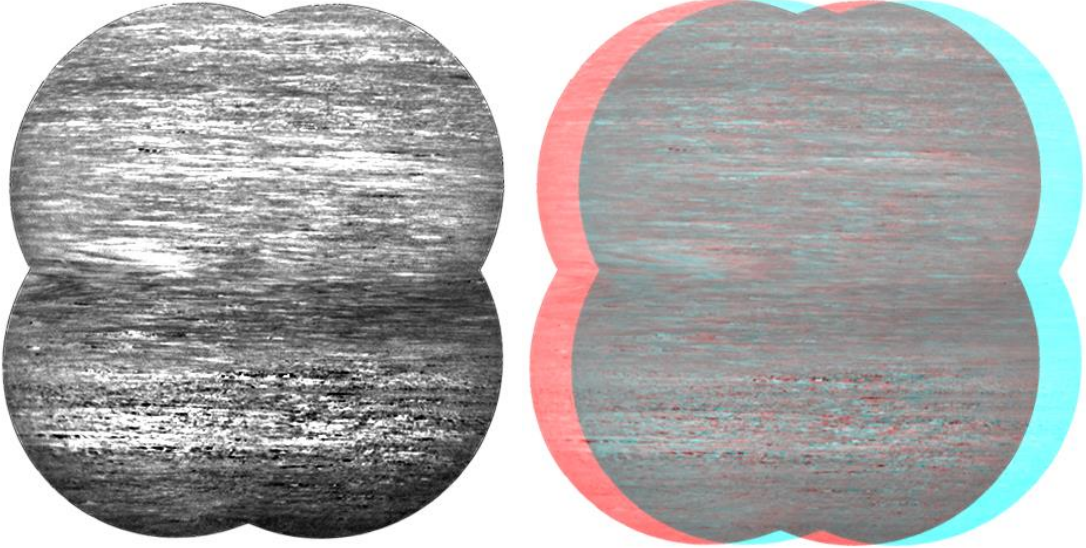
A twenty-frame mosaic was acquired on Sol 1984 in the ChemCam long-distance RMI sequence CCAM02984. This observation targeted distal deposits on the central sector of the fan surface. A contact between the fan surface and crater floor deposits is observed as a continuous contrast across the bottom of the mosaic.



Sol 1991

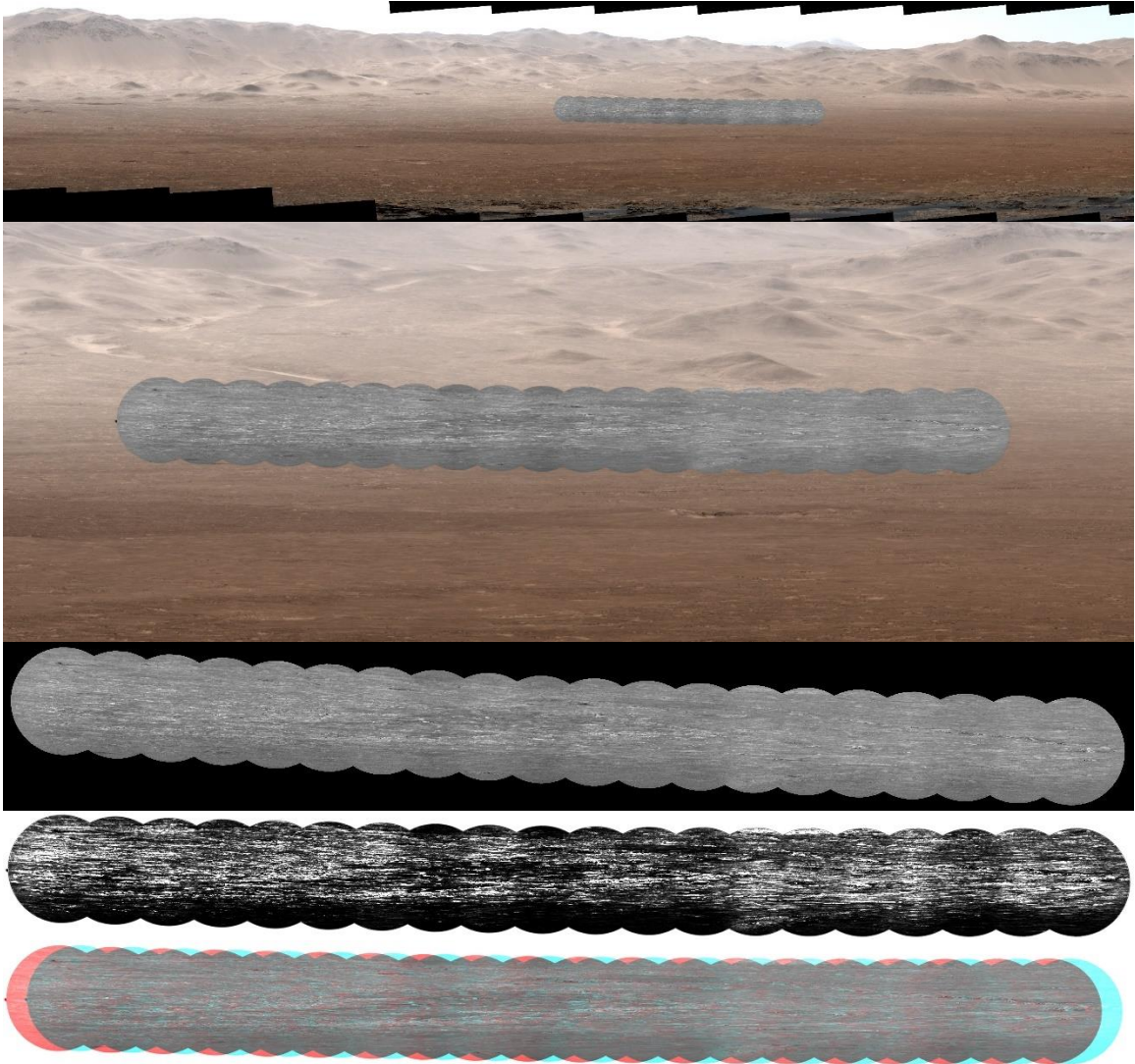
A four-frame mosaic was acquired on Sol 1991 in the ChemCam long distance RMI sequence CCAM05991. The observation targeted distal deposits of the mantling, discontinuous AF fan unit on the east-lateral sector of the fan apron. This sequence experienced a rover anomaly due to the ChemCam “hardstop” and was cut short of the intended 10x2 raster.





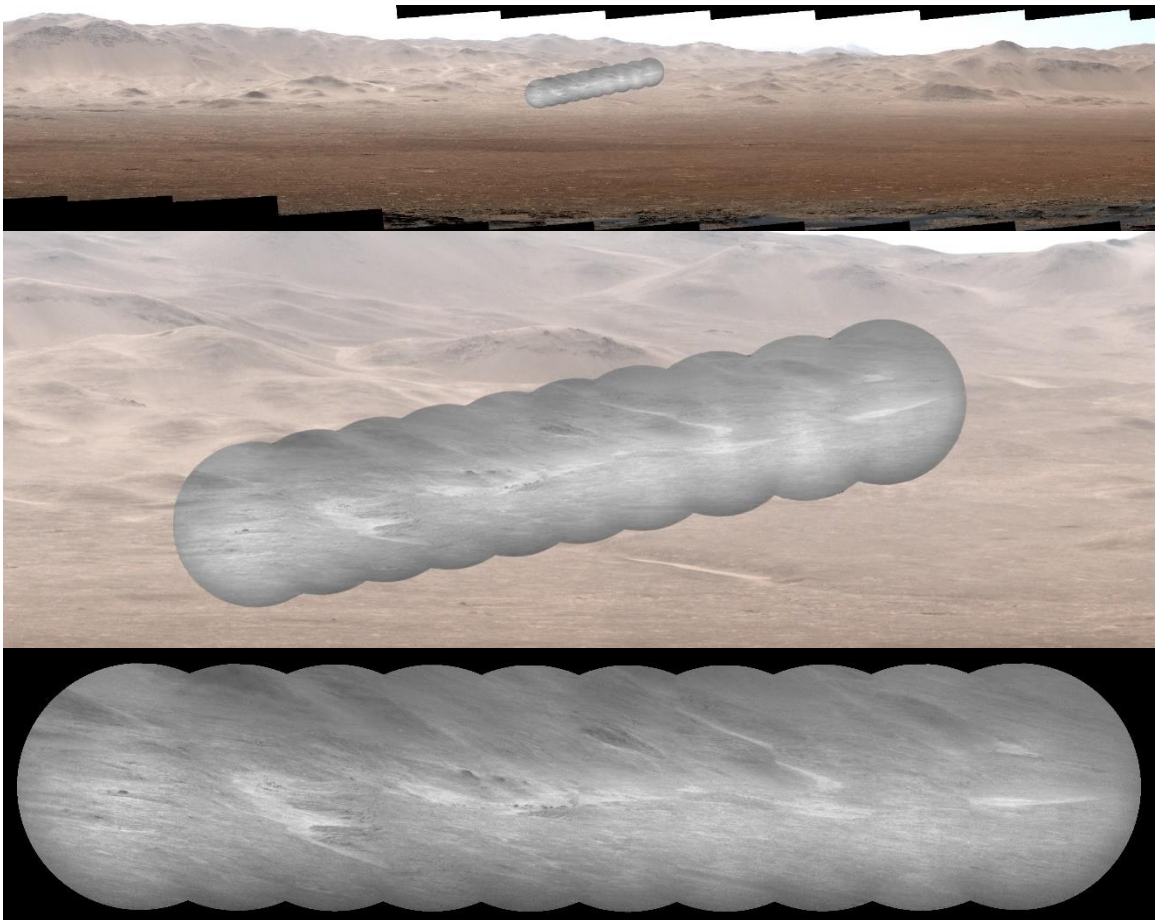
Sol 1998

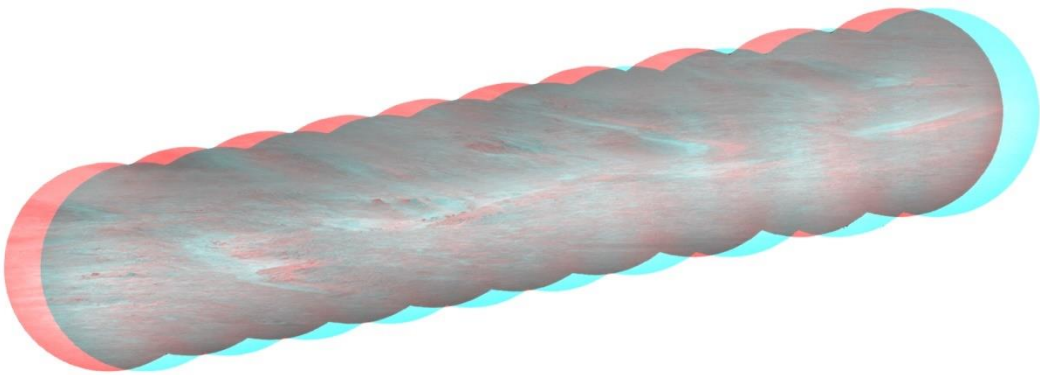
A twenty-frame mosaic was acquired on Sol 1998 in the ChemCam long-distance RMI sequence CCAM03998. This observation targeted proximal deposits near the apex of the Peace Vallis DFS. A prominent inverted channel feature can be seen running from the top-central part of the image to the left middle of the image.



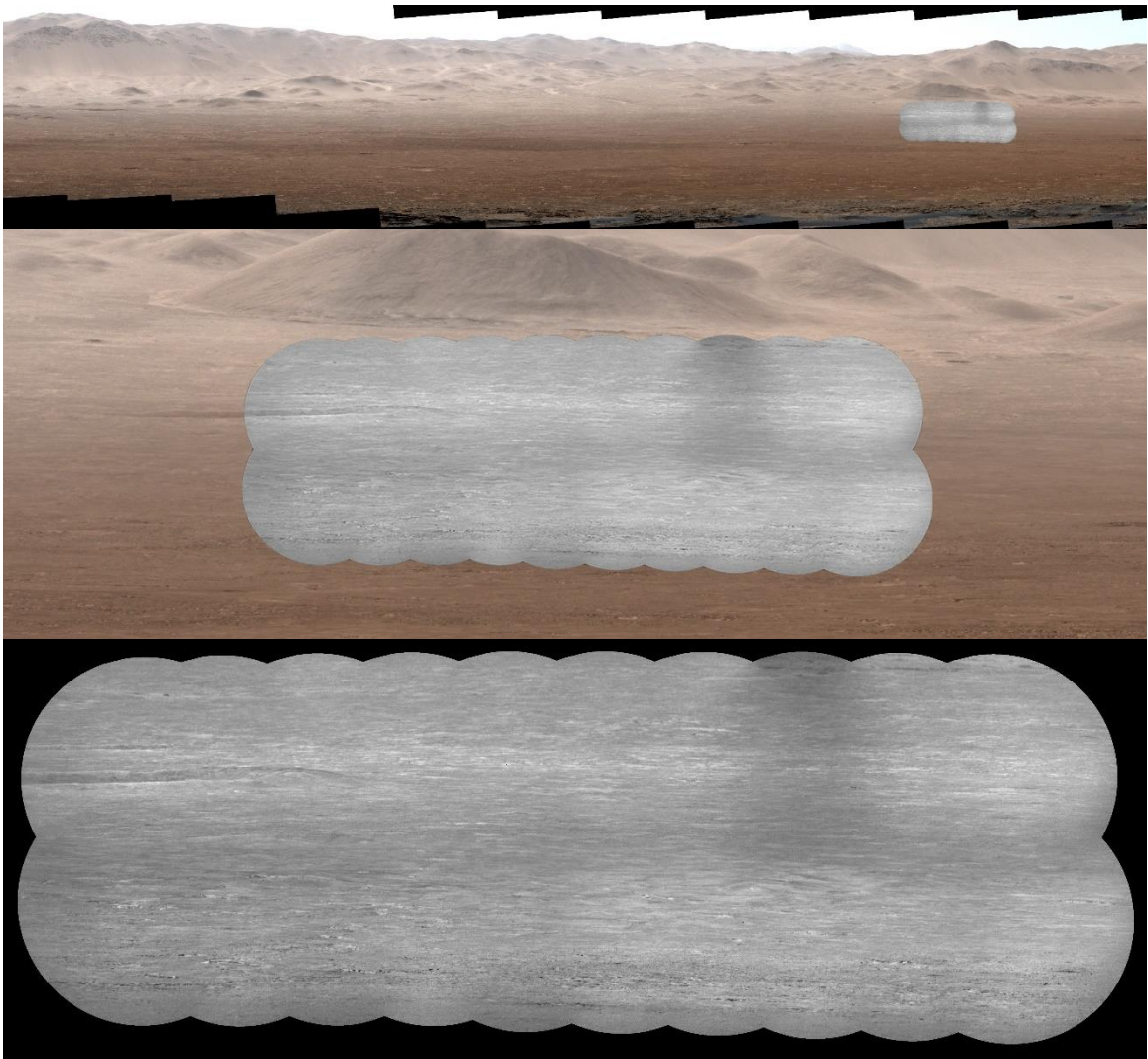
Sol 2011

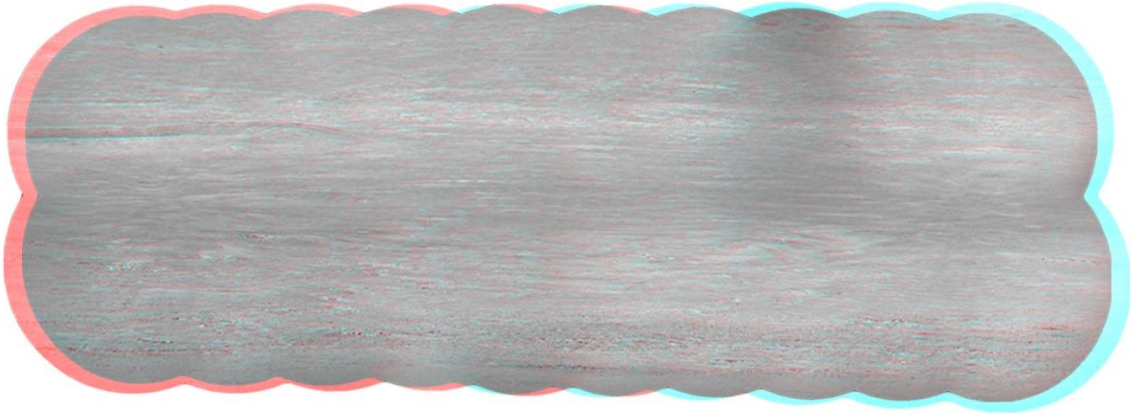
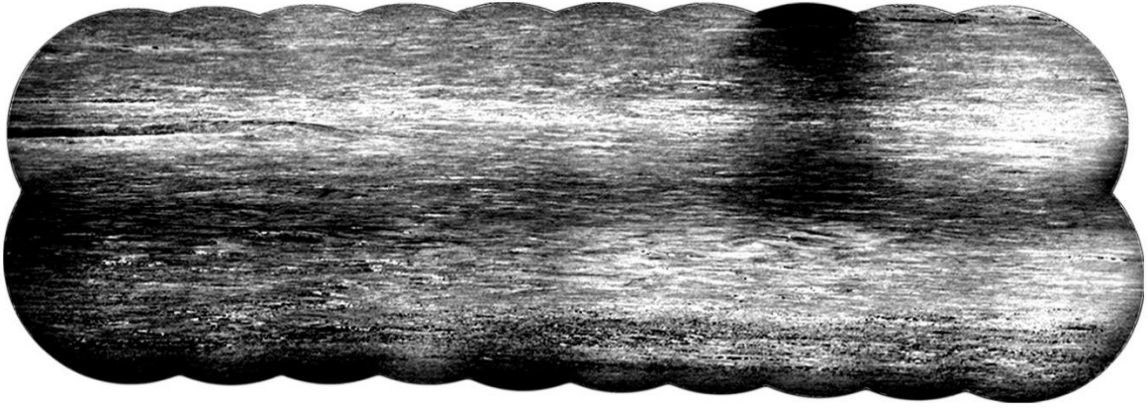
A ten-frame mosaic was acquired on Sol 2011 in the ChemCam long-distance RMI sequence CCAM01011. This was a horizontal mosaic targeted on the Peace Vallis channel while the rover was at a high tilt. The channel contains fluvial fill and boulders eroded from the channel wall. A series of flat-lying outcrops can be seen perched above the west side of the channel at the left-center of the mosaic.





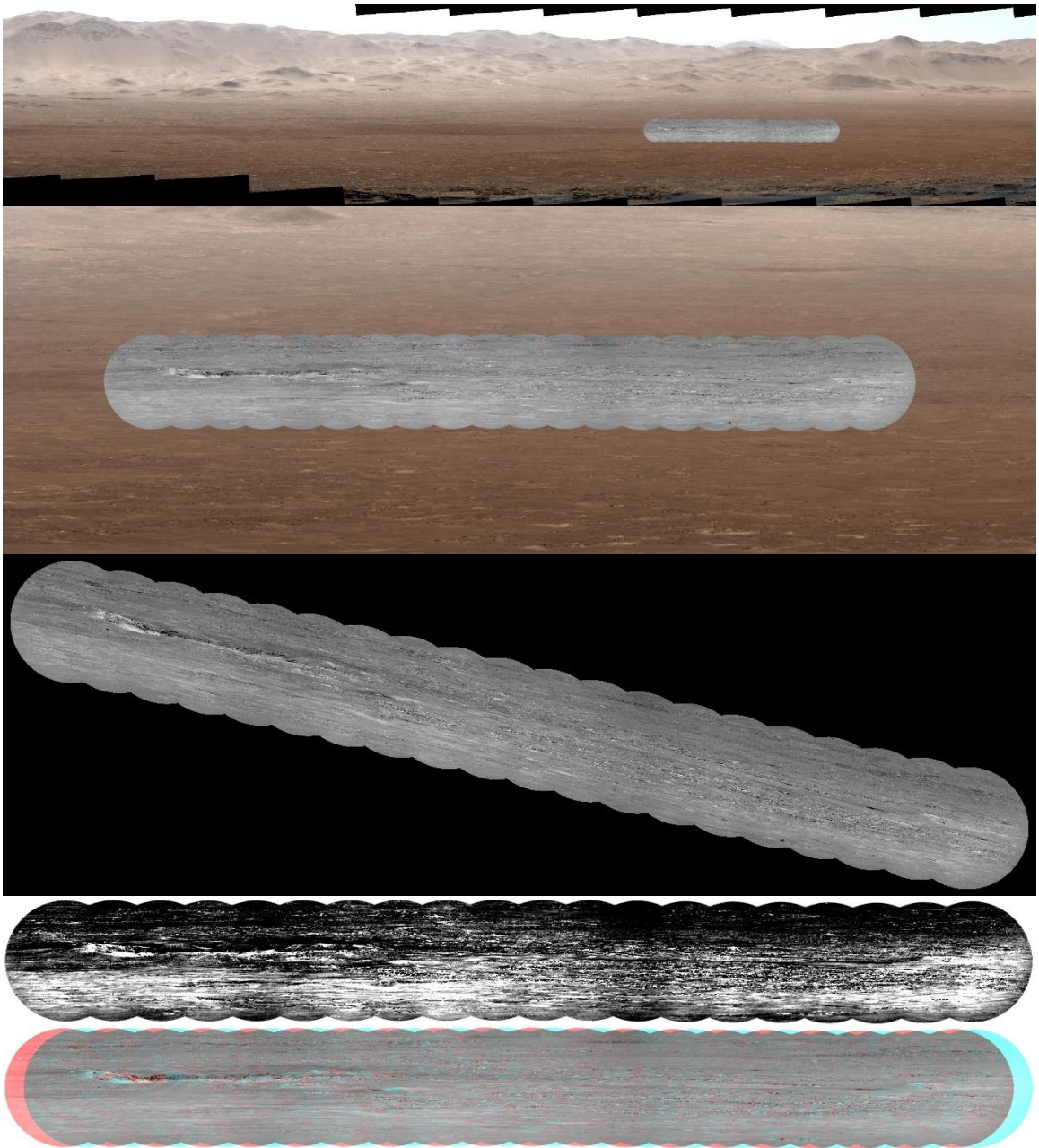
A twenty-frame mosaic was acquired on Sol 2011 in the ChemCam long-distance RMI sequence CCAM02011. This observation targeted the medial deposits of the fan on the left-lateral sector of the fan. A large, .75 km crater is seen on the left side of the top raster. The AF fan surface is observed over most of the middle of the mosaic. The lower section of the bottom raster is lined with BF unit outcrops. The older fan surfaces in the Peace Vallis system are observed at the top of the image.





Sol 2012

A twenty-frame mosaic was acquired on Sol 2012 in the ChemCam long-distance RMI sequence CCAM02012. This observation targeted the distal deposits on the central sector of the apron. An impact crater is seen on the left side of the mosaic.



References

- Anderson, R. B., and Bell III, J. F. "Geologic mapping and characterization of Gale Crater and implications for its potential as a Mars Science Laboratory landing site." *Mars 5* (2010): 76-128.
- Anderson, R. et al., "Change monitoring on Aeolis Mons using ChemCam RMI and HiRISE." *Lunar and Planetary Science Conference* (2017).
- Armitage, J. J., et al. "Timescales of alluvial fan development by precipitation on Mars." *Geophysical research letters* 38.17 (2011).
- Baedke, S. J., et al. "Reconstructing paleo lake levels from relict shorelines along the Upper Great Lakes." *Aquatic Ecosystem Health & Management* 7.4 (2004): 435-449.
- Baker, V. R. "The channels of Mars." *Research supported by NASA, NSF, and Australian-American Educational Foundation Austin, TX, University of Texas Press, 1982. 204 p.* (1982).
- Baker, V. R. "Water and the Martian landscape." *Nature* 412.6843 (2001): 228.
- Blissenbach, E. "Geology of alluvial fans in semiarid regions." *Geological Society of America Bulletin* 65.2 (1954): 175-190.
- Blair, T. C., and J. G. McPherson. "Alluvial fan processes and forms." *Geomorphology of desert environments*. Springer, Dordrecht, 1994. 354-402.
- Bristow, T. F., et al. "The origin and implications of clay minerals from Yellowknife Bay, Gale crater, Mars." *American Mineralogist* 100.4 (2015): 824-836.
- Bull, William B. "Recognition of alluvial fan deposits in the stratigraphic record." (1972).
- Bull, W. B. "The alluvial-fan environment." *Progress in Physical geography* 1.2 (1977): 222-270.
- Chan, M. A., et al. "The Significance of a Mars Hydrograph: Shoreline Synthesis Constrained from Integrated Terrestrial Analog Studies." *Lunar and Planetary Science Conference*. Vol. 42. 2011.
- D'Arcy, M., et al. "Measuring alluvial fan sensitivity to past climate changes using a self-similarity approach to grain-size fining, Death Valley, California." *Sedimentology* 64.2 (2017): 388-424.

Davidson, S. K., et al. "Geomorphic elements on modern distributive fluvial systems." *Geomorphology* 180 (2013): 82-95.

Dromart, G., et al., "The light-toned yardang unit, Mount Sharp, Gale crater, Mars spotted by the long distance Remote Micro-imager of ChemCam (MSL mission)." *Lunar and Planetary Science Conference* (2018).

Dufour, C., et al. "Determination of the first level image processing of the ChemCam RMI instrument for the Mars Science Laboratory (MSL) rover." *International Conference on Space Optics*. Vol. 4. 2010.

Fairén, Alberto G., et al. "A cold hydrological system in Gale crater, Mars." *Planetary and Space Science* 93 (2014): 101-118.

Fassett, C. I., and Head III, J. W., "Fluvial sedimentary deposits on Mars: Ancient deltas in a crater lake in the Nili Fossae region." *Geophysical Research Letters* 32.14 (2005).

Fraeman, A. A., et al. "A hematite-bearing layer in Gale Crater, Mars: Mapping and implications for past aqueous conditions." *Geology* 41.10 (2013): 1103-1106.

Fraeman, A. A., et al. "Curiosity's Investigation at Vera Rubin Ridge." (2018).

Gaines, Daniel, et al. "Expressing Campaign Intent to Increase Productivity of Planetary Exploration Rovers." *Proc. Int. Workshop on Planning and Scheduling for Space (IW PSS'17), Pittsburgh, Pennsylvania, USA*. 2017.

Gallegos, Z. E., et al. "Recent Results and Future Plans for the Peace Vallis Campaign Including ChemCam RMI Super-Resolution Observations." *Lunar and Planetary Science Conference*. Vol. 49. 2018.

Golombek, M., et al. "Selection of the Mars Science Laboratory landing site." *Space science reviews* 170.1-4 (2012): 641-737.

Grant, J. A., et al. "The timing of alluvial activity in Gale crater, Mars." *Geophysical Research Letters* 41.4 (2014): 1142-1149.

Grant, J. A., et al. "Possible geomorphic and crater density evidence for late aqueous activity in Gale crater." *Lunar and Planetary Science Conference*. Vol 49. 2018.

Grotzinger, J. P., et al. "Mars Science Laboratory mission and science investigation." *Space science reviews* 170.1-4 (2012): 5-56.

Grotzinger, J. P., et al. "A habitable fluvio-lacustrine environment at Yellowknife Bay, Gale Crater, Mars." *Science* 343.6169 (2014): 1242777.

Grotzinger, J. P., et al. "Deposition, exhumation, and paleoclimate of an ancient lake deposit, Gale crater, Mars." *Science* 350.6257 (2015): aac7575.

Harvey, A. M., Mather, A. E., and Stokes, M. "Alluvial fans: geomorphology, sedimentology, dynamics—introduction. A review of alluvial-fan research." *Geological Society, London, Special Publications* 251.1 (2005): 1-7.

Hooke, R. LeB. "Processes on arid-region alluvial fans." *The Journal of Geology* 75.4 (1967): 438-460.

Irwin, R. P. "Testing links between impacts and fluvial erosion on post-Noachian Mars." *Lunar and Planetary Science Conference*. Vol. 44. 2013.

Johnston, J. W., Thompson T. A., and Baedke, S. J., "Systematic pattern of beach-ridge development and preservation: Conceptual model and evidence from ground penetrating radar." *SPECIAL PAPERS-GEOLOGICAL SOCIETY OF AMERICA* 432 (2007): 47.

Kite, E. S., et al. "Seasonal melting and the formation of sedimentary rocks on Mars, with predictions for the Gale Crater mound." *Icarus* 223.1 (2013): 181-210.

Kraal, E. R., et al. "Catalogue of large alluvial fans in martian impact craters." *Icarus* 194.1 (2008a): 101-110.

Kraal, E. R., et al. "Martian stepped-delta formation by rapid water release." *Nature* 451.7181 (2008b): 973.

Le Deit, L., et al. "Model age of Gale Crater and origin of its layered deposits." *Hydrologic, and Climatic Evolution and the Implications for Life*. Vol. 1680. 2012.

Le Deit, L., et al. "Lower Mount Sharp, Gale crater, Mars: key study areas as observed by Curiosity remote cameras." *Lunar and Planetary Science Conference* (2018).

Le Mouélic, S., et al. "The ChemCam Remote Micro-Imager at Gale crater: Review of the first year of operations on Mars." *Icarus* 249 (2015): 93-107.

Le Mouélic, S., et al. "Correction of stray light in ChemCam Remote Micro-imager long distance images." *Lunar and Planetary Science Conference*. Vol 50. 2019.

Malin, M. C., and Edgett, K. S., "Evidence for persistent flow and aqueous sedimentation on early Mars." *Science* 302.5652 (2003): 1931-1934.

Malin, M. C., et al. "The Mars Science Laboratory (MSL) mast-mounted cameras (Mastcams) flight instruments." *Lunar and Planetary Science Conference*. Vol. 41. 2010.

Maurice, S., et al. "Characterization of the ChemCam (MSL) Imaging Capability." *Lunar and Planetary Science Conference*. Vol. 40. 2009.

Maurice, S., et al. "The ChemCam instrument suite on the Mars Science Laboratory (MSL) rover: Science objectives and mast unit description." *Space science reviews* 170.1-4 (2012): 95-166.

Mège, D., and Bourgeois, O., "Equatorial glaciations on Mars revealed by gravitational collapse of Valles Marineris wallslopes." *Earth and Planetary Science Letters* 310.3-4 (2011): 182-191.

Metz, J. M., et al. "Sublacustrine depositional fans in southwest Melas Chasma." *Journal of Geophysical Research: Planets* 114.E10 (2009).

Milliken, R. E., J. P. Grotzinger, and B. J. Thomson. "Paleoclimate of Mars as captured by the stratigraphic record in Gale Crater." *Geophysical Research Letters* 37.4 (2010).

Moore, Jeffrey M., et al. "Martian layered fluvial deposits: Implications for Noachian climate scenarios." *Geophysical Research Letters* 30.24 (2003).

Moore, J. M., and Howard, A. D., "Large alluvial fans on Mars." *Journal of Geophysical Research: Planets* 110.E4 (2005).

Morgan, A. M., et al. "Utilizing a global database to explore morphologic trends of Martian alluvial fans." *Lunar and Planetary Science Conference*. Vol. 50. 2019.

Nachon, M., et al. "Calcium sulfate veins characterized by ChemCam/Curiosity at Gale crater, Mars." *Journal of Geophysical Research: Planets* 119.9 (2014): 1991-2016.

Nachon, M., et al. "Chemistry of diagenetic features analyzed by ChemCam at Pahrump Hills, Gale crater, Mars." *Icarus* 281 (2017): 121-136.

Newsom, H. E., et al. "Long distance observations with the ChemCam Remote Micro-Imager: Eroded Mount Sharp deposits on Gale Crater floor?" *AAS/Division for Planetary Sciences Meeting Abstracts# 48*. Vol. 48. 2016.

Newsom, H. E., et al. "Inverted channel deposits on the floor of Miyamoto crater, Mars." *Icarus* 205.1 (2010): 64-72.

Newsom, H. E., et al. "Upper Drainage and Watershed of the Multi-Stage Peace Vallis Alluvial Fan System, Gale Crater, Mars." *Lunar and Planetary Science Conference*. Vol. 50. 2019.

Oehler, D. Z., et al. "Origin and significance of decameter-scale polygons in the lower Peace Vallis fan of Gale crater, Mars." *Icarus* 277 (2016): 56-72.

Okon, A. B. "Mars science laboratory drill." (2010).

Palucis, M. C., et al. "The origin and evolution of the Peace Vallis fan system that drains to the Curiosity landing area, Gale Crater, Mars." *Journal of Geophysical Research: Planets* 119.4 (2014): 705-728.

Palucis, M. C., et al. "Sequence and relative timing of large lakes in Gale crater (Mars) after the formation of Mount Sharp." *Journal of Geophysical Research: Planets* 121.3 (2016): 472-496.

Postma, G. "Slumps and their deposits in fan delta front and slope." *Geology* 12.1 (1984): 27-30.

Rampe, E. B., et al. "Mineralogy of an ancient lacustrine mudstone succession from the Murray formation, Gale crater, Mars." *Earth and Planetary Science Letters* 471 (2017): 172-185.

Rice, Melissa S., et al. "Geologic overview of the Mars Science Laboratory rover mission at the Kimberley, Gale crater, Mars." *Journal of Geophysical Research: Planets* 122.1 (2017): 2-20.

Sautter, V., et al. "In situ evidence for continental crust on early Mars." *Nature Geoscience* 8.8 (2015): 605.

Sharp, R. P., and Michael C. Malin. "Channels on mars." *Geological Society of America Bulletin* 86.5 (1975): 593-609.

Scuderi, L. A., et al. "An Amazonian Groundwater Springline at Peace Vallis Fan, Gale Crater; Implications for a Late Period of Surface Water Flow." *Lunar and Planetary Science Conference*. Vol. 50. 2019.

Stack, K. M., et al. "Diagenetic origin of nodules in the Sheepbed member, Yellowknife Bay formation, Gale crater, Mars." *Journal of Geophysical Research: Planets* 119.7 (2014): 1637-1664.

Stack, K. M., et al. "Evidence for plunging river plume deposits in the Pahrump Hills member of the Murray formation, Gale crater, Mars." *Sedimentology* (2018).

Stein, N., et al. "Desiccation cracks provide evidence of lake drying on Mars, Sutton Island member, Murray formation, Gale Crater." *Geology* 46.6 (2018): 515-518.

Strahler, A. N. "Physical Geography. John Wiley & Sons, New York 1975 (1975): 8385.

Sumner, D. Y., et al. "Preliminary geological map of the Peace Vallis fan integrated with in situ mosaics from the Curiosity rover, Gale Crater, Mars." (2013).

Thomson, B. J., et al. "Constraints on the origin and evolution of the layered mound in Gale Crater, Mars using Mars Reconnaissance Orbiter data." *Icarus* 214.2 (2011): 413-432.

Vaniman, D. T., et al. "Mineralogy of a mudstone at Yellowknife Bay, Gale crater, Mars." *Science* 343.6169 (2014): 1243480.

Vasavada, A. R., et al. "Overview of the Mars Science Laboratory mission: Bradbury landing to Yellowknife Bay and beyond." *Journal of Geophysical Research: Planets* 119.6 (2014): 1134-1161.

Weissmann, G. S., et al. "Factors controlling sequence development on Quaternary fluvial fans, San Joaquin Basin, California, USA." *Special Publication-Geological Society of London* 251 (2005): 169.

Weissmann, G. S., et al. "Fluvial form in modern continental sedimentary basins: distributive fluvial systems." *Geology* 38.1 (2010): 39-42.

Weissmann, G. S., et al. "Prograding distributive fluvial systems: geomorphic models and ancient examples." *New Frontiers in Paleopedology and Terrestrial Paleoclimatology: SEPM, Special Publication* 104 (2013): 131-147.

Wiens, R. C., et al. "The ChemCam instrument suite on the Mars Science Laboratory (MSL) rover: Body unit and combined system tests." *Space science reviews* 170.1-4 (2012): 167-227.

Williams, R. ME., et al. "Martian fluvial conglomerates at Gale crater." *science* 340.6136 (2013): 1068-1072.